

# Optimization and in-depth analysis of alginate nanocellulose hydrogels for 3D printing of vascular and integumentary systems

---

Šurina, Paola

Master's thesis / Diplomski rad

2023

Degree Grantor / Ustanova koja je dodijelila akademski / stručni stupanj: **University of Split, Faculty of Science / Sveučilište u Splitu, Prirodoslovno-matematički fakultet**

Permanent link / Trajna poveznica: <https://um.nsk.hr/um:nbn:hr:166:642604>

Rights / Prava: [Attribution 4.0 International](#) / [Imenovanje 4.0 međunarodna](#)

Download date / Datum preuzimanja: **2025-02-07**

Repository / Repozitorij:

[Repository of Faculty of Science](#)



**UNIVERSITY OF SPLIT**  
**FACULTY OF SCIENCE**

Master thesis

**Optimization and in-depth analysis of alginate nanocellulose  
hydrogels for 3D printing of vascular and integumentary  
systems**

Paola Šurina

**September 2023, Split**



Ovaj rad, izrađen u Splitu, pod vodstvom doc. dr. sc. Perice Boškovića, predan je na ocjenu Odjelu za kemiju Prirodoslovno-matematičkog fakulteta Sveučilišta u Splitu radi stjecanja zvanja magistra edukacije biologije i kemije.

## ***Acknowledgment***

*I would like to thank my professor and mentor Perica Bošković for always providing advice, guidance and help during my student years, as well as mentoring both of my bachelor and master thesis. Thank you for making my trip to Graz possible and connecting me with my supervisors.*

*The work for this thesis was done at the IBioSys institute (Institute of Chemistry and Technology of Biobased Systems) in Graz, Austria, as a part of an Erasmus+ project. I would like to thank everyone there for their welcome, help and support. Especially professors Karin Stana Kleinschek and Rupert Kargl as well as PhD student Florian Lackner, with whom I worked more closely.*

*Lastly, a big thank you to my family for always being there for me.*

## TEMELJNA DOKUMENTACIJSKA KARTICA

Sveučilište u Splitu  
Prirodoslovno – matematički fakultet  
Odjel za kemiju  
Rudera Boškovića 33, 21000 Split, Hrvatska

Diplomski rad

### **OPTIMIZACIJA I DUBINSKA ANALIZA ALGINATNIH NANOCELULOZNIH HIDROGELOVA ZA 3D PRINTANJE KRVOŽILNIH I KOŽNIH SUSTAVA**

Paola Šurina

Diplomski sveučilišni studij biologija i kemija – smjer nastavnički

**Sažetak:** U zadnjih nekoliko desetljeća velika pažnja usmjerena je na inženjering tkiva i regenerativnu medicinu. Iako tkivni inženjering uključuje širok spektar primjena, ovaj rad fokusira se uglavnom na optimizaciju i razvoj hidrogelova za takvu primjenu. Analizirana su brojna svojstva 3D isprintanih i umreženih alginatnih i nanoceluloznih hidrogelova kao što su proces ispiranja kalcija važnog za procese regeneracije tkiva, zatim ispitivanja vlačnim povlačenjem kako bi se dobio uvid u elastična, odnosno plastična svojstva materijala važna za primjenu u krvožilnim sustavima. Zatim, procesi difuzije za dokazivanje permeabilnosti hidrogela, vrlo važnog svojstva koje omogućuje prijenos nutrijenata do oštećenog tkiva, te na kraju ispitivanje citotoksičnosti materijala. Postignuta su i optimizirana važna svojstva biomaterijala za biomedicinske primjene, kao što su biokompatibilnost i kontrolirana degradacija. Uočeno je da veća koncentracija kalcija pozitivno utječe na mehanička svojstva hidrogelova. Tijekom testova rastezanja te testova bubrenja i skupljanja uočena je anizotropija materijala važna kod primjene u krvožilnim sustavima. Dobiveni rezultati obećavajući su za buduće primjene u biomedicini i tkivnom inženjeringu.

**Ključne riječi:** nanoceluloza, biomaterijali hidrogelovi, 3D printanje, umreženje, difuzija, inženjering tkiva

**Rad sadrži:** 83 stranice, 48 slika, 13 tablica, 107 literaturnih navoda.

Izvornik je na engleskom jeziku.

**Mentor:** Dr. sc. Perica Bošković, docent

**Neposredni voditelj:** Dr. sc. Rupert Kargl, docent

**Ocjenjivači:** Dr. sc. Perica Bošković, izv. prof  
Dr.sc. Ivica Ljubenkov, izv. Prof.  
Martina Gudelj, mag. educ. biol. et chem.

**Rad prihvaćen:**

*Rad je pohranjen u knjižnici Prirodoslovno-matematičkog fakulteta, Sveučilišta u Splitu.*

## BASIC DOCUMENTATION CARD

University of Split  
Faculty of Science  
Department of Chemistry  
33 Ruđer Bošković Street, 21000 Split, Croatia

Master thesis

### **OPTIMIZATION AND IN-DEPTH ANALYSIS OF ALGINATE NANOCCELLULOSE HYDROGELS FOR 3D PRINTING OF VASCULAR AND INTEGUMENTARY SYSTEMS**

Paola Šurina

Graduate university study programme biology and chemistry, specialization in education

**Abstract:** In recent decades, tissue engineering and regenerative medicine have received much attention. Although tissue engineering covers a wide range of applications, this work focuses mainly on the optimization and processing of hydrogels for such applications. Numerous properties of 3D printed and crosslinked alginate and nanocellulose hydrogels were analyzed, such as the calcium leaching process important for tissue regeneration processes, tensile properties to gain insight into the elastic and/or plastic properties of materials important for pressurized vascular systems, diffusion processes to demonstrate the permeability of the scaffolds for the transfer of nutrients to the cells and testing of the cytotoxicity of the material. Important biomaterial properties such as biocompatibility and controlled degradation for biomedical applications have been reached and optimized. It was observed that higher calcium concentration positively influences mechanical properties of the hydrogels. During tensile testing as well as shrinking and swelling tests, material anisotropy important for application in vascular systems was observed. The obtained results are promising for future applications in biomedicine and tissue engineering.

**Keywords:** nanocellulose, biomaterials, hydrogels, 3D printing, crosslinking, diffusion, tissue engineering

**The thesis consists of:** 83 pages, 48 figures, 13 tables, 107 literature references



**Mentor:** Perica Bošković, Ph.D., assistant professor

**Assistant Supervisor:** Rupert Kargl, Ph.D., assistant professor

**Reviewers:** Perica Bošković, Ph.D., assistant professor

Ivica Ijubenkov, Ph.D., assistant professor

Martina Gudelj, mag. educ. biol. et chem.

**Thesis accepted:**

*The thesis is deposited in the Faculty of Science Library, University of Split.*

## Summary

Cellulose, known for its biocompatibility, biodegradability and mechanical strength has emerged as a promising material for 3D manufacturing in field of biomedicine and tissue engineering. Through precise layer by layer fabrication, cellulose based materials offer unique advantages in constructing scaffolds for tissue regeneration and engineering. This thesis describes a detailed investigation of the properties of bio inks fabricated from nanocellulose, alginate and calcium carbonate, with the latter providing the calcium ions for cross-linking. When preparing inks for extrusion-based 3D printing, the rheological behavior of the materials is one of the most important issues to consider. The inks (with different calcium concentrations) prepared for this work have significant shear thinning properties and retain their shape after printing. Homogeneity of the prepared inks was observed using light microscopy before printing.

After printing, the scaffolds were crosslinked with appropriate amounts of glucono- $\delta$ -lactone (GDL) for 24 hours, then stored in different calcium concentration solutions previously optimized for each ink. After that, the scaffolds were ready for various mechanical and physical analyses. Firstly, calcium leaching tests were performed and optimized for each ink. The ink with the lowest calcium concentration stored in appropriate solutions retained almost all of its calcium, while the ink with the highest amount of calcium, also stored in its appropriate solution, retained about 60% of its initial calcium.

Second, shrinkage and swelling of the scaffold stored in crosslinking and storage solutions were observed, and during this process a strong anisotropic behavior of the material was observed. Anisotropic behavior was also observed during uniaxial tensile tests and cyclic tests. The stress-strain curves obtained after the tensile tests were then used to calculate the tensile modulus. In general, the longitudinally printed scaffolds exhibited a higher tensile strength and modulus compared to the perpendicularly printed scaffolds which is an effect of nanocellulose fiber alignment. Increasing the  $\text{CaCO}_3$  content in the scaffolds also improved the tensile properties and stability after crosslinking.

Furthermore, the porosity of the printed scaffolds was tested by diffusion of NaCl,  $\text{CaCl}_2$ , glucose, riboflavin, dextran (20 kDa), and bovine serum albumin (BSA) through 1-, 2-, and 3-layer scaffolds. The pores of the scaffolds were too small for diffusion of dextran and BSA molecules due to their large structure, while all other tested substances penetrated with values comparable to those reported in the literature.

For a material to be considered biocompatible, it must promote cell growth. Therefore, cell viability tests were performed and found no toxicity to HUVECs and HEK 293 cells.

Lastly, to ensure that the damaged tissue heals, and the scaffold gradually breaks down and integrates with the surrounding tissue, the degradation of the scaffold needs to be triggered. For this reason, degradation tests were performed to determine which substances may promote degradation.

In summary, the analyzed properties make the tested material promising for application in biomedicine as a material for tissue engineering and wound healing.

## Contents

1. INTRODUCTION AND AIM.....	1
2. THEORETICAL BACKGROUND.....	3
2.1. Biomaterials.....	3
2.2. Cellulose.....	4
2.2.1. Cellulose structure and polymorphs.....	5
2.2.2. Plant vs. bacterial nanocellulose.....	7
2.3. Alginate.....	11
2.3.1. Crosslinking.....	12
2.3.2. Applications.....	14
2.4. Polymers.....	15
2.4.1. Chain conformation.....	15
2.4.2. Rheology.....	15
2.4.3. Molecular mass distribution (MMD).....	17
2.4.4. Charge complexes.....	17
2.5. Direct ink writing.....	18
3. EXPERIMENTAL SECTION.....	19
3.1. Materials.....	19
3.2. Scaffold preparation and 3D printing.....	19
3.2.1. Preparation of the ink for direct ink writing (DIW).....	19
3.2.2. General printer and software description.....	20
3.2.3. 3D printing process.....	22
3.2.4. Crosslinking process.....	24
3.2.5. Leaching process.....	25
3.2.6. Scaffold preparation for cell viability test.....	25
3.3. Analytic methods.....	27

3.3.1.	Swelling/shrinking tests.....	27
3.3.2.	Calcium titrations .....	27
3.3.3.	Tensile and cycle tests.....	28
3.3.4.	Light microscopy .....	30
3.3.5.	Diffusion tests .....	31
3.3.6.	Cell viability tests.....	34
3.3.7.	Degradation process .....	35
4.	RESULTS AND DISCUSSION .....	38
4.1.	Calcium Leaching and Leaching Kinetics .....	38
4.1.1.	Rectangular shaped scaffolds.....	38
4.1.2.	Disks for cell viability .....	39
4.2.	Shrinking/swelling of the scaffolds.....	42
4.3.	Tensile testing .....	44
4.4.	Cycle test .....	45
4.5.	Light microscopy.....	49
4.6.	Diffusion tests .....	50
4.6.1.	Sodium and calcium chloride.....	51
4.6.2.	Riboflavin .....	52
4.6.3.	Dextran (20 kDa).....	54
4.6.4.	Bovine albumin serum (BSA).....	55
4.6.5.	Glucose .....	55
4.7.	Cell viability tests.....	57
4.8.	Degradation process .....	58
4.8.1.	Solutions .....	58
4.8.2.	Cellulase .....	60
5.	CONCLUSIONS.....	65

6.	LIST OF PUBLICATIONS AND TALKS .....	67
7.	ABBREVIATIONS .....	68
8.	LIST OF FIGURES .....	69
9.	LIST OF TABLES .....	72
10.	References .....	73
11.	METHODICAL PART .....	I

## 1. INTRODUCTION AND AIM

Cellulose is very abundant organic polymer on Earth and is known for its remarkable physical, chemical, and biological properties. It is one of the important structural components of plant cell walls and is also produced by several bacteria and algae. The only known animals to biosynthesize cellulose are tunicates. Cellulose has been processed and consumed for thousands of years in the form of paper, textiles, wood, feed, and as dietary fiber in foods. Nowadays, cellulosic materials are gaining renewed attention to meet modern societies' requirements of carbon neutrality, sustainability, and biodegradability. Due to the hierarchical arrangement of cellulose fibrils and crystallites, nanomaterials can be extracted from renewable resources. This yields products with high performance and good mechanical, physical and chemical properties. Rheological properties, selective fiber orientation and alignment, surface chemical reactivity are other aspects of interest.<sup>1,2</sup> Cellulose dimensions less or equal to 100 nm in diameter or length are considered as nanocellulose which is most commonly divided into rod-like nanocrystals (CNC) and more elongated nanofibers (NFC). The latter form of cellulose was first reported by Turbak A. F. in 1983, who described its remarkable properties and potential applications.

Over the past two decades, 3D printing, or additive manufacturing has gained tremendous popularity and has also found its way into bioprinting, a technology that aims to replace damaged or infected tissues and organs with the help of cell seeded scaffolds and tissue culture. Many of these printing techniques make use of bio-inks, which are viscous polymer solutions, optionally containing biological molecules and cells. Several methods exist to 3D print and cross-link these scaffolds with or without incorporated live cells. In this respect, nanocellulose has attracted great interest as a material for tissue scaffolds in various applications since NFC provides mechanical strength to biocompatible hydrogels. The use of NFC in wound healing, bone tissue regeneration, blood vessel or soft tissue replacement and drug delivery has been reported.<sup>2-5</sup> When using NFC in extrusion based bioprinting, the methods of cross-linking, and the physio-chemical and biological properties of the resulting materials are essential. Cross-linking is necessary to stabilize the 3D printed structure after extrusion and during use. For cross-linking, either covalent chemical methods, or physical methods such as charge complexation of sodium alginate with calcium ions are known.<sup>6,7</sup> Alginate is already used as a medical biomaterial in wound dressings and appears to be very suitable for blends with NFC as biocompatible hydrogels in 3D printing.<sup>6</sup> This work is a contribution to the investigation of the mechanical and biological properties of NFC alginate blend

bio-inks useful for 3D bioprinting.<sup>6,8</sup> It has been reported that the calcium concentration of bio-inks comprising NFC/Alg affects their mechanical properties and stability due to variations in the crosslinking density.<sup>6</sup> Therefore, mechanical properties, such as maximum stress and elongation, were tested for inks with different calcium concentrations. In addition, the calcium leaching process was determined and optimized for each ink. Following, to get an insight into the porosity of the scaffolds, nutrient diffusion through the materials and degradation on-demand were tested.

The aims of the thesis are to:

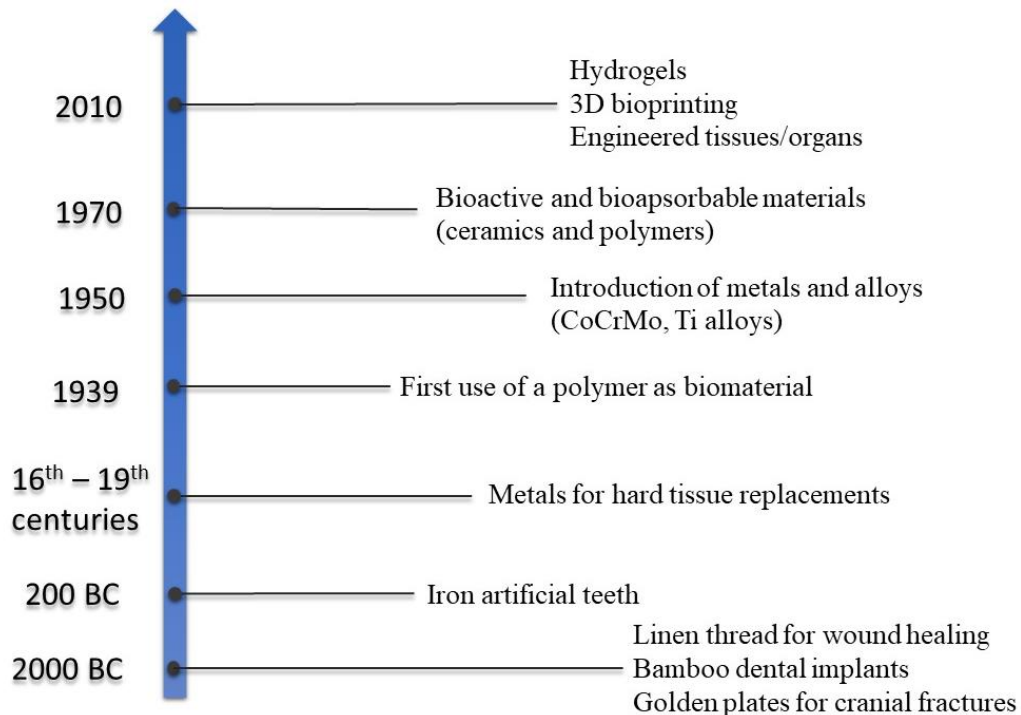
1. Prepare bio-inks from cellulose nanofibril/alginate hydrogels.
2. Characterize the mechanical and chemical properties of the printed hydrogels.
3. Investigate the influence of the calcium concentrations on the scaffold properties.
4. Perform leaching, diffusion and cell viability tests and investigate scaffold degradation.



## 2. THEORETICAL BACKGROUND

### 2.1. Biomaterials

Materials designed to interact with biological systems for either therapeutic or diagnostic purposes are commonly referred to as biomaterials, even though their scope extends beyond the medical field.<sup>9</sup> Biomaterials are part of biomedical engineering and combine scientific fields such as biology, chemistry, medicine, engineering, etc., they are multidisciplinary and can be naturally or synthetically derived or can be a hybrid of both. Biomaterials have probably been used since the existence of humankind, as there is evidence that Neanderthals used wood as dental implants, the ancient Egyptians used various biomaterial based mummification methods, and later various materials were used to heal wounds and immobilize fractures.<sup>10</sup> Today, biomaterials have come a long way and their use is broad and includes countless applications, some of which are shown in **Figure 1**.



**Figure 1** Biomaterials throughout history until today<sup>10-12</sup>

Important properties of biomaterials are biocompatibility, biodegradability, and non-cytotoxicity. One of the materials that have a very high level of compatibility with biological systems is cellulose. It has been reported that incorporating cellulose with other materials increases their biocompatibility, making them more suitable to interact with biological systems.<sup>13</sup> In addition, cellulose is considered to be one of the biopolymers with the highest biocompatibility and the lowest cytotoxicity and is therefore of great interest as a biomaterial for 3D printing of tissue substitutes.<sup>13,14</sup>

Another polysaccharide commonly used in biomedical applications and 3D bioprinting is alginate. It has numerous advantageous material properties of which its gelling behavior is of particular importance. Various techniques have been developed to control the gelling process of alginate, which is very important for its properties.<sup>15</sup> Like cellulose, alginate is biocompatible and can be easily combined with other biomaterials such as cellulose to achieve cell affinity and increase stability.<sup>6,16</sup>

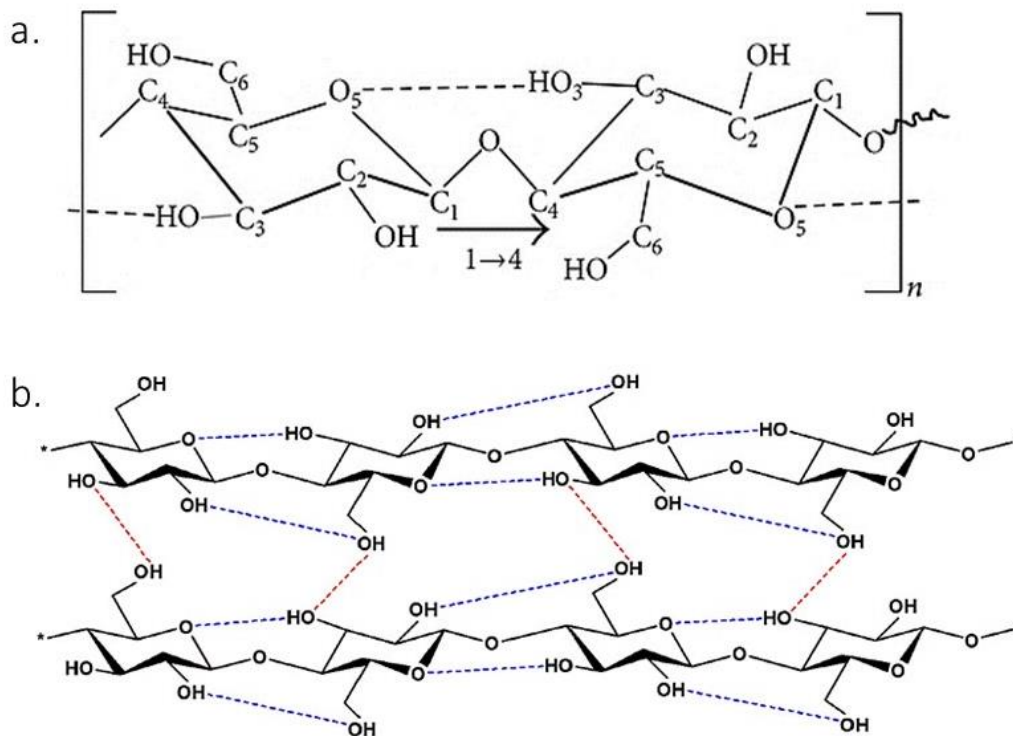
Although natural polymers are widely used in 3D printing and tissue engineering there are still some challenges, such as mechanical properties that need to mimic natural tissues, biodegradation rate control, biostability of manufactured materials, etc.<sup>17</sup> Combining different materials, adapting the best crosslinking process for each material and developing different techniques are a great step forward to produce suitable materials for tissue engineering in the future.

## **2.2. Cellulose**

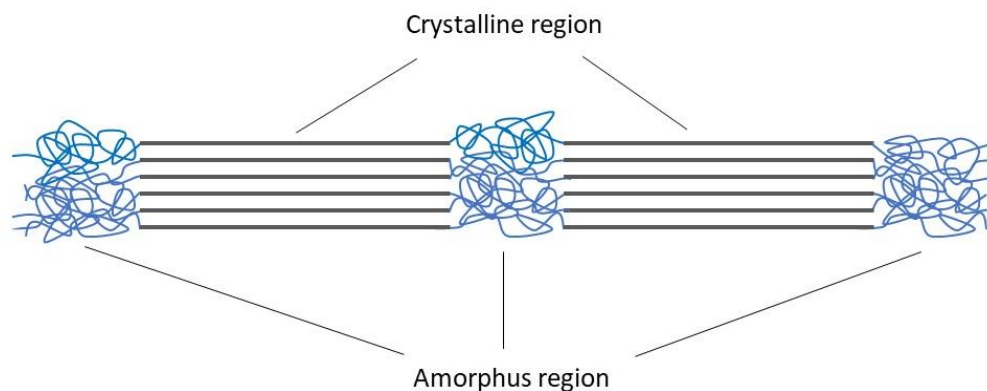
As mentioned earlier, cellulose is the most abundant organic compound known to humankind. Although it is highly associated with plants and trees because this is the largest industrial source, it is also produced by some prokaryotes such as bacteria (e.g. *Acetobacter*, *Pseudomonas*, *Rhizobium*, *Sarcina*) and cyanobacteria (*Scytonema hofmanni*)<sup>18</sup> and eukaryotes including fungi (*Aspergillus*, *Trichoderma*), green algae (*Cladophorales* and some members of *Siphonocladales*)<sup>19</sup>, amoebae, cellular slime molds and a very small group of animals, tunicates (*Ciona intestinalis*, *Ascidia sp.*, *Halocynthia roretzi*).<sup>20,21</sup>

### 2.2.1. Cellulose structure and polymorphs

Native cellulose consists of D-glucopyranose subunits linked together via  $\beta$  1 $\rightarrow$ 4 glycosidic bonds (**Figure 2 (a)**)<sup>22</sup> The cellulose morphology can be described by two terms, crystalline and amorphous (**Figure 2 (b)**). Owing to the hydroxyl groups in cellulose, intra- and inter-molecular hydrogen bonds can be formed which play a major role in the structure of cellulose and thus in its properties.<sup>23,24</sup> Although cellulose is hydrophilic, it is not soluble in water but rather interacts with it forming hydrogen bonds and is therefore considered amphiphilic, in other words having both hydrophilic and hydrophobic properties.<sup>25-27</sup> The crystalline structure occurs as long cellulose chains stacked next to each other which is a result of Van der Waals forces and intermolecular and intramolecular hydrogen bonding, whereas amorphous cellulose is the result of the breaking of these bonds and these types of cellulose chains are shorter than the crystalline ones and can be as short as one cellobiose unit.<sup>23,28,29</sup>



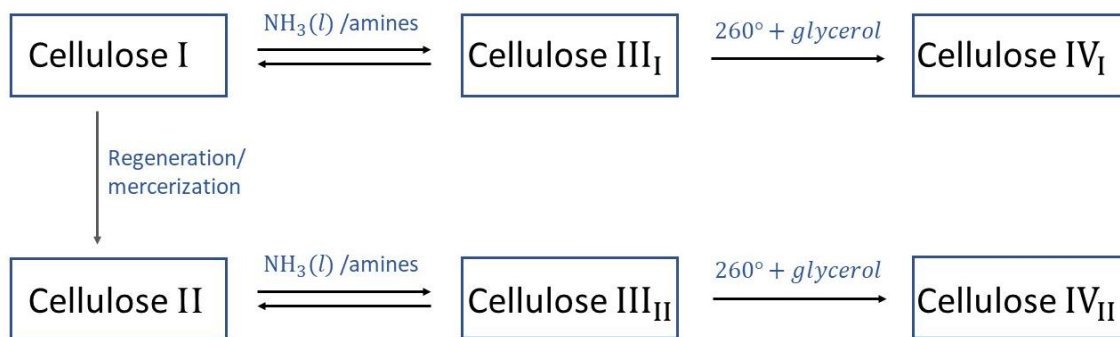
**Figure 2 (a.)** Cellulose repeat unit showing  $\beta$  1 $\rightarrow$ 4 glycosidic bond<sup>22</sup> **(b.)** intermolecular (red) and intramolecular (blue) hydrogen bonding in cellulose<sup>30</sup>



**Figure 3** Schematic representation of the crystalline and amorphous region of cellulose, crystalline region is obtained by hydrogen bonds and Van der Waals forces, when they are disrupted amorphous region occurs

Compounds that exist in two or more crystalline structures are called polymorphs. As reported, cellulose exists in six different polymorphs.<sup>28,31,32</sup> They all differ in molecular orientation and in the hydrogen bonds that occur in the crystalline regions which is a result of different sources, treatments, or methods of production.<sup>33</sup> Cellulose I (CI) and cellulose II (CII) are the most common polymorphs, and are commonly referred to as native cellulose and regenerated cellulose.<sup>23,24</sup> Native cellulose (CI) occurs only in nature and is usually found as a combination of CI $\alpha$  and CI $\beta$ . Their ratio depends on the source. In bacteria and green algae, the predominant cellulose polymorph is CI $\alpha$  and for wood and animal (tunicates) cellulose CI $\beta$  is the dominant one.<sup>28</sup> For example, a ratio of CI $\alpha$ /CI $\beta$  = 60/40 has been reported for some algae such as *Valonia ventricosa*, which have a crystallinity of up to 100%.<sup>34</sup> On the other hand, cellulose extracted from higher plants contains a higher proportion of CI $\beta$ .<sup>22</sup>

CI has many applications, among all in tissue engineering as a wound dressing component.<sup>35-37</sup> CII can be obtained from CI by two different processes: Regeneration (dissolving CI in a suitable solution and re-precipitating with water) and mercerization (swelling of the cellulose fibers in concentrated sodium hydroxide solution). Chemical treatments with liquid ammonia or some amines can convert CI and CII into CIII<sub>I</sub> and CIII<sub>II</sub> (index numbers indicate the origin, either CI or CII) which are less densely packed compared to CI.<sup>28,31</sup> Cellulose IV<sub>I</sub> and IV<sub>II</sub> are produced by heating CIII<sub>I</sub> and CIII<sub>II</sub> to 260°C in glycerol, they cannot be obtained directly from cellulose I. Described conversion processes are shown in **Figure 4**.



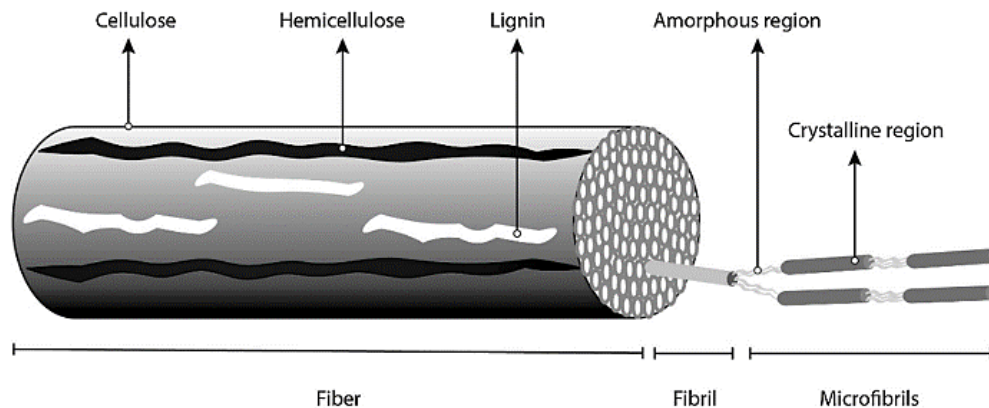
**Figure 4** Cellulose polymorphs conversions

### 2.2.2. Plant vs. bacterial nanocellulose

As mentioned earlier, cellulose is the most abundant organic polymer on Earth and can be obtained from different sources. The most common sources for obtaining cellulose for research and various applications are plants and bacteria.<sup>38,39</sup> Nanocellulose is classified into three groups depending on the source of extraction: Cellulose nanocrystals (CNC), cellulose nanofibers (CNF), which are subgroups of plant cellulose, and bacterial cellulose (BC).<sup>40</sup>

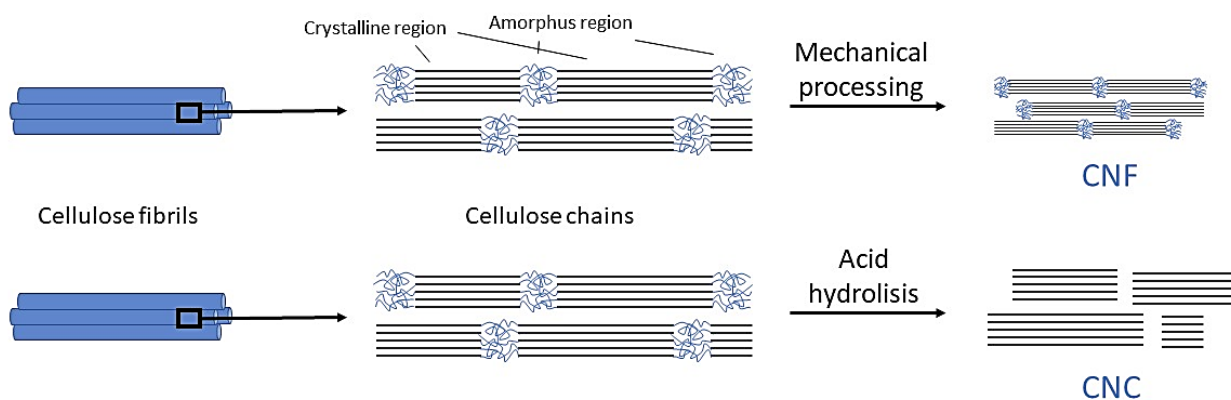
#### 2.2.2.1. Production

Plant cellulose differs from bacterial cellulose because of its occurrence in nature. While plant cellulose is synthesized by cellulose synthase complexes found in Golgi apparatus with carbon dioxide as a source of carbon, cellulose producing bacteria converts glucose, fructose, or any other organic compound into cellulose. That process is occurred with presence of many different precursors and enzymes such as hexoses, hexanoates, pyruvate, etc. and cellulose is then released to extracellular matrix.<sup>41</sup> Cellulose produced by bacteria is a pure cellulose, however plant cellulose occurs as impure and contains lignin and hemicellulose, which play an important role in improving the mechanical strength of the plant stem and the stability of the cell walls.<sup>42</sup> Due to its hierarchical structure (**Figure 5**), plant nanofibers and nanocrystals are extracted using top-down methods, either using mechanical or chemical methods.



**Figure 5** Plant cellulose hierarchical structure. Cellulose chains are bond together with hydrogen bonds and Van der Waals interactions forming microfibrils. Crystalline and amorphous regions aggregate and form fibrils which are held together with hemicellulose and lignin to form fibers.<sup>43</sup>

The first step in the production of nanocellulose from plants is the removal of lignin and hemicellulose from the cellulose by milling, pulping, and bleaching.<sup>43</sup> The cellulose is then processed either mechanically, enzymatically or chemically. Mechanical processes such as homogenization, milling, refining, blending, ultrasonication, etc., result in the production of CNFs containing both amorphous and crystalline domains.<sup>30</sup> On the other hand, CNCs are usually extracted from CNFs by acid hydrolysis with strong acids such as  $H_2SO_4$  and  $HCl$ .<sup>30,40</sup>



**Figure 6** Schematic representation of CNF and CNC production

In addition, cellulose obtained from cellulose producing bacteria is referred to bacterial nanocellulose due to bacterial polymerization of glucose monomers, linkage of monomers via

$\beta$ 1→4 bonds and secretion of nanofibers to the extracellular matrix. For this reason, BC is obtained by the bottom-up method.<sup>43</sup> To stimulate the production of nanocellulose, optimal media must be provided to the bacteria. The most used media today for BC was developed by Hestrin and Schramm in 1954 which is composed of 2% glucose, 0.5% peptone, 0.5% yeast extract, 0.15% citrate and 0.27% anhydrous disodium phosphate. Cultivation usually takes two weeks, after which the bacteria and media residues are removed. This process includes washing with distilled water, two or more treatments with NaOH in a heat bath, and finally washing with distilled water to a neutral pH.<sup>44</sup> The final product is a purified bacterial nanocellulose film ready for further processing such as homogenization and application in various fields. BC as well as CNF from PC (plant cellulose) contains amorphous and crystalline regions.

BC production has an advantage over PC production, an important reason is environmental impact. Hemicellulose and lignin must be removed to produce PC, which is done with extremely polluting reactions. Nevertheless, the production costs for both BC and PC are still very high, which is due to the high cost of the Hestrin-Schramm medium and the lack of more efficient fermentation systems for BC, as well as the high cost of equipment, chemicals, high energy consumption, etc. for PC.<sup>43</sup>

#### 2.2.2.2. Properties

In addition to the fact that plant and bacterial cellulose differ in terms of source and production, they also differ in different chemical and mechanical properties. As described previously both plant and bacterial cellulose have the same chemical structure however different morphology, which affects their properties. Some of the properties for PC and BC are compared and described in the **Table 1**.

**Table 1** Comparison of different properties for plant and bacterial cellulose<sup>43</sup>

Property	Plant cellulose		Bacterial cellulose
	Nanofibers	Nanocrystals	
<b>Crystallinity</b>	59-64% <sup>45</sup>	54-88% <sup>45</sup>	69-85% <sup>46</sup>
<b>Degree of polymerization</b>	$\geq 500$ <sup>47</sup>	500 – 15 000 <sup>47</sup>	800 – 10 000 <sup>47</sup>
<b>Tensile strength</b>	25 – 200 MPa <sup>48</sup>		20 – 300 MPa <sup>49</sup>

<b>Young's modulus</b>	39 – 78 GPa <sup>43</sup>	50 – 100 GPa <sup>43</sup>	15 – 30 GPa <sup>43</sup>
<b>Fiber diameter</b>	85 – 225 nm <sup>43</sup>	150 – 300 nm <sup>43</sup>	70 – 80 nm <sup>43</sup>
<b>Purity</b>	< 80% <sup>47</sup>		>99% <sup>47</sup>
<b>Relative hydrophilicity</b>	20 – 30% <sup>50</sup>		40 – 50% <sup>50</sup>
<b>Toxicity</b>	Slight cytotoxicity reported on HEK 293 cells <sup>51</sup> , cytotoxicity on other cells weren't reported		No cytotoxicity reported

### 2.2.2.3. Applications

Due to their remarkable properties bacterial and plant cellulose have gained huge popularity in a variety of fields in both research, and industry. The development of various techniques for modifying cellulose has also increased, leading to even more potential applications of cellulose. Most applications of cellulose are in civil engineering, biomedical engineering, and the food industry due to its non-toxicity, but cellulose has also found its way in electronic devices. Some of the applications of plant and bacterial cellulose are shown in **Table 2**.

**Table 2** Plant and bacterial cellulose applications<sup>43</sup>

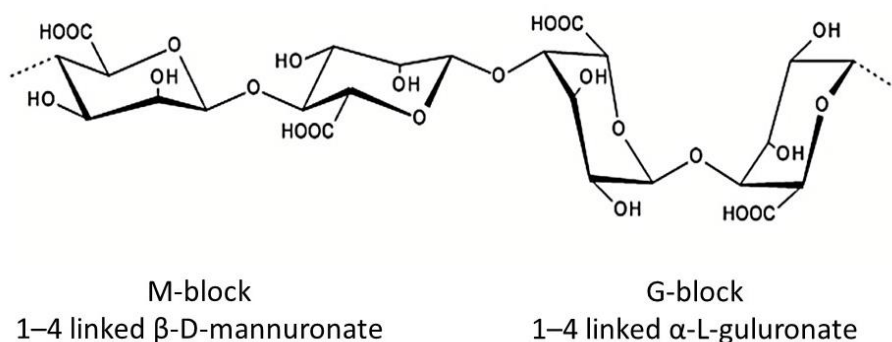
	<b>Plant cellulose</b>	<b>Bacterial cellulose</b>
<b>Biomedical engineering</b>	<ul style="list-style-type: none"> <li>• Drug carriers<sup>52,53</sup></li> <li>• Wound dressings<sup>53</sup></li> </ul>	<ul style="list-style-type: none"> <li>• Wound dressings<sup>54</sup></li> <li>• Research for tissue engineering for heart valves<sup>43</sup></li> </ul>
<b>Food industry</b>	<ul style="list-style-type: none"> <li>• Package coatings (carboard and bioactive packaging)<sup>55,56</sup></li> </ul>	<ul style="list-style-type: none"> <li>• Package coatings<sup>57</sup></li> <li>• Texture modifier for ice cream<sup>58</sup></li> <li>• Fat replacer<sup>58</sup></li> </ul>
<b>Cosmetics</b>	<ul style="list-style-type: none"> <li>• Cellulose as emulsifier, film former and humectant<sup>59</sup></li> </ul>	<ul style="list-style-type: none"> <li>• Anti-inflammatory mask for acne treatment<sup>60</sup></li> <li>• Vitamin B loaded membranes for dermal care<sup>61</sup></li> </ul>



<b>Civil engineering</b>	<ul style="list-style-type: none"> <li>• Cement composites (improvement of the mechanical strength)<sup>62</sup></li> </ul>	/
<b>Electronic devices</b>	<ul style="list-style-type: none"> <li>• OLEDs (CNC substrates)<sup>63</sup></li> </ul>	<ul style="list-style-type: none"> <li>• Biological electrodes and flexible biosensors for medical devices<sup>64</sup></li> </ul>

### 2.3. Alginate

Alginate is a polysaccharide composed of 1–4 linked  $\beta$ -D-mannuronic acid (M segment) and  $\alpha$ -L-guluronic acid (G segment) monomers, which can occur as consecutive M segments, consecutive G segments or alternating M and G segments (**Figure 7**). usually extracted from brown algae, *Phaeophyceae* such as *Laminaria japonica*, *Macrocystis pyrifera*, and *Ascophyllum nodosum* but it can also be synthesized by some bacteria of the genera *Pseudomonas* and *Azotobacter*.<sup>7</sup> Alginate is usually extracted with sodium hydroxide or some other alkali solution, following, in order to precipitate sodium or calcium chloride is added. It can then be converted into alginic acid with hydrochloric acid treatment.<sup>7</sup>



**Figure 7** Alginate chemical structure<sup>65</sup>

Depending on the ratio of G and M blocks, alginate can exhibit different mechanical properties. A higher level of G blocks results in stiffer and brittle alginate gels, while a higher level of M blocks gives the alginate soft and elastic properties.<sup>65</sup> For this reason, the properties of alginate gels can be adjusted by changing the molecular weight and ratio of G and M blocks. The molecular weight

of alginate can range from 33 000 to 40 000 g/mol, and as the molecular weight increases, the viscosity of the alginate gel increases, which is not always desirable. It is important to control the viscosity of the gels since it also affects the stiffness of the gel post gelation.<sup>7</sup> In addition, the ratio of M and G blocks depends on the source of extraction and thus on the mechanical and chemical properties. Another factor affecting the mechanical and chemical properties of alginate gels is the crosslinking process, more specifically the crosslinking method, the crosslinking density and the crosslinking agent.<sup>15</sup>

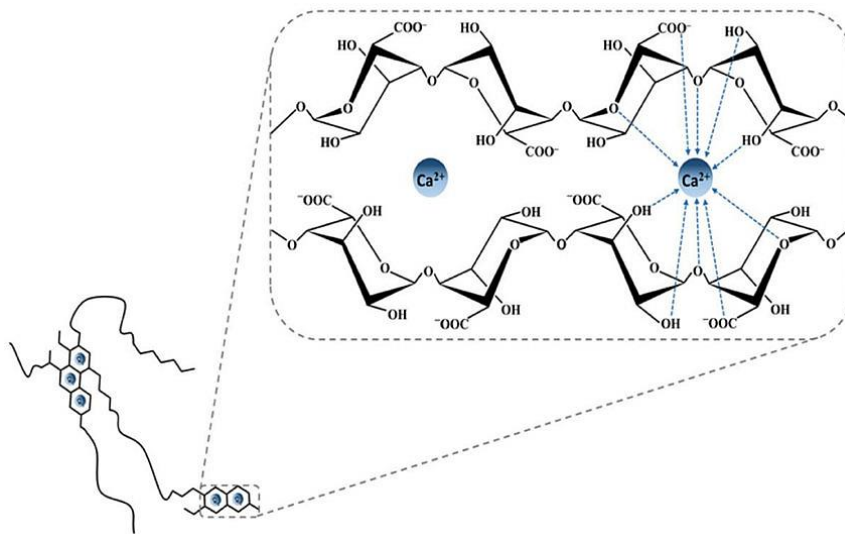
### 2.3.1. Crosslinking

To prepare alginate hydrogels for various applications, crosslinking of the alginate gel is required to achieve the desired mechanical properties. Crosslinking of alginate results in the formation of a hydrogel. Hydrogels are 3D structures consisting of a crosslinked polymer network capable of binding large amounts of water.<sup>66</sup> Various methods have been developed for the preparation of alginate hydrogels, some of which are described below.

**Ionic crosslinking** is the most common method for preparing alginate hydrogels.<sup>7</sup> In ionic crosslinking, divalent cations such as  $\text{Ca}^{2+}$  and  $\text{Mg}^{2+}$  are bound to the G blocks of the alginate forming so called “egg-boxes” (**Figure 8**). This gelation process occurs very rapidly when  $\text{CaCl}_2$  is used due to its high-water solubility, which affects the other properties of a hydrogel and thus its applications. Controlling the gelation rate plays a major role in the stability and uniformity of the hydrogel.<sup>7,15,16,67</sup> To achieve slower and more controlled gelation,  $\text{CaCl}_2$  can be replaced by less water soluble substances such as  $\text{CaCO}_3$  or  $\text{CaSO}_4$ .<sup>7,16,67</sup> To dissolve them, the pH must be lowered using acid such as glucono- $\delta$ -lactone.<sup>6,7</sup>

In addition to their importance in crosslinking, calcium ions have many other important functions in hydrogels. Calcium concentration affects the mechanical properties of the scaffolds. It was reported that with increasing  $\text{CaCO}_3$  concentration in the scaffolds, the maximum tensile stress increased.<sup>6</sup> However, obtaining hydrogels with higher amounts of calcium (>5 wt%) represents a great challenge.<sup>68</sup> Calcium ions play an important role in tissue regeneration because they are involved in cell signaling. They are involved in angiogenesis, differentiation, keratinocytes, fibroblasts, and different extracellular matrix proteins synthesis. The average calcium concentration of a healthy human varies between 2.1 and 2.6 mM. Following, extracellular calcium

ions at concentrations of 2.5 and 3.5 mM have been reported to affect cell migration, protein synthesis, metabolic activity, MMP activity, contractile capacity, and gene expression associated with wound healing.<sup>69</sup> On the other hand, lower  $\text{Ca}^{2+}$  concentrations (0.1 and 1.25 mM) showed faster and stronger contraction of the collagen matrix compared with the higher  $\text{Ca}^{2+}$  concentrations (2.5 and 3.5 mM).<sup>69</sup>



**Figure 8** “Egg-box” structure as a result of interaction between alginate G blocks and  $\text{Ca}^{2+}$ <sup>70</sup>

**Covalent crosslinking** gained interest in order to produce hydrogels with more stability and improved physical properties in general.<sup>7</sup> In order to covalently crosslink, two polymer chains have to be linked via their functional groups with different crosslinking agents such as polyethylene glycol (PEG) or glutaraldehyde.<sup>67</sup> The mechanical properties and swelling can be strongly influenced by the choice of the crosslinking agent, sometimes second molecules have been used to compensate for the loss of hydrophilic property after covalent crosslinking.<sup>7</sup> It has been reported that covalently crosslinked hydrogels exhibit elastic properties, while ionically crosslinked hydrogels exhibit plastic deformation due to their water loss.<sup>7,71</sup> However, covalently crosslinked hydrogels require many purification steps to obtain a product without toxicity.<sup>7</sup>

**Cell crosslinking** allows the alginate to be crosslinked without the use of crosslinking chemicals. The most widely studied adhesive peptide in the biomaterials field is the tri-amino acid sequence, arginine-glycine-aspartate, or “RGD”. RGD-modified alginate can be crosslinked with cells by a ligand-receptor reaction.<sup>7,16,67</sup> The arginyl-glycyl-aspartic acid sequence responsible for cell adhesion to the extracellular matrix; it is also involved in cell-cell interactions and cell differentiation and migration.<sup>72</sup> The addition of cells to RGD-modified alginate results in the

formation of a polymer network that does not have as high a strength as other crosslinking methods described, resulting in application limitations.<sup>16,67</sup>

**Free radical polymerization** is an alginate crosslinking method in which modified alginate chains (usually with methacrylates) are converted into a 3D polymer network and are enabled for radical polymerization. Covalent crosslinking occurs between methacrylate groups when initiated with UV light.<sup>67</sup> This method has many advantages due to the chemical used to modify alginate hydrogels.<sup>16,67</sup>

### 2.3.2. Applications

Due to its rheological properties alginate has various applications in biomedical, pharmaceutical, cosmetics and textile industries.<sup>73</sup> Alginate plays an important role as a thickening agent in pharmaceuticals and biomedical engineering. In pharmacy, it serves as a stabilizing agent and plays an important role in controlled release drugs. Subsequently, due to its low toxicity and biocompatibility, it is used as a component for materials used in 3D bioprinting for tissue engineering.<sup>16,67</sup> Traditional wound dressings such as gauze help with the prevention of the pathogen wound contact while keeping the wound dry which leads to secondary skin damages while taking the dressing off. However, modern wound dressings are designed to retain wound moisture as it speeds up the healing process.

In food industry thickening and gelling properties of alginate can be used in various food products such as syrups, marmalade, jam, condiments, etc. It can also be used as an additive in probiotics because of its possibility to encapsulate some strains of living cells of probiotics.<sup>73</sup> **Table 3** shows some of the alginate applications in various fields.

**Table 3** Alginate applications in various fields

Field	Applications
<b>Pharmacy</b>	<ul style="list-style-type: none"> <li>• Drug delivery<sup>7,67</sup></li> <li>• Protein delivery<sup>7</sup></li> </ul>
<b>Biomedicine</b>	<ul style="list-style-type: none"> <li>• Tissue engineering (wound dressings, bone regeneration, cartilage repair)<sup>7,16,67,73</sup></li> </ul>

---

	<ul style="list-style-type: none"> <li>• Cell culture (RDG-modified alginate serves as <i>in vitro</i> cell substrate)<sup>7</sup></li> </ul>
<b>Food industry</b>	<ul style="list-style-type: none"> <li>• Modifying food characteristics (water binding, coatings, emulsion stabilizer)<sup>73</sup></li> <li>• As additive in probiotics and prebiotics<sup>73</sup></li> <li>• Antioxidant activity<sup>73</sup></li> </ul>
<b>Textile and paper industry</b>	<ul style="list-style-type: none"> <li>• Stabilizer and thickener<sup>73</sup></li> </ul>

---

## 2.4. Polymers

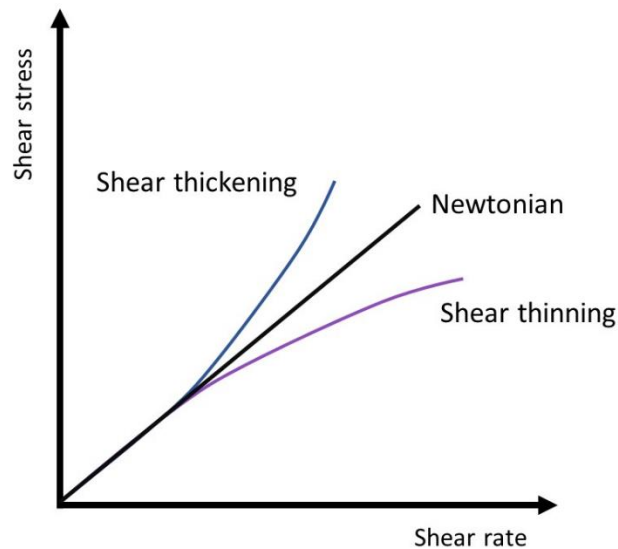
### 2.4.1. Chain conformation

The shape of each polymer chain is determined by the spatial arrangement of the atoms, and polymers by their own macromolecular nature have a very large number of possible structural spatial forms. They consist of a series of linked repeating units, and the position of the atoms in the molecule in the three-dimensional space which is determined by their molecular structure and the surrounding environment. After polymerization, a single molecular chain can adopt many different conformations which are statistically distributed, and which can change over time depending on chain flexibility. The conformation that polymer adopts depends on many factors like its molecular weight, chain flexibility, interactions with neighboring chains, temperature solvent conditions and concentration.<sup>74</sup> Understanding chain conformation and its time dependent behavior is a crucial in material science as it directly influences physical and mechanical properties of polymers and their applications.

### 2.4.2. Rheology

Due to their different properties resulting from the long chains, side branches and their entanglements, polymers are used as materials in various fields. For this reason, the characterization of their properties is of great interest. To get an insight into important properties of polymer, rheological tests can be performed. Rheological properties to consider for different applications include viscosity, viscoelasticity, flow behavior, temperature dependent behavior, etc.

The viscosity ( $\eta$ ) of a fluid is defined as a resistance to flow when pressure is applied and can be expressed as the ratio of shear stress ( $\tau$ ), versus shear rate ( $\dot{\gamma}$ ). There are different types of fluids, Newtonian, which show a linear relationship of shear stress and shear rate, and non-Newtonian fluids. Polymers in the melt or solution state are usually non-Newtonian fluids and show either shear-thickening behavior with an increase in viscosity while increasing shear stress or shear-thinning behavior with decrease in viscosity as shear stress increases (**Figure 9**).



**Figure 9** Flow curves of Newtonian and non-Newtonian fluids

Polymers, to be used as inks for extrusion-based 3D printing, need to meet certain mechanical properties including minimal viscosity for retaining its shape after printing and shear thinning behavior.<sup>75</sup> Without shear thinning it wouldn't be easily possible to extrude the ink through the nozzle because of its high viscosity. Further, a yield stress which is defined as certain stress above which the ink can flow and behave like a liquid, shouldn't be increased to the point of using higher extrusion pressure as it can negatively affect the cell viability in the printing process.<sup>75</sup>

Different polymers are often mixed together in order to obtain an ink with improved properties.<sup>76</sup> For example, alginate is a non-Newtonian fluid often used as a material for 3D printing due to its mechanical properties, low cost and rapid gelation.<sup>75</sup> However, 3D printed alginate has a low form fidelity and it is not stable in physiological conditions therefore it is often combined with different synthetic or natural polymer such as cellulose.<sup>6,67,76</sup>

### 2.4.3. Molecular mass distribution (MMD)

The property of polymer molecules that gives polymer materials special properties at production, processing, and application, compared to other classes of materials is their large molecular mass. While some natural polymers, such as proteins and nucleic acids have a clearly defined molecular mass, molecules of other natural polymers, such as polysaccharides and practically all synthetic polymers have oscillations in their molecular mass. They are referred to as polydisperse polymers and they exist as a distribution of molecular masses and chain lengths. Molecules of different sizes may be present in a material sample in varying proportions. For example, there may be a situation where two polymer samples with the same average molecular weight have completely different properties because they all have molecules of approximately the same size in one sample, and in the second sample there are many relatively small and large molecules.<sup>77</sup> In the first case, the polymer sample is said to have a narrow distribution, and in the second case, a broad MMD. Polymer's molecular mass has a big influence on its mechanical properties.<sup>78</sup> Polymers with narrow MMD tend to have higher modulus and strength, while polymers with broad MMD tend to have elastomeric properties such as low strength and large elongation at the break ( $E_b$ ).<sup>77</sup> When MM is  $>10^5$ ,  $E_b$  increases and rubbery behavior occurs.<sup>77</sup>

### 2.4.4. Charge complexes

Charge complexes in polymer chemistry refers to the association between polymers and oppositely charged species, resulting in the formation of complexes that exhibit unique properties and behaviors. These complexes are often form between polymers possessing ionizable groups referred as polyelectrolytes and oppositely charged species, such as ions, small molecules and other polymers.<sup>79</sup> The interaction between polymers and charged species can result in the formation of complexes through electrostatic attractions. These complexes can have various structures, including particle-like aggregates, coacervates, or even extended networks, depending on the polymer's nature, concentration, and the ionic strength of the solution.

An example of the polymer-polymer interaction that leads to the formation of the charge complexes with unique properties is the interaction between cellulose, alginate and calcium ions. These complexes have several applications such as hydrogels in tissue engineering<sup>15</sup>, drug delivery<sup>67</sup> and wound healing<sup>37</sup> due to their hydrogel formation, bioactive encapsulation due to their ability to

encapsulate bioactive molecules<sup>80</sup>, such as proteins which are usually sensitive to a harsh conditions, and biomaterial coatings.<sup>81</sup>

## 2.5. Direct ink writing

Direct ink writing (DIW) is an extrusion-based additive manufacturing (AM) process that allows a wide range of materials to be fabricated into desired 3D structures. Different materials in the form of inks can be extruded through small nozzle layer by layer until the software designed structure is obtained. Ink fabricated for DIW must meet certain requirements, one of the most important is rheological behavior. In order to maintain the shape fidelity of the filaments during printing, the shear thinning property and high yield stress (>200 Pa) as well as high storage modulus (>1000 Pa) of the ink play a crucial role in smooth ink flow through nozzle and in retaining the shape during printing.<sup>6,82</sup>

As mentioned above, the design of functional scaffolds for biomedical purposes must be taken into account, among other things, mechanical and structural properties corresponding to the replaced tissue, biocompatibility, and controlled biodegradability.<sup>83</sup> The mechanical and structural properties can be improved by proper design of the scaffold before printing. Following, the microstructure of the printed scaffold can be easily controlled when using the DIW process for manufacturing 3D structures as the shear flow created between the ink extruded by pressure and the walls of the nozzle results in fiber orientation and alignment of the printed material in the printing direction.<sup>6,84</sup> Fiber orientation plays an important role in mechanical properties of the scaffolds printed using anisotropic materials as it affects the tensile strength and the stiffness. For example, higher values of max. tensile strength have been reported for scaffolds with nanocellulose fibers aligned in the same direction as the loading stress.<sup>6,84,85</sup>

Advantages of DIW include cost efficiency, high material versatility as ink for printing (ceramics, metals, polymers, glass, cement, etc.), easy to use and low material consumption.<sup>82,86,87</sup>



### 3. EXPERIMENTAL SECTION

The following section describes materials and methods for the analysis of alginate nanocellulose hydrogels, as well as the optimization of these materials for imitating the blood vessels of the vascular systems and for skin/tissue engineering.

#### 3.1. Materials

NFC suspension (3 wt% solid content) was purchased from the University of Maine, USA. Sodium salt of alginic acid from brown algae, glucono- $\delta$ -lactone ( $\geq 99\%$ ), ethylenediaminetetraacetic acid disodium salt dihydrate, calcium chloride, DTAF, calconcarboxylic acid, cellulase from *Trichoderma viride*, celotetraose, celotriose, acetic acid, TRIS, potassium chloride, sodium phosphate dibasic dihydrate and sodium dihydrogen phosphate dihydrate were purchased from Sigma Aldrich, Austria. Calcium carbonate nanoparticles ( $\geq 99\%$ ) were purchased from Solvay Chemicals International, Belgium. Ethanol ( $\geq 99\%$ ), methanol and ammonium hydroxide were purchased from VWR Chemicals, Austria. Hydrochloric acid, sodium hydroxide and ethyl acetate were purchased from Fisher Scientific, Austria.

SmoothFlow tapered tips (410  $\mu\text{m}$ ), syringe barrel pistons, and fluid dispensing polyethylene-based plastic cartridges were purchased from Nordson, UK.

#### 3.2. Scaffold preparation and 3D printing

##### 3.2.1. Preparation of the ink for direct ink writing (DIW)

Ink for 3D printing was made by mixing 24.5 grams of NFC (3.0 w%) with 0.5 grams of distilled water and a specified amount of calcium carbonate in a 50 mL falcon tube using a custom-made 3D printed stirrer. Different inks were made with different calcium carbonate concentrations according to **Table 4**. After initial mixing at 2000 rpm for 60 seconds, 1.66 grams of alginic acid was added and mixed again at 2000 rpm for 10 to 15 minutes until visual homogeneity. Due to mixing, warm ink was let to cool down before printing for a few minutes or it was stored in a refrigerator at  $\approx 4^\circ\text{C}$  prior to use for maximum 6 hours.

The ink was stirred using a mechanical laboratory stirrer RZR 2005 (Heidolph, Germany) which was equipped with a 3D-printed UV resin stirrer printed with a resin 3D printer (Anycubic Photon Mono) that fits perfectly into 50 mL falcon tubes and was described already in detail in earlier work<sup>6,8</sup>.

**Table 4** Different inks used for 3D printing

<b>Ink</b>	<b>w% NFC (dry mass)</b>	<b>w% CaCO<sub>3</sub></b>	<b>w% Alg</b>	<b>w% H<sub>2</sub>O</b>
	[%]	[%]	[w%]	[w%]
<b>LOW</b>	2.37	0.30	6.21	91.12
<b>MEDIUM</b>	2.35	1.12	6.16	90.07
<b>HIGH</b>	2.29	3.30	6.02	88.39

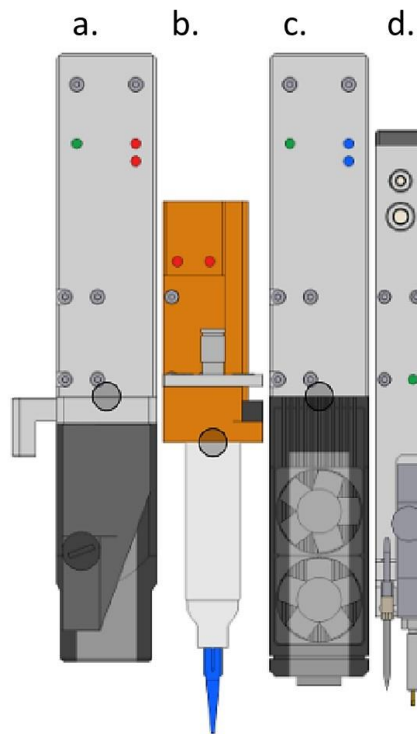
### 3.2.2. General printer and software description

GeSiM BioScaffolder 3.2. (GeSim, Germany) shown in **Figure 10**, using a computer-controlled extrusion cartridge, prints highly viscous bio ink layer by layer. A printer step width accuracy is  $\pm 2 \mu\text{m}$  in x or y and  $\pm 10 \mu\text{m}$  in z direction. It features four independent z-axes (**Figure 11**), three of them for cartridge extruding for simultaneous printing with different materials which allows printing different materials without changing cartridges. The fourth z-axis is reserved for the piezoelectric pipetting system and/or z-sensor for measuring printing point height. At the base of the cartridge dispenser (30 mL, Nordson, UK) tapered tips (Nordson, UK Limited) were attached with an inner diameter of  $410 \mu\text{m}$ .

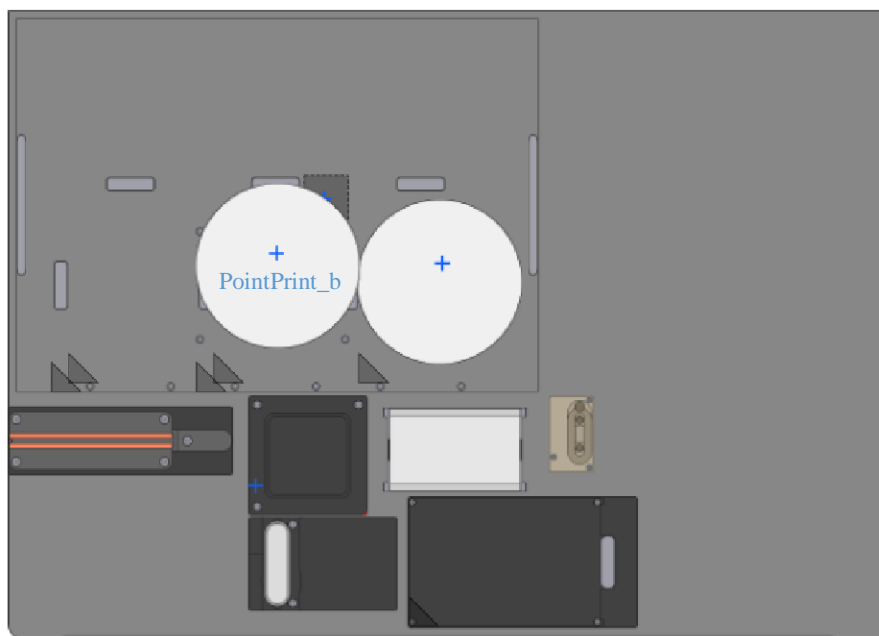
There are three main segments in GeSiM Robotic software: Configuration, Manual, and Scaffold in which configuration of the 3D printer and different printing parameters, such as angles between layers, strand width/height, pressure, infill offset/distance, z-offset, printing point, position (x, y, and z), etc. can be set and/or adjusted later. During printing, it is only possible to adjust the pressure and height of the printing nozzle. The scaffold segment offers the possibility to design simple rotation symmetric scaffold shapes. However, for more complex scaffolds 3D Builder 18.0.1931.0 (Microsoft Corporation) was used and imported to the software as a 3MF file. Clicking on the “Generate G code” software will calculate the time and material required for the printing process.



**Figure 10** GeSiM BioScaffolder 3.2. (GeSim, Germany)



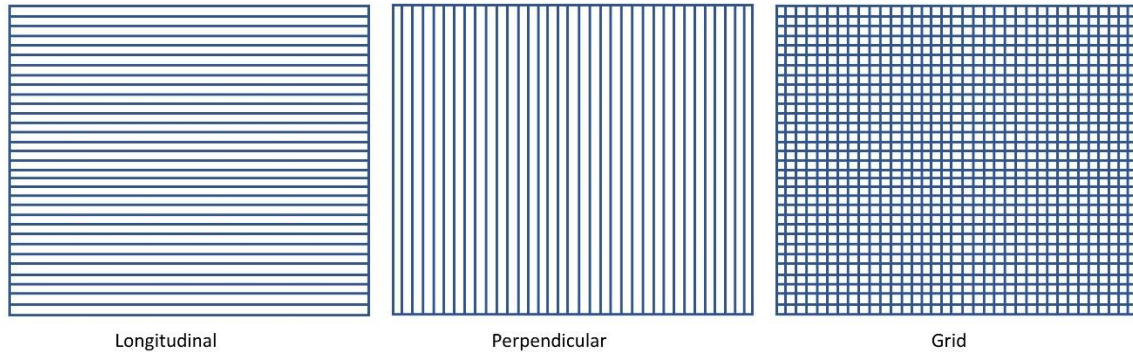
**Figure 11** Used printhead with 4 different axis. Axis 7 which features Internal Heating (a.), Axis 5 with cartridge dispenser (50 mL) and plastic nozzle (410  $\mu\text{m}$ ) (b.), Axis 3 that features Internal Cooler (c.) and Axis 1 (Piezo Pipette Nano, Z-sensor) (d.)



**Figure 12** Target tray with the petri dish selected for printing (PointPrint\_b)

### 3.2.3. 3D printing process

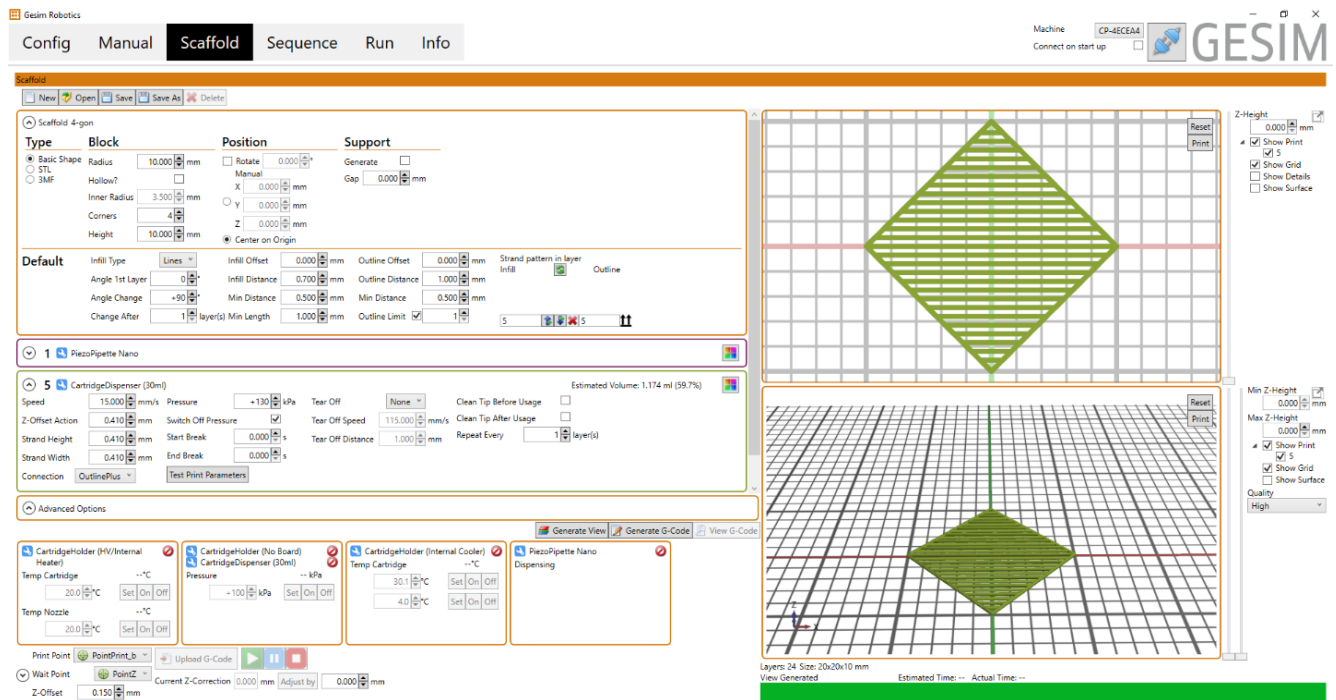
Different shapes of scaffolds (shown in **Table 5**) were printed using a GeSiM Robotics BioScaffolder 3.2 (GeSim, Germany) (**Figure 10**) with its included software. Cartridges (30 mL) with cartridge stoppers previously put in to eliminate air entrapment, were filled approximately to  $\frac{3}{4}$  with appropriate ink using a 10 ml syringe. Following, a 41 mm nozzle was attached, and the cartridge was ready to be installed to the printer axis. The shear forces forcing the ink through a small nozzle affect the fiber alignment in the printed scaffold in such a way that they are aligned with the direction axis of printing. Therefore, sheet scaffolds (**Table 5**) were printed in different orientations regarding fiber alignment; longitudinal, perpendicular, and grid alignment as shown in **Figure 13**. To get grid alignment, the print angle must be changed  $90^\circ$  at each layer. Different inks were printed with extrusion pressure that varies from 115 to 165 kPa depending on the printing speed (between 10 and 25 mm/s) with strand distance of 0.50 mm, strand height, and width of 0.44 mm onto polystyrene petri dishes and subjected to crosslinking described in the next passage.



**Figure 13** Different fiber alignment in scaffolds

**Table 5** Printing parameters for DIW (\*different layered scaffolds were printed for different tests)

	<b>Dimensions (l x w x h) [mm]</b>	<b>Printing speed [mm/s]</b>	<b>Printing pressure [KPa]</b>	<b>Nozzle diameter [mm]</b>	<b>Test</b>
<b>Sheet</b>	56 x 15 x 2	25	150-170	41	Leaching process/tensile tests
<b>Disks</b>	29 x 29 x 2	10	140-160	41	Cell viability test
<b>Disks</b>	74 x 78 x 1/2/3*	25	150-160	41	Diffusion test



**Figure 14** General settings for printing sheet scaffold

### 3.2.4. Crosslinking process

After printing the fresh scaffolds were put in crosslinking solution for 24h for solidification via ionic crosslinking. The solution was prepared freshly prior to use, containing a mixture of 50% w/w of EtOH and H<sub>2</sub>O with 4 molar equivalents (regarding CaCO<sub>3</sub>) of GDL dissolved in this solution. Per sample, 25 g of crosslinking solution (approximately 10 fold of the mass) was added to each petri dish, which was enough to cover the printed scaffolds. Scaffolds were gently shaken during the crosslinking process with a Unimax 2010 (Heidolf, Germany). After 24 hours scaffolds showed some shrinkage, no visible breaking, and were stable enough to be further processed. After crosslinking, scaffolds were patted dry and measured (height, width, and thickness) using a caliper and thickness measuring device (Digital Thickness Gauge 0-12.7mm/0.5") and they were ready for immediate tensile tests or could be further stored in a specific storage solution to investigate the calcium leaching process. The crosslinking solution was sampled for later titration to determine the amount of calcium ions left in the solution.



**Figure 15** Scaffold after crosslinking

### 3.2.5. Leaching process

Different storage solutions with varying concentrations of  $\text{CaCl}_2$  (**Table 6**) and 0.9 w% NaCl were prepared in order to investigate the calcium leaching process in scaffolds printed using **Medium ink** (described in **Table 4**), longitudinal scaffolds were printed as well as some of the perpendicular ones for comparison. After the scaffolds were stored in the crosslinking solutions for 24 hours under gentle shaking, the crosslinking solution was replaced with the corresponding storage solution and further shaken for 24 hours.

**Table 6** Storage solutions components

<b>Solution</b>	<b>c (<math>\text{CaCl}_2</math>) [mM]</b>	<b>w% (NaCl)</b>
<b>LOW <math>\text{Ca}^{2+}</math></b>	0,833	0.90
<b>MEDIUM <math>\text{Ca}^{2+}</math></b>	2.500	0.90
<b>HIGH <math>\text{Ca}^{2+}</math></b>	7.500	0.90

Scaffolds in storage solutions were gently shaken on Unimax 2010 (Heidolf, Germany). Storage solutions were exchanged five times, each after 24 hours and each solution was sampled in a falcon tube for volumetric titration to determine the amount of calcium ion leached.

### 3.2.6. Scaffold preparation for cell viability test

Preparation of the scaffold for cell viability tests differs slightly from the described process in such a way that the product must be as sterile as possible. Three different inks were made for printing that differ in the amount of calcium carbonate (**Low** 0.3 w%, **Medium** 1.12 w%, and **High** 3.3 w%) they contain as described in 3.2.1. After printing and crosslinking of the scaffolds according

to 3.2.3 and 3.2.4 they were put in a storage solution previously autoclaved using CertoClav MultiControl 2 at 121°C for 30 minutes. The sterile storage solutions also differ slightly in the amount of calcium chloride (CaCl<sub>2</sub>) as the **Low** calcium concentration solution contained 0,5 mM CaCl<sub>2</sub>, the **Medium** contained 0.9 mM of CaCl<sub>2</sub>, and the **High** calcium concentration one contained 7.5 mM of CaCl<sub>2</sub>. Storage solutions were exchanged five times, each after approximately 24 hours, and every storage solution was autoclaved at 121°C for 30 minutes before adding the scaffold. After the whole leaching process was done scaffolds were punched out into small discs (6 mm) using the metal hole punch tool shown in **Figure 16**, they were put back in the fifth leaching solution and autoclaved all together at 125°C for 10-15 minutes. After that samples were ready for cell viability tests. All autoclavation steps were done together with indicator stripes to prove successful autoclaving.

**Table 7** Calcium concentration in the ink and storage solution for Low, Medium, and High inks used for printing disks for cell viability testing

<b>INK</b>	<b>w% CaCO<sub>3</sub> in the ink [%]</b>	<b>CaCl<sub>2</sub> in storage solution [mM]</b>
<b>Low</b>	0.30	0.5
<b>Medium</b>	1.12	2.5
<b>High</b>	3.30	7.5



**Figure 16** Hole punching tool



### **3.3. Analytic methods**

#### **3.3.1. Swelling/shrinking tests**

Length, width, thickness, and mass of the printed scaffolds were measured using a caliper and thickness measuring device (Digital Thickness Gauge 0-12.7mm/0.5") after crosslinking, after the first leaching process, and at the end of the leaching process. For scaffolds after printing only mass was measured as the length, width, and thickness can be set in the printing process. Based on that, swelling/shrinking percentages were calculated as shown in following equation.

$$\text{swelling/shrinking}\% = \frac{\text{final size} - \text{original size}}{\text{original size}} * 100$$

#### **3.3.2. Calcium titrations**

Calcium titrations were done to determine the amount of calcium that was leached/absorbed from/by the scaffolds in crosslinking and leaching steps of the scaffold preparation as well as the amount of calcium left in the scaffold at the end of mentioned processes.

##### **3.3.2.1. Crosslinking solution**

The whole crosslinking solution was acidified with 1 mL of 37 w% HCl, transferred to a round bottom flask, and the ethanol was removed under vacuum. The remaining solution was transferred to a 100 mL measuring flask and an aliquot volume of 5-20 mL (depending on the starting calcium concentration) was brought to pH 12 using 40 w% NaOH. After cooling down to room temperature MgCl<sub>2</sub> was added as well as calconcarboxylic acid as an indicator and the solution was titrated with 2.00 mM EDTA solution from pale red to pale blue color.

##### **3.3.2.2. Storage solution**

The whole storage solution was acidified with 1 mL of 37 w% HCl, transferred to a measuring flask which was filled to the mark with distilled water. The aliquot volume of 5 to 10 mL was

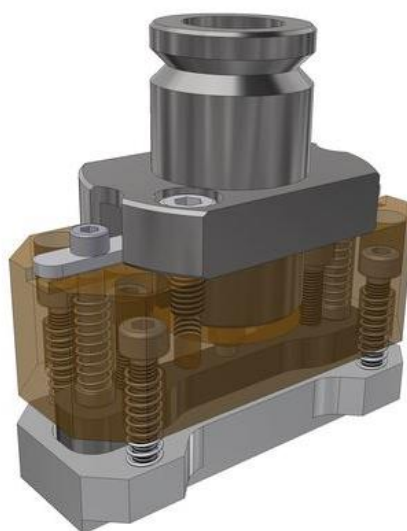
brought to pH 12 using 40 w% NaOH. The solution was ready for titration with 2.00 mM EDTA after adding  $MgCl_2$  and calconcarboxylic acid as an indicator.

### 3.3.2.3. Scaffolds

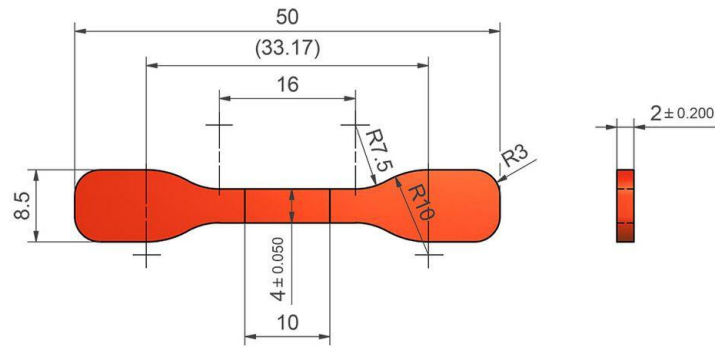
To determine the amount of calcium left in the scaffold calcium titrations were performed. Printed, crosslinked, and weighed scaffold was dissolved in 10 mL  $H_2SO_4$  (conc.), and 0.5 mL of a 30 w%  $H_2O_2$  solution was added. The solution was put on Heidolph MR Hei-Tec magnetic stirrer at  $80^\circ C$  for 30 minutes. To reduce the remaining  $H_2O_2$  2.0 g  $Na_2SO_4$  was added, and the remaining clear pale-yellow solution was transferred to a 50 mL measuring flask. After the solution was cooled down an aliquot volume of 5-10 ml (depending on the starting calcium concentration in the scaffold) was brought to pH 12 using 40 w% NaOH.  $MgCl_2$  was added as well as calconcarboxylic acid as an indicator and the solution was titrated with 2.00 mM EDTA solution from pale red to pale blue color.

### 3.3.3. Tensile and cycle tests

Crosslinked and calcium leached scaffolds were punched out using Q-tec punching knife DIN 53504 S3A (*Figure 17*) and manual toggle press RS PRO 254850. Dimensions of the punched-out specimens were 50 x 8.5 x t (thickness differed in each scaffold) as shown in *Figure 18*.



**Figure 17** Q-tec punching knife DIN 53504 S3A used to punch out scaffolds for tensile testing<sup>88</sup>



**Figure 18** Dimensions of the punched out scaffold ready for tensile testing according to DIN 53504 S3A<sup>88</sup>

All specimens were padded dry before testing and tested on the SHIMADZU AUTOGRAPH AGS-X 5 kN. Different speeds and strain percentages were used depending on the type of testing performed. Tensile testing was performed with a speed of 50 mm/min and cycle tests with four different speeds; 5, 10, 50, and 200 mm/min. Also, for cycle tests different strain percentages were selected, 5, 10, and 25% and each scaffold was tested with 10 cycles. Tensile modulus was calculated using the following (Young's modulus) equation,

$$E = \frac{\sigma}{\varepsilon}$$

where,

E is tensile modulus (Young's modulus),

$\sigma$  is tensile stress and

$\varepsilon$  is axial strain.

All samples were tested in quadruplicates and the standard deviation was calculated from measured values.

### 3.3.4. Light microscopy

Calcium and NFC distribution as well as homogeneity of developed ink was studied using light microscopy using a Panthera TEC MAT BD-T (Motic, China) (**Figure 19**). Different samples were tested, with and without calcium.

Samples include:

- a. standard printing ink (NFC, CaCO<sub>3</sub>, Alg and H<sub>2</sub>O),
- b. standard printing ink without CaCO<sub>3</sub> (NFC, Alg and H<sub>2</sub>O)
- c. standard printing ink without Alg (NFC, CaCO<sub>3</sub> and H<sub>2</sub>O)
- d. pure NFC

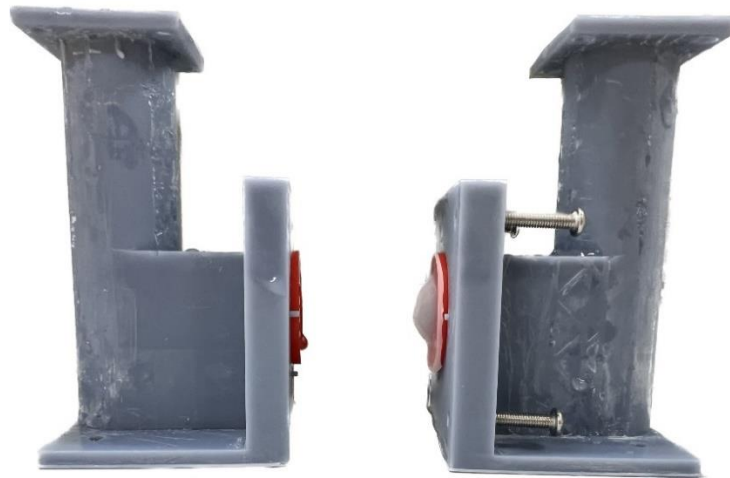
After mixing very well small amounts of samples were placed on a microscope slide, as thin as possible for light to get through the samples and it was covered with cover a slide to prevent the samples from drying.



**Figure 19** Motic: Panthera TEC MAT BD-T (6x4), microscope with Epi-LED fluorescence attachment<sup>89</sup>

### 3.3.5. Diffusion tests

To test the permeability, diffusion tests were done using different membranes that were put in between two cells printed with a resin 3D printer (Anycubic Photon Mono) shown in **Figure 20**. Membranes used for tests include the ZelluTrans membrane (Dialysis membrane ZelluTrans/ROTH T4: MWCO 12000-14000) and our 3D printed membranes (1, 2, and 3 layered). Permeability was tested using different molecules and ions. Sodium chloride, calcium chloride, glucose, dextran (20 000 Da), BSA, and riboflavin (vitamin B<sub>2</sub>) were used. A defined concentration of substance was added in one side of the cell, sampled at specific timespans, and measured depending on the sample which is described in the following sections.



**Figure 20** Diffusion cell

#### 3.3.5.1. Calibrations

Before starting the diffusion test calibration for each substance was made. A series of dilutions were made for each substance, and it was measured using corresponding measurements to get a calibration curve. Using a linear or cubic fitting curves a regression coefficient of minimum  $R^2 \geq xy$  could be used for the calculation.

#### 3.3.5.2. Sodium and calcium chloride

For both sodium and calcium chloride 1.7 M solution was used. Exactly, 1 mL of solution was pipetted in the left side of the cell, already containing 10 mL of MilliQ water, while in the right

side, containing 11 ml of MilliQ water. The conductivity sensor was placed into the low concentration side(right). Conductivity was measured every 10 seconds until equilibrium was reached for a minimum of 24 hours using METTLER TOLEDO S213 SevenCompact Duo pH/Conductivity with METTLER TOLEDO Conductivity probe InLab 731-ISM. From collected data, flux (J) and diffusion coefficient (D) were calculated.

#### **3.3.5.3. Riboflavin**

To 10 mL of 0.1 M ammonium buffer containing 0.05 M CaCl<sub>2</sub> in the left side of the diffusion cell, 150 µL of 0.133 mM riboflavin solution was added while in the left side, also containing 10 mL 0.1 M ammonium buffer containing 0,05 M CaCl<sub>2</sub>, 150 µL same buffer was added. Samples of 200 µL were collected from the left and right side of the diffusion cell until the equilibrium was reached. For analytics, they were put in a well plate and fluorescence was measured using Tecan Spark te-cool multimode microplate reader. Fluorescence was measured with excitation 445 nm, excitation bandwidth 10 nm, emission 550 nm, emission bandwidth 10 nm, and gain set to 50. Flux and diffusion coefficients were calculated from the measured data.

#### **3.3.5.4. Dextran (20 000 Da)**

Before diffusion tests, dextran was labeled using fluorescein isothiocyanate isomer 1 (FITC) to be able to detect fluorescence signals. The fluorescein reagent (27.7 mg) dissolved in DMSO (1 mL) was added to a solution of dextran (500 mg) in distilled water (15 mL) which was brought to pH 10 using 0.01 M NaOH prior addition of the dye. For pH measurements METTLER TOLEDO S213 SevenCompact Duo pH/Conductivity with METTLER TOLEDO pH electrode InLab Expert Pro-ISM. After two hours, the FITC-dextran was precipitated with ethanol, filtered, and dried. The purification step was repeated x times. To prepare a solution for the diffusion test, 20 mg of dried FITC-dextran was dissolved in 20 mL of distilled water. To 10 mL of 0.1 M ammonium buffer containing 0,05 M CaCl<sub>2</sub> in the left side of the diffusion cell, 5 mL of FITC-dextran solution was added while in the left side, 15 mL of 0.1 M ammonium buffer containing 0,05 M CaCl<sub>2</sub> was added. Samples (200 µL) were collected from the left and right side of the diffusion cell for x hours. Samples were transferred into the well plate and fluorescence was measured using Tecan Spark te-cool multimode microplate reader. Fluorescence was measured with excitation 491 nm, excitation bandwidth 10 nm, emission 525 nm, emission bandwidth 10 nm and gain set to 50.

### 3.3.5.5. Bovine serum albumin (BSA)

To 13 mL of 0.1 M ammonium buffer containing 0,05 M CaCl<sub>2</sub> in the left side of the diffusion cell, 1 mL of 2.12 mmol/L BSA solution was added while in the left side, also containing 13 mL 0.1 M ammonium buffer and 0,05 M CaCl<sub>2</sub>, 1 mL of same buffer was added. Samples (300 µL) were collected from left as well as the right side of the diffusion cell until the equilibrium was reached. To prepare the samples for absorbance measurement, Pierce™ BCA Protein Assay Kit from ThermoFisher Scientific was used according to the manufacturer. Samples were placed in a well plate and absorbance was measured using Tecan Spark te-cool multimode microplate reader at 562 nm.

### 3.3.5.6. Glucose

To get a 0.5 w% glucose solution in the left side of the diffusion cell, 14 mL of 0.1 M ammonium buffer containing 0,05 M CaCl<sub>2</sub> was spiked with 1.0 ml of 7.5 w% glucose solution, while in the right side of the cell, 15 ml of the same buffer was added. Samples (0.5 mL) were collected from left as well as the right side of the diffusion cell until the equilibrium was reached. The refractive index (RI) of the samples was then measured using Anton Paar Abbemat 550 Refractometer. From the collected data, flux and diffusion coefficients were calculated.

### 3.3.5.7. Calculations

To calculate the flux, Fick's Law of diffusion was used shown in the following equation<sup>90</sup>,

$$J = \frac{N}{A} = \frac{n}{A * t}$$

where:

J is the flux, [mol\*m<sup>2</sup>/s]

N is the rate of mass transfer of components, [mol/s]

A is the area across which mass transfer [m<sup>2</sup>]

occurs and

x is the distance. [m]

In this work, it was assumed that distance (x) was constant. Therefore, it was measured before the diffusion process using a thickness measuring device (Digital Thickness Gauge 0-12.7mm/0.5”) and that value was considered as a distance.

When flux and the change in the concentration over time were known, then the diffusion coefficient was calculated also using Fick’s Law:

$$J = -D \times \frac{dc}{dx}$$

From which diffusion coefficient is equal to:

$$D = \frac{-J \times dx}{dc}$$

where:

D is the diffusion coefficient and [m<sup>2</sup>/s]

c is concentration [mol/L]

The final equation used for the diffusion coefficient calculation is shown below. The time point at which was calculated was 8 hours after starting the diffusion process.

$$D = \frac{1}{2} \ln \left[ \frac{c_{up}}{c_{up} - 2c_{down}} \right] \left[ \frac{V_{down} \times h}{A \times t} \right]$$

### 3.3.6. Cell viability tests

Scaffold samples were sent to Institute for Biomedical Research and Technologies, Graz for cell viability tests where transwell cytotoxicity tests were performed to determine whether the scaffolds release any cytotoxic substances that adversely affect the cells. Cells were separated from the scaffold discs with a semipermeable membrane to avoid direct contact.

HEK293 cells were cultured in Dulbecco's Modified Eagle Medium/Nutrient Mixture F-12 (DMEM/F12, Thermo Fisher Scientific (Gibco), MA, USA) containing 1% penicillin/streptomycin (P/S, Thermo Fisher Scientific (Gibco)) and 10% fetal bovine serum (Thermo Fisher Scientific (Gibco)). Primary HUVECS (Promocell, Heidelberg, Germany) were cultured in endothelial cell growth media (Promocell, Heidelberg, Germany) supplemented with 1 % P/S. A monolayer culture



of each cell type was seeded on the bottom of a 24-well plate ( $4 \times 10^4$  cells/well) and grown until reaching a confluency of at least 60 – 70%.

After an incubation period of 48 hours, percentage of surviving cells was quantified by using the PrestoBlue™ cell viability reagent (MolecularProbes by life technologies™, CA, USA). Absorbance is measured at 570/600 nm (excitation/emission) using a SpectraMax® iD3 plate reader (MolecularDevices, CA, USA). Three independent experiments were performed. Cells without the addition of a scaffold were used as negative controls and indicated as 100% viable.

### 3.3.7. Degradation process

#### 3.3.7.1. Solutions

Briefly, 300 mg of tubular printed and crosslinked scaffold was cut and used throughout all degradation tests. That corresponds to 0.033 mmol of calcium remaining in the scaffold. All solutions were prepared and diluted with 0.9 w% NaCl to reach a 4-molar excess regarding the used calcium amount. **Table 8** shows the composition and concentration of the substances used to make solutions for the degradation process. In parallel, all solutions were tested separately (**Table 8**) containing an additionally 100 mg of CaCl<sub>2</sub> for stabilization.

Solutions with scaffolds were shaken on Unimax 2010 (Heidolf, Germany) and pictures were taken immediately after putting them in solutions for comparison. Following that pictures were taken after 6 hours, 24 hours, and after 1 week.

**Table 8** Solutions used for scaffold degradation process (pH values were set using 0,1 M NaOH)

	Substance	Concentration [g/L]	pH
<b>PBS</b>	Na <sub>2</sub> HPO <sub>4</sub>	5.76	7.00
	NaH <sub>2</sub> PO <sub>4</sub>	0.98	
	KCl	0.80	
	NaCl	9.0	
<b>TRIS</b>	TRIS	4.84	5.51
	NaCl	9.0	
<b>NaCl</b>	NaCl	9.0	6.22

<b>EDTA</b>	EDTA	3.27	7.00
<b>Citric acid</b>	Citric acid	2.27	4.50 and 7.00
<b>HCl</b>	HCl	0.365	1.15
<b>NaOH</b>	NaOH	0.399	13.41

### 3.3.7.2. Cellulase

Different degradation experiments were done using cellulase enzyme isolated from *Trichoderma viride*. Firstly, 500 mg of the scaffold was put in a round bottom flask in 4 molar equivalents of EDTA solution whose pH was previously brought to 9. Meaning, if 500 mg of the scaffold contains 0.055 mmol of calcium, that's 0.22 mmol of EDTA needed for the solution (15 mL). When a blurry solution occurred (scaffold structure was degraded), it was diluted to 100 mL and 15 mg of cellulase was added and put in a water bath at 35°C until the solution was completely clear. It was then put on Hei-VAP Core rotavapor with Hei-VAC Valve Control pump at 40°C, 150 rpm, and 72 mbar until the water evaporates completely. To the remaining solids, 20 mL of methanol was added, filtered through a glass filter (filtrate - S1 sample) and put on rotavapor at 40° C, 150 rpm and 330 mbar. The same procedure was done afterwards with ethanol as a solvent instead of methanol (filtrate - S2 sample), and put on rotavapor at 40° C, 150 rpm, and 115 mbar.

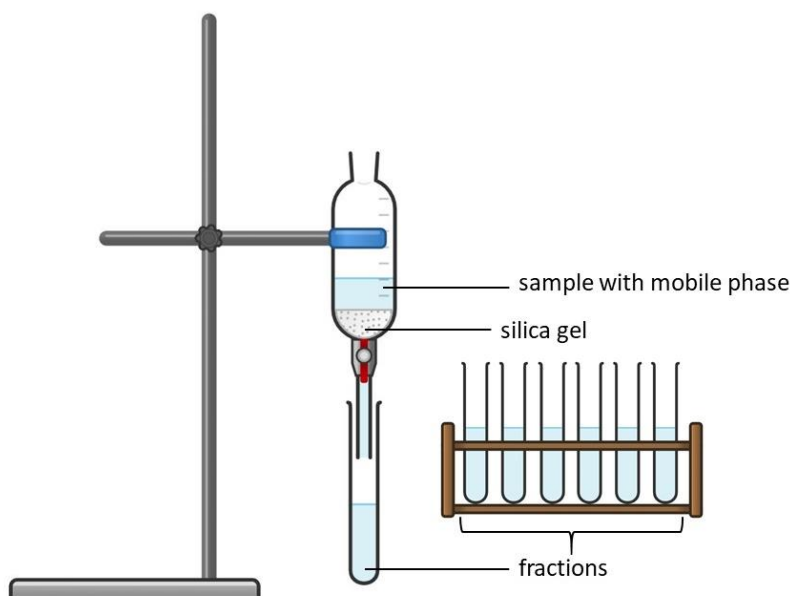
#### 3.3.7.2.1. Thin layer chromatography

The product was tested using thin layer chromatography (TLC). The samples (product, S1, S2-solid residue from S1, S3 and S4-solid residue from S3, as well as glucose and EDTA as a reference) were applied to the pre-coated TLC-sheets ALUGRAM SIL G/UV254 and put in ethyl acetate–acetic acid–methanol–water (2.5:1:1:0.5) mobile phase.

#### 3.3.7.2.2. Column chromatography

To separate the product from EDTA, column chromatography was performed. The columns were plugged with cotton to prevent loss of the stationary phase out the bottom. As the stationary phase, a silica gel (SiO<sub>2</sub>) was placed in a column and for the mobile phase, ethyl acetate–acetic acid–methanol–water (2.5:1:1:0.5) was used and pushed down through the column by gravity and external pressure. Fraction size of 3 mL were taken. Fractions were then tested with TLC the same

way it was described previously. Samples suspected of containing glucose were combined and subjected to NMR testing.



**Figure 21** Schematic illustration of column chromatography technique

### 3.3.7.2.3. NMR

To determine if the scaffold sample after cellulase degradation process contains only glucose,  $^1\text{H}$ -NMR test was performed on Bruker 300 MHz NMR spectrometer. As a solvent  $\text{D}_2\text{O}$  was used, 0.0464 grams of the sample was dissolved in 0.7 mL  $\text{D}_2\text{O}$ . As a reference, 0.0211 grams of glucose was dissolved in 0.8 mL  $\text{D}_2\text{O}$ .

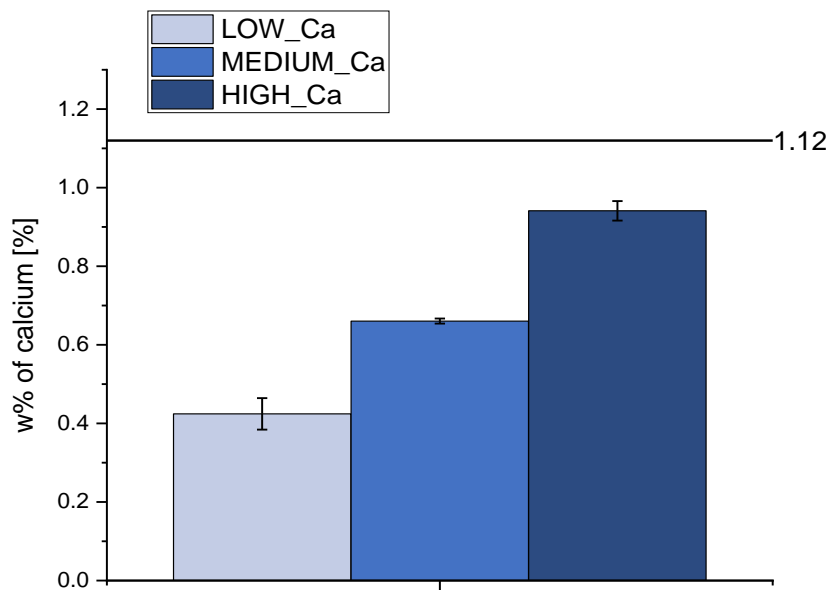
## 4. RESULTS AND DISCUSSION

### 4.1. Calcium Leaching and Leaching Kinetics

#### 4.1.1. Rectangular shaped scaffolds

Since it has been proven that storage media, as well as the calcium concentration in scaffolds can effect mechanical properties of the scaffolds themselves<sup>6</sup> different storage solutions with varying concentration of CaCl<sub>2</sub> (described in 3.2.5 and **Table 6**) and 0.9 w% NaCl were tested in order investigate the calcium leaching process in scaffolds printed using **Medium** ink (described in **Table 4**). As **Figure 22** shows, after the whole leaching process consisting of five complete media changes (cycles), it was determined that in scaffolds that were leached in **LOW Ca<sup>2+</sup>** storage solution  $37.82 \pm 2.65$  % of the calcium remained. This results in a new calcium weight concentration in the scaffolds with  $0.42 \pm 0.03$  % and  $11.57 \pm 1.45$  % of the scaffolds mass was lost during the process. Scaffolds stored in **MEDIUM Ca<sup>2+</sup>** could retain  $58.87 \pm 3.66$  % of the initially added calcium after, while  $26.41 \pm 4.28$  % of mass was lost, which results in  $0.66 \pm 0.04$  % Ca in the scaffold after leaching. As for scaffolds stored in **HIGH Ca<sup>2+</sup>**,  $83.89 \pm 1.04$  % of calcium remained in scaffold, a significant amount of  $44.95 \pm 0.62$  % of scaffold mass was lost and w% of calcium resulted in  $0.94 \pm 0.01$  %.

Also, longitudinal, and perpendicular printed scaffold stored in **MEDIUM Ca<sup>2+</sup>** solutions were compared during this process and no differences were observed. Perpendicular fiber alignment scaffold remained  $58.93 \pm 0.02$  % of calcium, mass loss was  $28.85 \pm 0.47$  % and new w% of the calcium in scaffold was  $0.66 \pm 0.01$  % which is equal within the standard deviation to the longitudinal ones.



**Figure 22** Remaining w% of calcium in the scaffolds leached in different leaching solutions at the end of the leaching process after five cycles. Line indicated the starting amount of calcium.

#### 4.1.2. Disks for cell viability

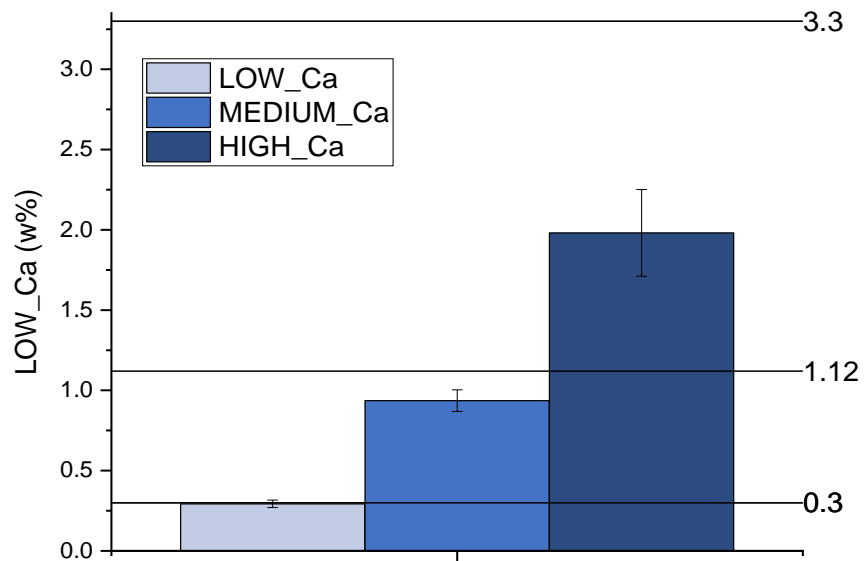
After medium ink was tested in different storage solutions for calcium leaching, different inks were made with different concentrations of  $\text{CaCO}_3$  (**Table 4**) to determine the difference of the amount of calcium leached for each ink. Starting already from an ink with a similar calcium concentration as in the storage solution should lead to a reduced number of leaching cycles and reduced calcium leaching until equilibrium.

As shown in **Figure 23**, scaffolds that were printed using **LOW** ink and leached in **LOW**  $\text{Ca}^{2+}$  solution retained  $97.65 \pm 7.79$  % of calcium after the whole leaching process, their mass even increased by  $17.41 \pm 2.79$  % with a resulting weight percent of the calcium in the scaffold of  $0.29 \pm 0.02$  w%. The ones printed with **MEDIUM** ink and leached in **MEDIUM**  $\text{Ca}^{2+}$  showed already more leaching with  $83.55 \pm 5.99$  % of the initial calcium, while the mass decreased by  $27.01 \pm 1.99$  %. This results finally in w%  $0.93 \pm 0.07$  w% after five leaching cycles. **HIGH** ink scaffolds leached in **HIGH**  $\text{Ca}^{2+}$  showed the most pronounced leaching with  $60.04 \pm 8.18$  % of the calcium remaining from the beginning of the leaching process, mass loss was  $49.57 \pm 1.11$  % and end w% was  $1.98 \pm 0.27$  %. Comparing the results of **LOW** and **MEDIUM** inks with the ones in previous

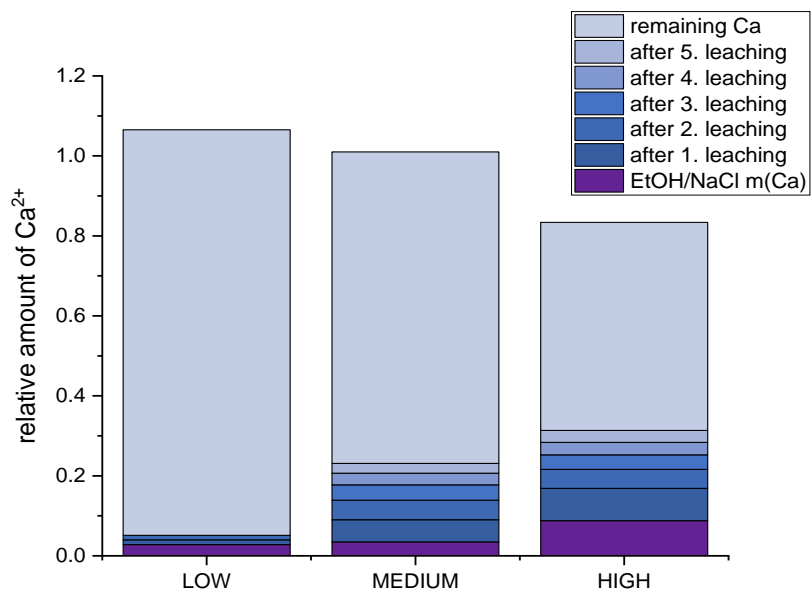
passage where only **MEDIUM** ink was used, it was noticed that different concentrations of calcium in leaching solutions with appropriate concentrations of calcium in the inks affects the leaching process in such way that less amount of calcium is leached. However, the higher the initial concentration of calcium in the ink is the more pronounced is the leaching. This process might be suppressed or reduced by even higher calcium concentrations in the storage solution.

Looking in more detail at the leaching of each complete media change in **Figure 24**, it was noticed that different amounts of calcium are leaching at every leaching step.

At the crosslinking step in EtOH/H<sub>2</sub>O, for **LOW/LOW Ca<sup>2+</sup>** 2.8223 ± 1.9225 % of calcium was leached, for **MEDIUM/MEDIUM Ca<sup>2+</sup>** it was 3.5033 ± 0.11809 % and for **HIGH/HIGH Ca<sup>2+</sup>** 8.7940 ± 0.5152 % of calcium was leached. This trend of more pronounced leaching for higher calcium starting concentrations also remains for the leaching in the different storage solutions for example in the first leaching step, 4.82 % for **LOW/LOW Ca<sup>2+</sup>**, 22.31 % for **MEDIUM/MEDIUM Ca<sup>2+</sup>** and 32.29 % for **HIGH/HIGH Ca<sup>2+</sup>** calcium was leached. Throughout the five leaching cycles less calcium was lost at each leaching step. For the **LOW/LOW Ca<sup>2+</sup>**, case the leaching after the amounts were below our limit of detection after the second cycle. Also, for **MEDIUM/MEDIUM Ca<sup>2+</sup>** and **HIGH/HIGH Ca<sup>2+</sup>** the relative amounts reduced to 9.88 % and 11.87 % for the fifth cycle to more than half in both cases. This indicates that with increasing number of cycles the equilibrium of calcium within the scaffold and the storage solution is reached.



**Figure 23** Changes in w% of calcium in the different scaffolds (regarding different ink concentration) leached in different leaching solutions at the end of the leaching process after five cycles.



**Figure 24** Amount of calcium leached into the crosslinking solution and storage solutions in 24 hours for each solution for LOW, MEDIUM and HIGH inks leached in LOW  $\text{Ca}^{2+}$ , MEDIUM  $\text{Ca}^{2+}$  and HIGH  $\text{Ca}^{2+}$  storage solutions.

## 4.2. Shrinking/swelling of the scaffolds

The mechanical property of the biomaterial is greatly influenced by swelling of the fiber networks<sup>91</sup> also the swelling property of the biomaterial is important for nutrient diffusion<sup>92</sup>. It was proven that the rate of epithelization is twice as high while using moist dressing compared to dry ones<sup>93</sup>. Important to mention, risk of infection does not increase in moist environment compared to dry methods of wound healing<sup>94</sup>. It can be said that moist environment is attainable by desired swelling capacity of the scaffold therefore it mimics natural tissue. On the other hand, structural shrinkage are assumed to play a role in the structural stabilization<sup>6</sup>. Therefore, swelling and shrinking percentages were calculated as described in heading 3.3.1.

After crosslinking in EtOH/H<sub>2</sub>O all scaffolds showed a decrease in the mass by  $47.13 \pm 2.37$  %. On the other hand, after the first calcium leaching step all scaffolds reswelled and showed an increase in the mass. For scaffolds leached in **LOW Ca<sup>2+</sup>** storage solution it was observed that the mass increased by  $30.35 \pm 1.83$  %, for scaffold leached in **MEDIUM Ca<sup>2+</sup>** mass increased by  $21.84 \pm 2.22$  %. Scaffolds leached in **HIGH Ca<sup>2+</sup>** storage solution showed the smallest increase in the mass with  $12.02 \pm 1.38$  %. At the end of the calcium leaching process mass increase was still observed. Mass of the scaffolds leached in **LOW Ca<sup>2+</sup>** storage solution was increased by  $29.88 \pm 4.07$  % from the first leaching step, scaffolds leached in **MEDIUM Ca<sup>2+</sup>** storage solution showed mass increase by  $15.81 \pm 1.82$  % from the first leaching step and scaffolds leached in **HIGH Ca<sup>2+</sup>** storage solution showed the least mass increase by  $1.69 \pm 0.99$  % from the first leaching step. These results indicate that increasing amounts of calcium in the scaffold increase network density and stability and thus suppress the swelling. This is also in correlation with the increase in mechanical properties described in section 4.3.

One important finding was that considering only the increase of mass due to swelling there is no large difference between different aligned structures. For example, the mass of the scaffolds with longitudinal fiber alignment after crosslinking decreased by  $46.79 \pm 0.53$  %, for the one with perpendicular fiber alignment that it decreased by  $45.42 \pm 0.92$  % and for the scaffolds with grid fiber alignment mass decreased by  $44.94 \pm 0.84$  %. After the last leaching step, mass of the scaffold with longitudinal alignment shows the least amount of mass increase with the value of  $15.81 \pm 1.82$  % from the first leaching step, whereas the mass of the scaffolds with perpendicular alignment



increased by  $20.32 \pm 1.49$  % and the mass of the scaffolds with grid alignment increased by  $18.63 \pm 0.15$  %.

Although the mass was not significantly influenced by the printing alignment, strong anisotropic swelling was observed. While longitudinal printed samples mainly swelled in the width (perpendicular to their fiber direction) with an increase of just  $2.06 \pm 0.92$  % in length, samples printed perpendicular increased more than 4 percent.

Comparing length changes after the first leaching step, it was observed that perpendicularly printed scaffolds have increased in length by  $4.36 \pm 0.79$  % which is twice as much as for the longitudinally printed ones which length increased by  $2.06 \pm 0.92$  %. Interestingly, scaffolds with grid alignment show an increase in length similarly to the perpendicular ones with an increase of  $4.17 \pm 0.67$  %.

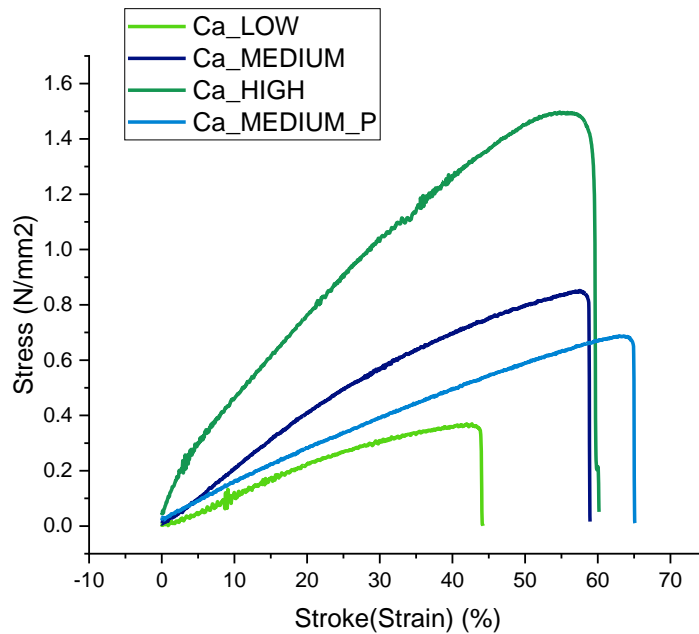
This anisotropic swelling was not observed for samples printed with the same geometry but changing calcium concentrations, and the increase in length is in accordance with the overall increase in mass. For example, the length of the scaffolds stored in **LOW Ca<sup>2+</sup>** increased by  $2.10 \pm 3.50$  % and the length of the scaffolds stored in **MEDIUM Ca<sup>2+</sup>** storage solution increased by  $2.06 \pm 0.92$  %. However, scaffolds stored in **HIGH Ca<sup>2+</sup>**, after the first leaching step, showed a decrease in length by  $3.26 \pm 0.26$  %. After the whole leaching process, the length of all the scaffolds increased slightly.

### 4.3. Tensile testing

To get an insight into properties such as yield stress and tensile strength of printed materials, tensile testing was done on samples printed with **Medium ink (Table 4)** and calcium leached in different storage solutions (**Table 6**).

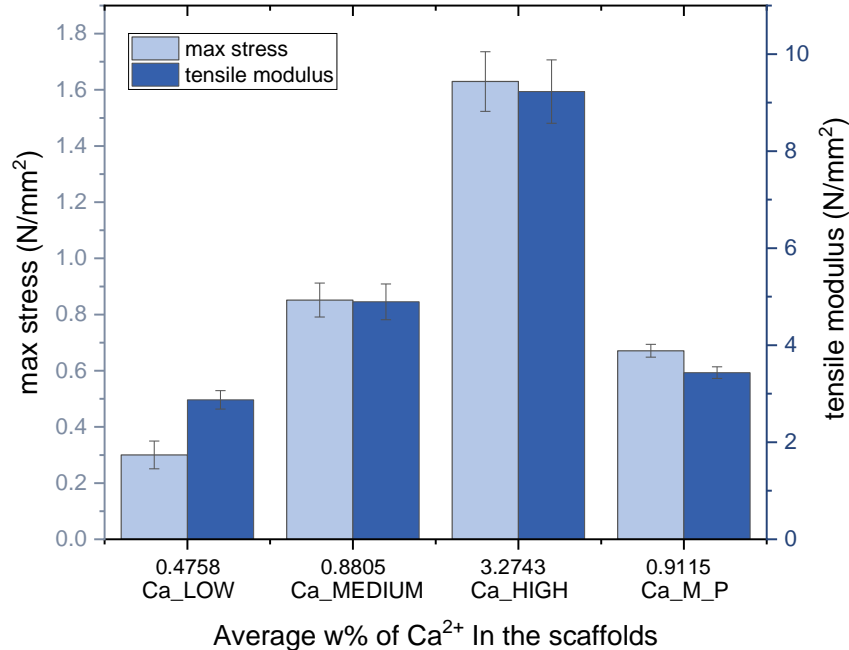
Sample **Ca\_LOW** (**Medium ink** leached **LOW Ca<sup>2+</sup>** storage solution) has the lowest maximum stress and modulus with  $0.30 \pm 0.05 \text{ N/mm}^2$  and  $2.87 \pm 0.19 \text{ N/mm}^2$  compared to the other samples with the same fiber alignment, **Ca\_M** (**Medium ink** leached in **MEDIUM Ca<sup>2+</sup>** storage solution) with maximum stress and modulus of  $0.85 \pm 0.06 \text{ N/mm}^2$  and  $4.89 \pm 0.37 \text{ N/mm}^2$  and **Ca\_H** (**Medium ink** leached in **HIGH Ca<sup>2+</sup>** storage solution) with maximum stress and modulus of  $1.63 \pm 0.11 \text{ N/mm}^2$  and  $9.22 \pm 0.65 \text{ N/mm}^2$ .

Samples that were stored in the same calcium concentration solutions (**Ca\_M** and **Ca\_M\_P**) show differences depending on their predominant fiber orientation. Samples with the longitudinal fibers (**Ca\_M\_1**) show higher strength with a modulus of  $4.89 \pm 0.37 \text{ N/mm}^2$ , than the sample with perpendicular fibers (**Ca\_M\_P1**) with a modulus of  $3.43 \pm 0.12 \text{ N/mm}^2$ . This anisotropic behavior was already described in previous works.<sup>6</sup>



**Figure 25** Tensile stress-strain curves for scaffolds stored in different storage solutions and with different fiber alignment. **Ca\_LOW**, **Ca\_MEDIUM** and **Ca\_HIGH** have longitudinal fiber

alignment, whereas **Ca\_MEDIUM\_P** has perpendicular fiber alignment relative to the pulling direction.



**Figure 26** Comparison of the mechanical properties (maximum stress and tensile modulus) for scaffolds printed using **Medium ink** (Table 4) leached in different storage solutions (Table 6). Values on x-axis indicate remaining Ca concentration in w% after leaching.

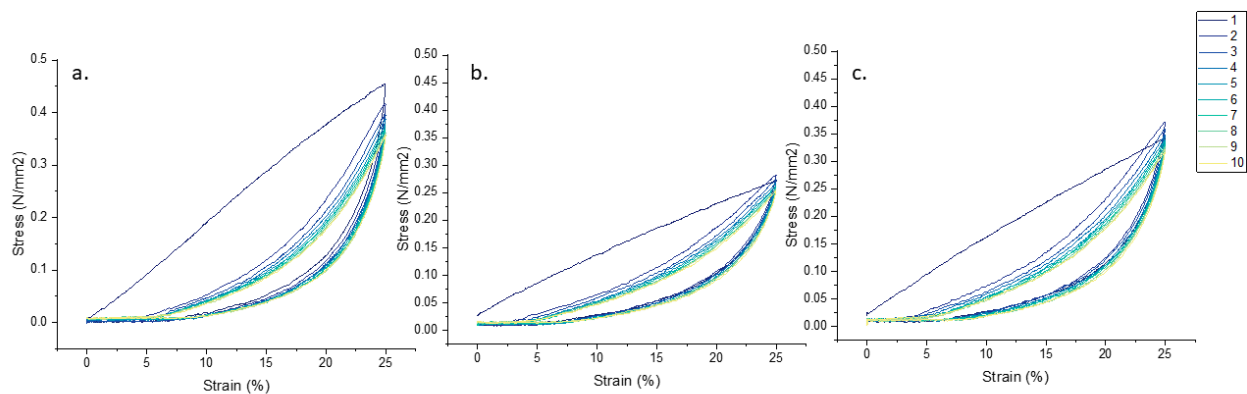
#### 4.4. Cycle test

To investigate elastic properties, different scaffolds were subjected to a 10 cycle tensile tests without resting time. Cycle stress-strain curves are shown in **Figure 27**, **Figure 28** and **Figure 29**. It is visible from the graphs that plastic (or inelastic) deformation occurs. For each sample the stress-strain hysteresis curves change gradually, and no sample fully returned to its original state when unloaded to a zero stress.

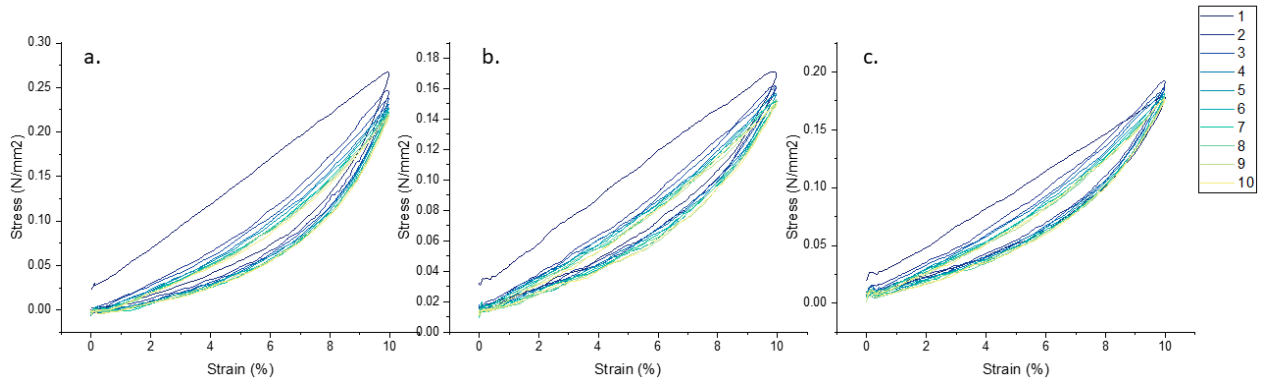
The changes in maximum and minimum stresses during cycle testing are shown in **Figure 30**. Every tested material shows slight decrease in maximum stress over each cycle. However, when comparing the first cycle with the following ones shown in **Figure 27**, **Figure 28** and **Figure 29**, it is visible that for some of them (perpendicular and grid fiber alignment scaffolds at speed 10

mm/min and 25 % strain and 50 mm/min and 25 % strain, as well as for grid alignment at 50 mm/min and 10 % strain) max stress for first cycle is lower and it slightly increases over the cycles. One possible explanation for this could be the changes of fiber alignment during stretching. When stretching the first cycle fibers in perpendicular and grid printed scaffolds aligned in the direction of the pulling strain. Therefore, the next cycle shows increase in max stress which is after that slowly decreasing in the same way as the longitudinally printed scaffolds.<sup>95</sup> Furthermore, from comparing the **Figure 27**, **Figure 28** and **Figure 29** it can be concluded that different extensional speed also affects the fiber alignment change. For example, max stress after first cycle increased by 0.2241 N/mm<sup>2</sup> for scaffold with grid alignment at speed 50 mm/min and 0.0138 N/mm<sup>2</sup> for scaffold with grid alignment at speed 10 mm/min for the same strain percentage (25%).

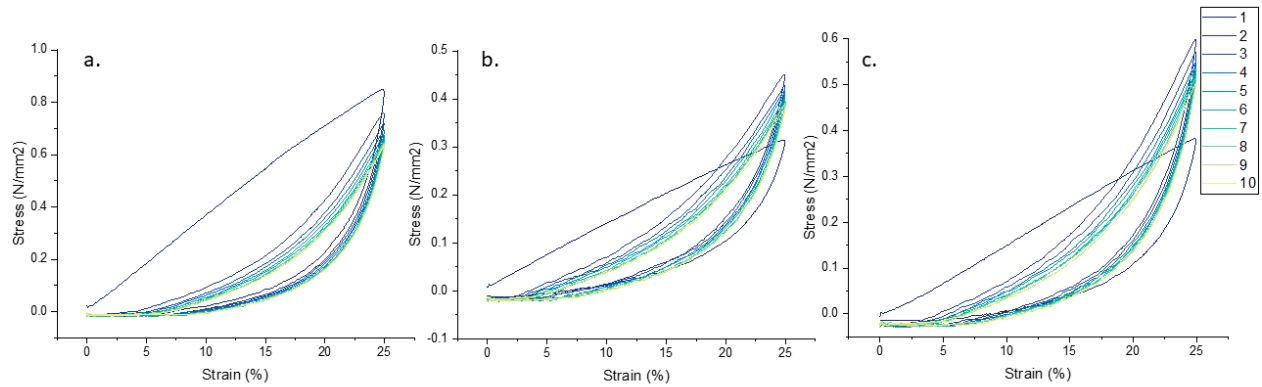
Further **Figure 30** shows that the elastic deformation mainly occurs at the starting circles and the maximum stress values even out towards the later cycles. For example, looking at the sample tested with 50 mm/min and 25% strain, the difference between cycle 1 and 10 is 0.22 N/mm<sup>2</sup> while the difference between cycle 9 and 10 is only 0.005 N/mm<sup>2</sup>.



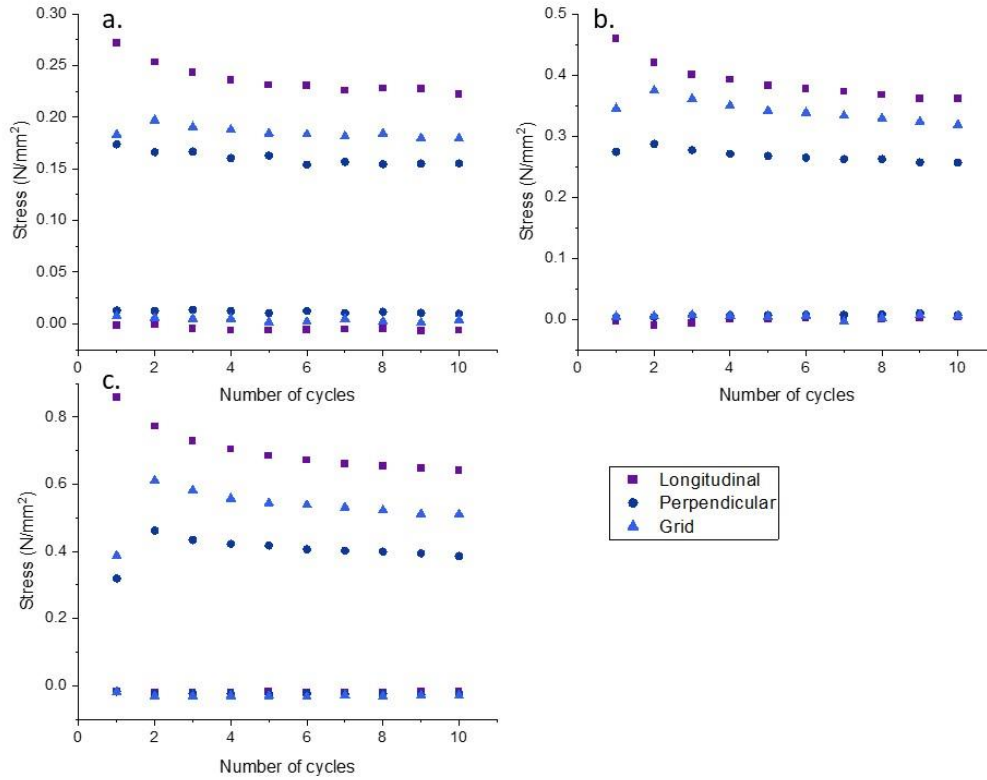
**Figure 27** Cycle tests stress-strain graphs for scaffold with different fiber alignment (a. longitudinal, b. perpendicular and c. grid alignment) tested with speed 10 mm/min and 25 % strain



**Figure 28** Cycle tests stress-strain graphs for scaffold with different fiber alignment (a. longitudinal, b. perpendicular and c. grid alignment) tested with speed 50 mm/min and 10 % strain



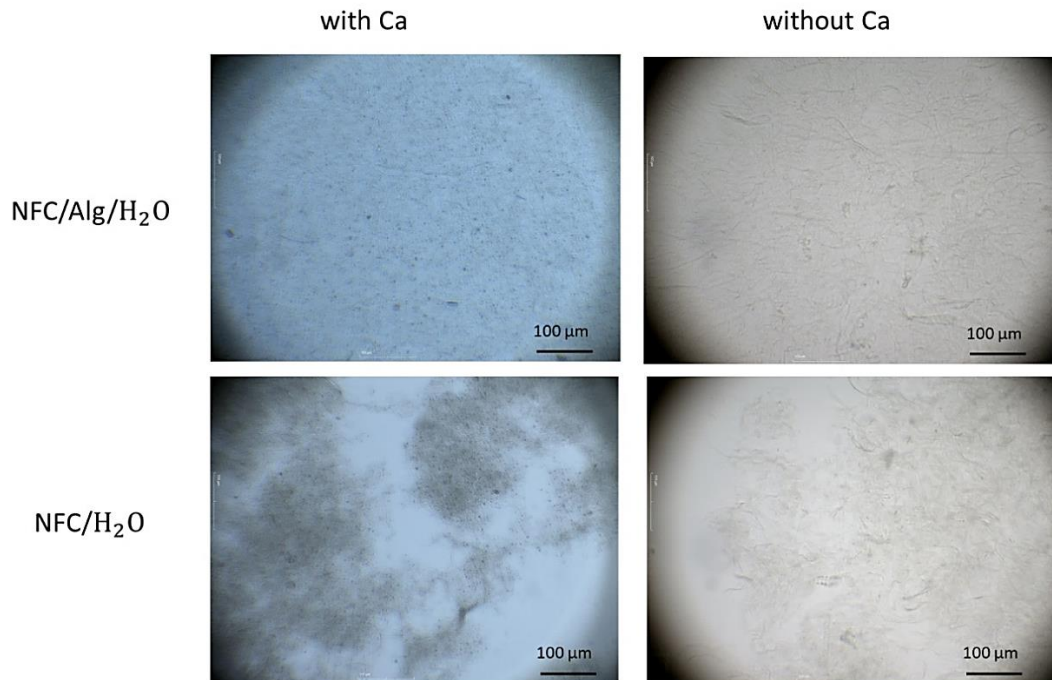
**Figure 29** Cycle tests stress-strain graphs for scaffold with different fiber alignment (a. longitudinal, b. perpendicular and c. grid alignment) tested with speed 50 mm/min and 25 % strain



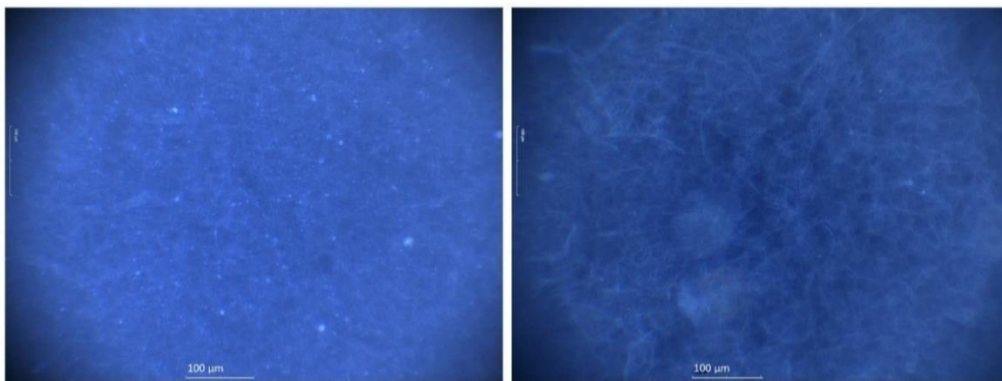
**Figure 30** Maximum and minimum stress during cycle testing for (a.) speed 50 mm/min, strain 10%, (b.) speed 10 mm/min, strain 25% and (c.) speed 50 mm/min, strain 25%

## 4.5. Light microscopy

Biomaterial 3D printing requires homogeneous distribution of components that make up its composition. Homogeneity is important for controlling the properties of the printed scaffold for its further use either in tissue engineering or similar biomedical applications. For that reason, different ink components were investigated by light microscopy to determine the homogeneity of each one in the ink used for printing. It is visible in **Figure 31** and **Figure 32** that calcium carbonate and nanocellulose fibers are very well distributed in the alginate gel that appears transparent under the microscope. It can therefore be stated that the ink is homogeneous and that alginate strongly aids the dispersibility.



**Figure 31** Brightfield microscopic pictures of different ink components



**Figure 32** Darkfield microscopic pictures of ink with calcium carbonate (left) and without (right)

## 4.6. Diffusion tests

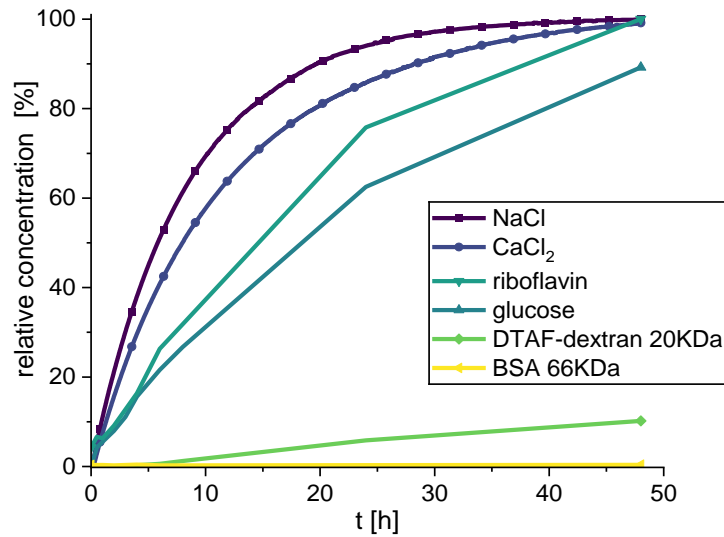
Living tissues rely on transport of nutrients to the individual cells, therefore it is important for scaffolds designed for tissue engineering to have optimal porosity for transporting nutrients and ions. For that reason, different diffusion tests were done on a variety of molecules to test the membrane permeability.

**Table 9** Diffusion coefficients for NaCl, CaCl<sub>2</sub>, riboflavin, dextran (20 kDa), BSA and glucose measured through different membranes and compared to literature values.

\*D for FITC-dextran (17.2 Da)

Substance	Diffusion coefficient (2 layers membrane) [m <sup>2</sup> /s]	Diffusion coefficient (ZelluTrans membrane) [m <sup>2</sup> /s]	Literature value (tissue) [m <sup>2</sup> /s]	Literature value (water) [m <sup>2</sup> /s]
NaCl	$9.62 \times 10^{-10}$	$8.05 \times 10^{-11}$	$1.85 \times 10^{-10} - 2.50 \times 10^{-10}$ (pork tissue) <sup>96</sup>	$1.10 \times 10^{-9} - 2.80 \times 10^{-9}$ <sup>97</sup>
CaCl <sub>2</sub>	$6.99 \times 10^{-10}$	$5.86 \times 10^{-11}$		$1.11 \pm 0,008 \times 10^{-9}$ <sup>98</sup>
Riboflavin	$4.75 \times 10^{-10}$	$1.87 \times 10^{-11}$	$2.2 \times 10^{-10} - 7.5 \times 10^{-10}$ (alg-F68 composite hydrogels) <sup>99</sup>	
Dextran (20 kDa)	/	/	$2.70 \pm 0.9 \times 10^{-11}$ (MDCK cells) <sup>100</sup>	$6.4 \times 10^{-11}$ * <sup>101</sup>
BSA	/	/	$0.5 \times 10^{-10} - 7.5 \times 10^{-10}$ (alg-F68 composite hydrogels) <sup>99</sup>	$5.27 \times 10^{-10} - 5.44 \times 10^{-10}$ <sup>102</sup>
Glucose	$4.77 \times 10^{-10}$	$8.20 \times 10^{-12}$	$6.23 \times 10^{-10}$ (alginate gel) <sup>103</sup>	$7 \times 10^{-10}$ <sup>103</sup>





**Figure 33** Concentration profiles over time for all tested substances

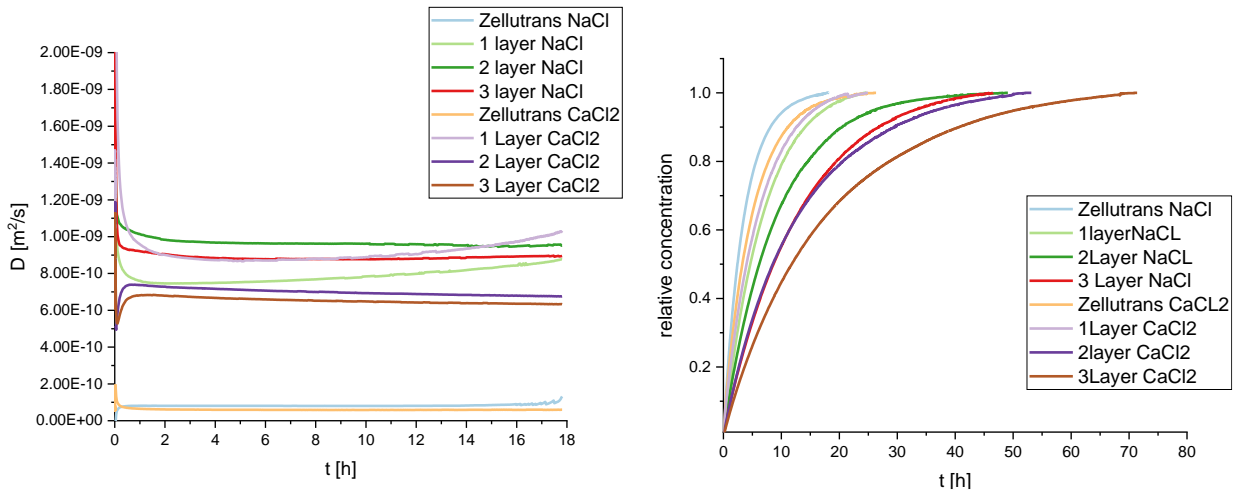
#### 4.6.1. Sodium and calcium chloride

Sodium and calcium chloride diffused through all tested membranes, ZelluTrans (a cellulose membrane) and all scaffold membranes. Differences in diffusion coefficients are shown in **Figure 34** as well as in **Table 10**.

All calculated diffusion coefficients show similar values for scaffold membrane, calcium chloride diffusion through 2 and 3 layered membranes show lowest value of them all which is expected due to the larger size of the calcium ion. Also, diffusion coefficient values for NaCl and CaCl<sub>2</sub> through ZelluTrans membrane are lower than the one for all scaffold membranes meaning diffusion is slower through ZelluTrans. Comparing calculated values to the one in literature<sup>96,97,99</sup>, we can conclude that diffusion coefficients for NaCl and CaCl<sub>2</sub> for tested membranes nicely correspond to the ones for living tissues as shown in **Table 9**.

**Table 10** Diffusion coefficients for NaCl and CaCl<sub>2</sub> for different membranes calculated at 8 hours.

Substance	ZelluTrans [m <sup>2</sup> /s]	1 layer [m <sup>2</sup> /s]	2 layers [m <sup>2</sup> /s]	3 layers [m <sup>2</sup> /s]
NaCl	$8.05 \times 10^{-11}$	$7.70 \times 10^{-10}$	$9.62 \times 10^{-10}$	$8.79 \times 10^{-10}$
CaCl <sub>2</sub>	$5.86 \times 10^{-11}$	$8.80 \times 10^{-10}$	$6.99 \times 10^{-10}$	$6.52 \times 10^{-10}$



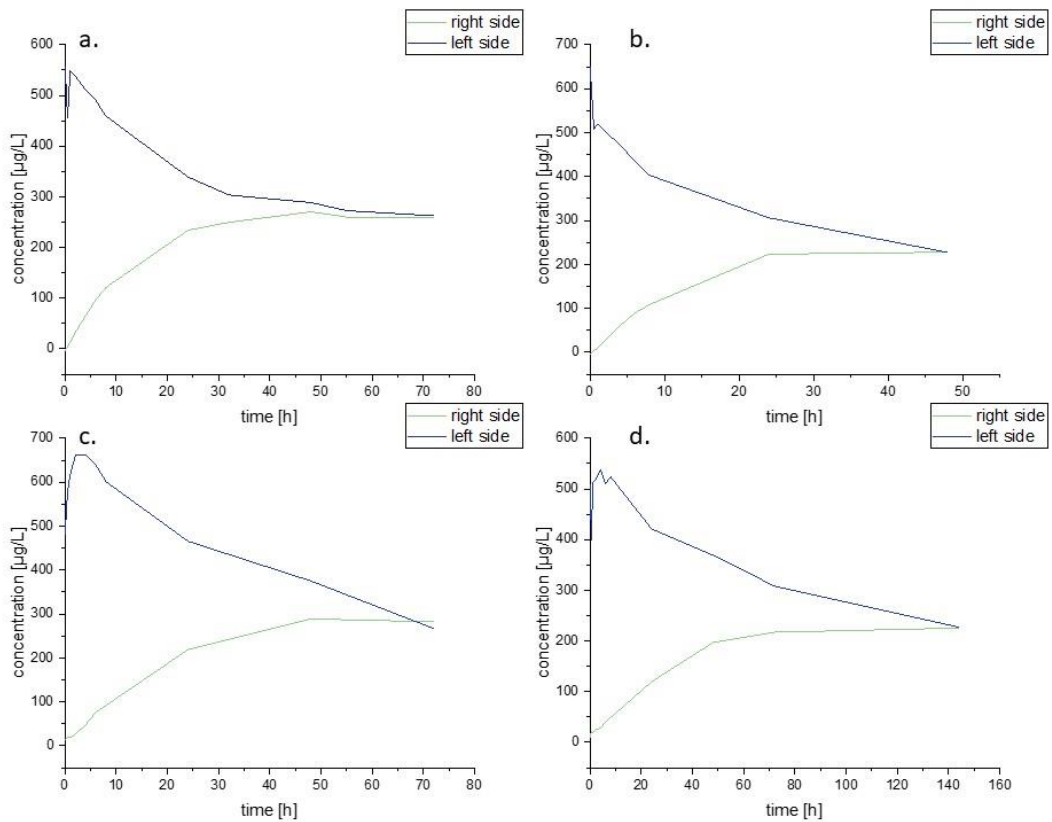
**Figure 34** Diffusion coefficient versus time and concentration versus time for sodium and calcium chloride

#### 4.6.2. Riboflavin

Riboflavin, also known as vitamin B<sub>2</sub> went through all tested membranes. Concentration changes in left and right diffusion cells are shown in **Figure 35**. From diffusion coefficient shown in **Table 11** it is visible that riboflavin went through a 1 layered membrane the fastest as expected, then follows 3 layered and finally 2 layered scaffold membrane. Surprisingly, riboflavin diffusion through ZelluTrans membrane shows lowest diffusion coefficient of all. As of the reported literature values shown in **Table 9**, diffusion coefficients show similar values.<sup>99</sup>

**Table 11** Diffusion coefficients for riboflavin for different membranes calculated at 8 hours

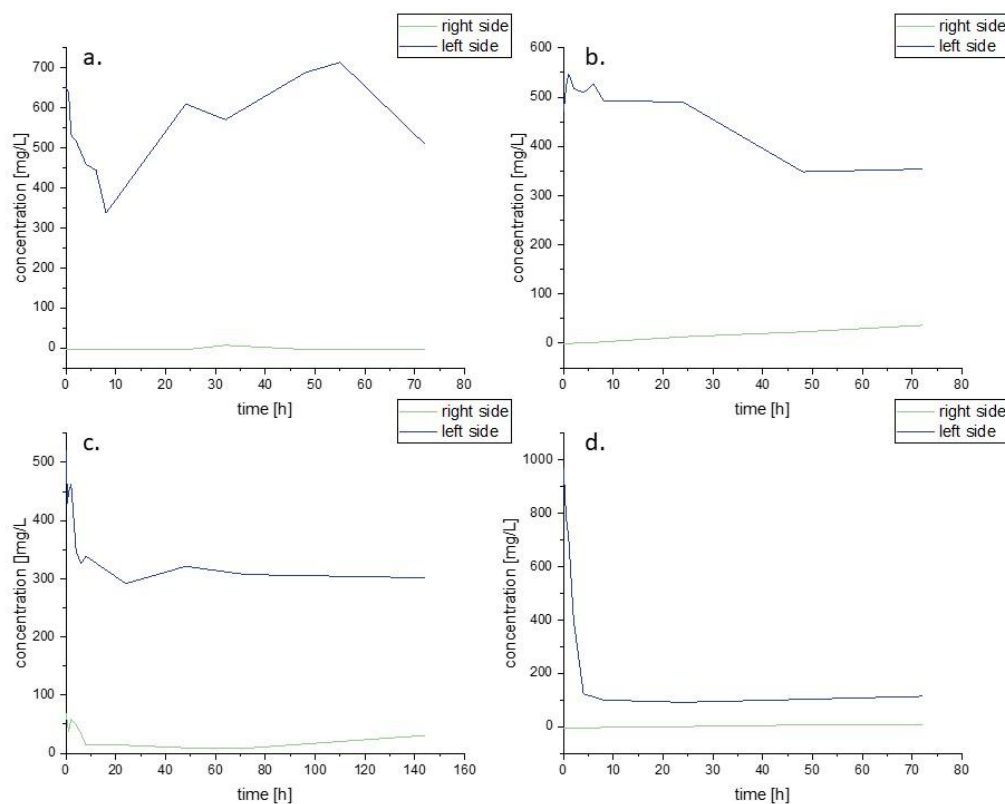
	<b>ZelluTrans</b>	<b>1 layer</b>	<b>2 layers</b>	<b>3 layers</b>
	[m <sup>2</sup> /s]	[m <sup>2</sup> /s]	[m <sup>2</sup> /s]	[m <sup>2</sup> /s]
<b>Riboflavin</b>	$1.87 \times 10^{-11}$	$2.36 \times 10^{-10}$	$4.75 \times 10^{-10}$	$2.70 \times 10^{-10}$



**Figure 35** Concentration versus time for riboflavin diffusion test through a. ZelluTrans membrane, b. 1 layered, c.2 layered and d. 3 layered scaffold membrane.

### 4.6.3. Dextran (20 kDa)

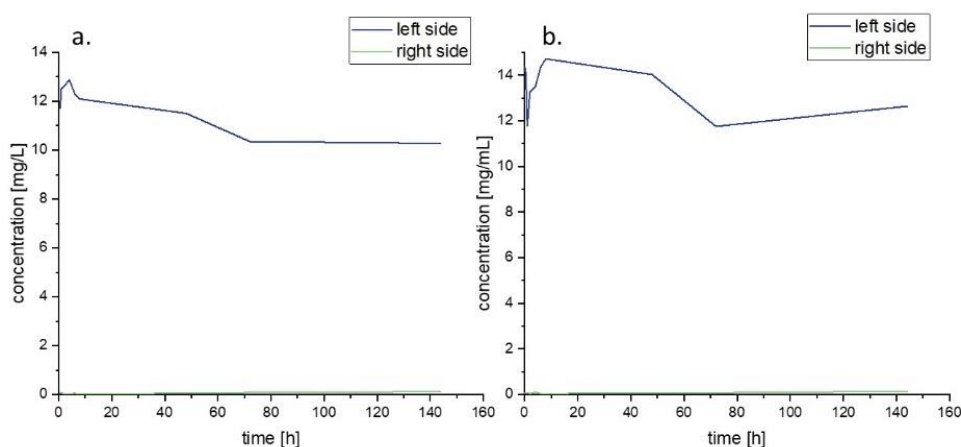
If we observe the concentration signal on the right side of the diffusion cell (cell with no dextran added) in **Figure 36**, we can assume that no or negligible amounts after several days went through the ZelluTrans nor the scaffold membranes. For that reason, no diffusion coefficients were calculated for dextran. On the other hand, oscillations in concentration line on the left side of the diffusion cell (cell with added dextran solution) can be attributed to dextran clinging and detaching on/off the diffusion cell walls or membrane.



**Figure 36** Concentration versus time for dextran (10 kDa) diffusion test through a. ZelluTrans membrane, b. 1 layered, c. 2 layered and d. 3 layered scaffold membrane.

#### 4.6.4. Bovine albumin serum (BSA)

Like dextran, BSA as shown in **Figure 37**, did not pass through ZelluTrans nor 2 layered scaffold membrane. Explainable with its large size of with 66 000 Da. The used ZelluTrans membrane has a molecular cut of weight from 12 000 to 14 000 Da. On the other hand, from previous experiments with dextran it is concluded that molecules larger than 20 000 Da did not pass through the scaffold membrane. Hence it is impossible for BSA to diffuse in the measurable range. For that reason, no diffusion coefficients were calculated for BSA.



**Figure 37** Concentration versus time for BSA diffusion test through a. ZelluTrans membrane and b. 2 layered scaffold membrane

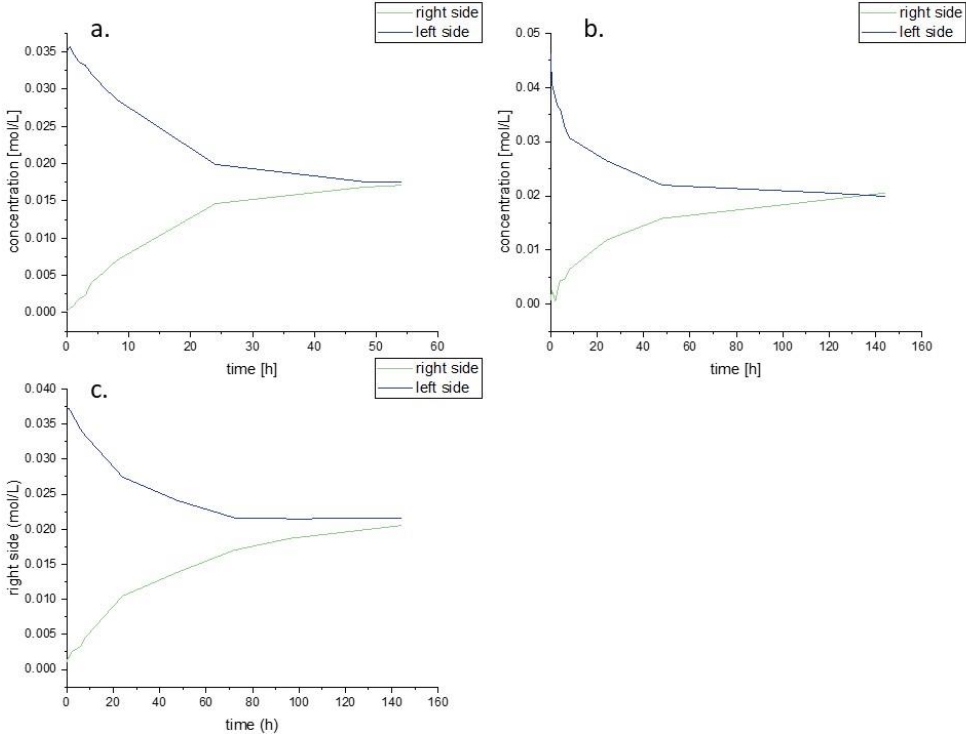
#### 4.6.5. Glucose

For glucose, diffusion through all tested membranes occurred as **Figure 38** shows. The diffusion coefficient of glucose through ZelluTrans membrane was determined with  $4.77 \times 10^{-10} \text{ m}^2/\text{s}$ , for 2 layered scaffold membrane with  $5.26 \times 10^{-9} \text{ m}^2/\text{s}$  and for 3 layered scaffold membrane with  $8.20 \times 10^{-9} \text{ m}^2/\text{s}$ .

Furthermore, from diffusion coefficients of **Table 9** and changes in concentrations visible from **Figure 38** it can be concluded that glucose diffuses faster through printed scaffold membranes rather than through ZelluTrans membrane or reported alginate gels.<sup>103</sup>

**Table 12** Diffusion coefficients for glucose for different membranes calculated at 8 hours.

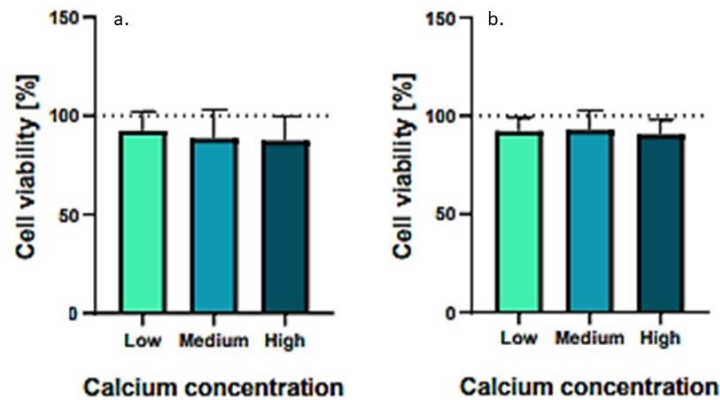
	ZelluTrans	2 layers	3 layers
	[m <sup>2</sup> /s]	[m <sup>2</sup> /s]	[m <sup>2</sup> /s]
Glucose	$8.20 \times 10^{-12}$	$4.77 \times 10^{-10}$	$5.26 \times 10^{-10}$



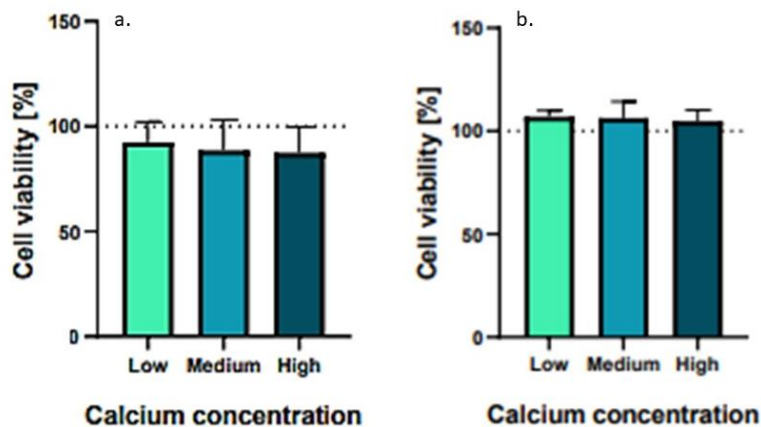
**Figure 38** Concentration versus time for glucose diffusion test through a. ZelluTrans membrane, b. 2 layered and c. 3 layered scaffold membrane.

## 4.7. Cell viability tests

In tissue engineering (TE) cells are necessary for inducing regeneration of the tissue or to secrete factors important for regeneration of the tissue. For that reason, cell viability is one of the most important parameters in TE (e.g. wound dressing) for evaluating cell response in different conditions. Therefore, to assess if printed are toxic to cells, cell viability tests were done.



**Figure 39** Cell viability test results tested for a. 24 hours and b. 48 hours on HEK 293 cells.



**Figure 40** Cell viability test results tested for a. 24 hours and b. 48 hours on HUVECs cells.

From **Figure 39** and **Figure 40** it is visible that HUVECs cells have higher cell viability after 48 hours comparing to the HEK293 cells which also corresponds with above mentioned literature, which states that no cytotoxicity was reported on HUVECs cells while slightly cytotoxicity of CNF and CNC from plant cellulose can be observed on HEK 293 cells.<sup>51</sup>

## 4.8. Degradation process

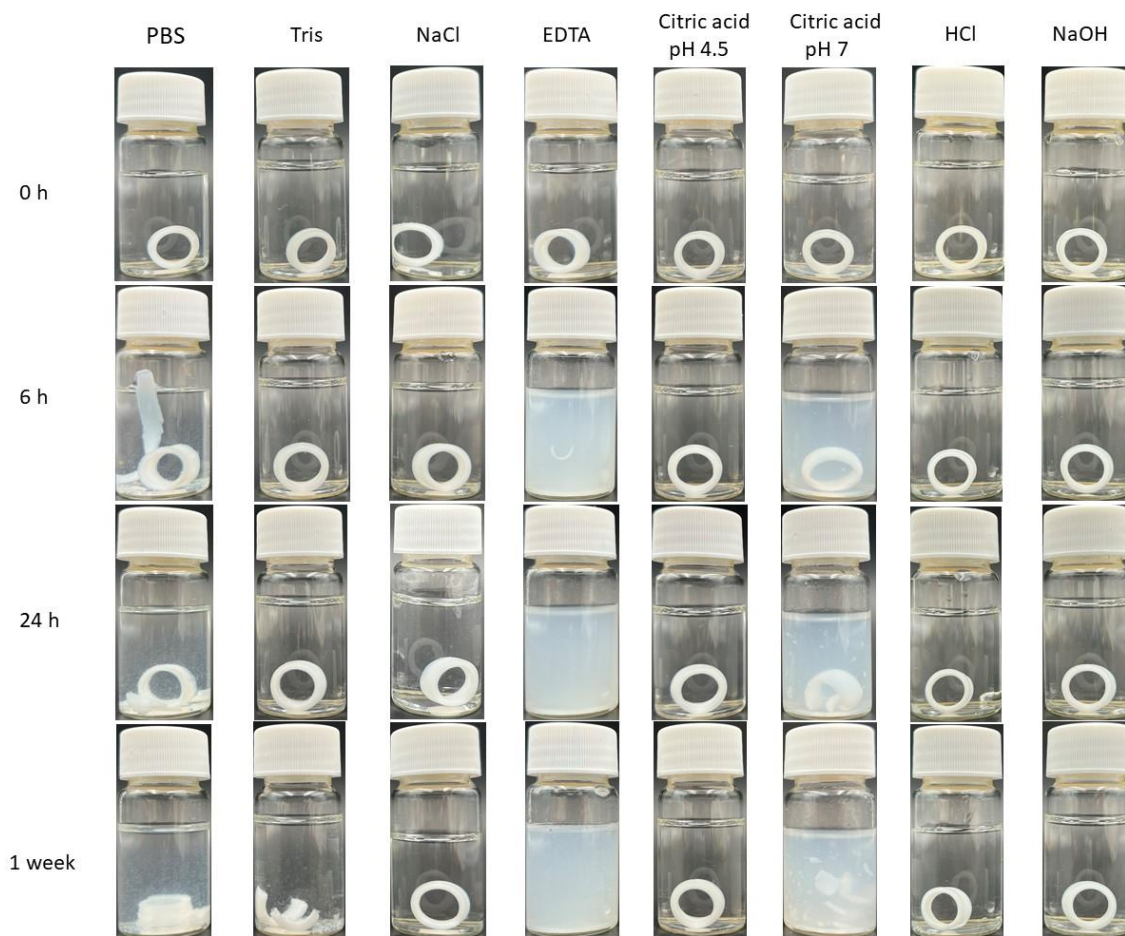
Until injured tissue is regenerated, scaffold should provide stability and mechanical properties that correspond to that tissue. Followed by that, important scaffold property is also ability to degrade and allow formation of a new tissue<sup>104</sup>. Therefore, two different degradation process tests were done on previously printed scaffolds to determine what solutions/substances trigger scaffold degradation and the time it takes for such process.

### 4.8.1. Solutions

Immediately after putting scaffolds in different solutions for degradation process (shown in **Table 8**) no changes in scaffolds nor solutions occurred. After 6 hours complete layer separation was visible for scaffold in PBS solution. The scaffold in TRIS solution appears to be softer on the touch than at the start. EDTA solution become cloudy due to the fibers which detached from the material and the scaffold was almost completely degraded. Also, citric acid solution with pH set to 7 showed cloudiness and scaffold was soft to the touch but structure of the scaffold remained the same. As for the scaffolds in NaCl, citric acid (pH 4.5), HCl and NaOH solutions, no changes were observed. After 24 hours scaffold in TRIS solution was soft to touch, the one in EDTA was completely degraded and the scaffold in citric acid (pH 7) lost its structure, small fragments and fibers were detached from the original scaffold. Scaffold in HCl solution become harder to touch and the rest of the scaffolds remained the same after 6 hours. After 1 week no changes were observed except for the scaffolds in TRIS and citric acid (pH 7) solutions where scaffolds degraded even more, and the materials disintegrated.

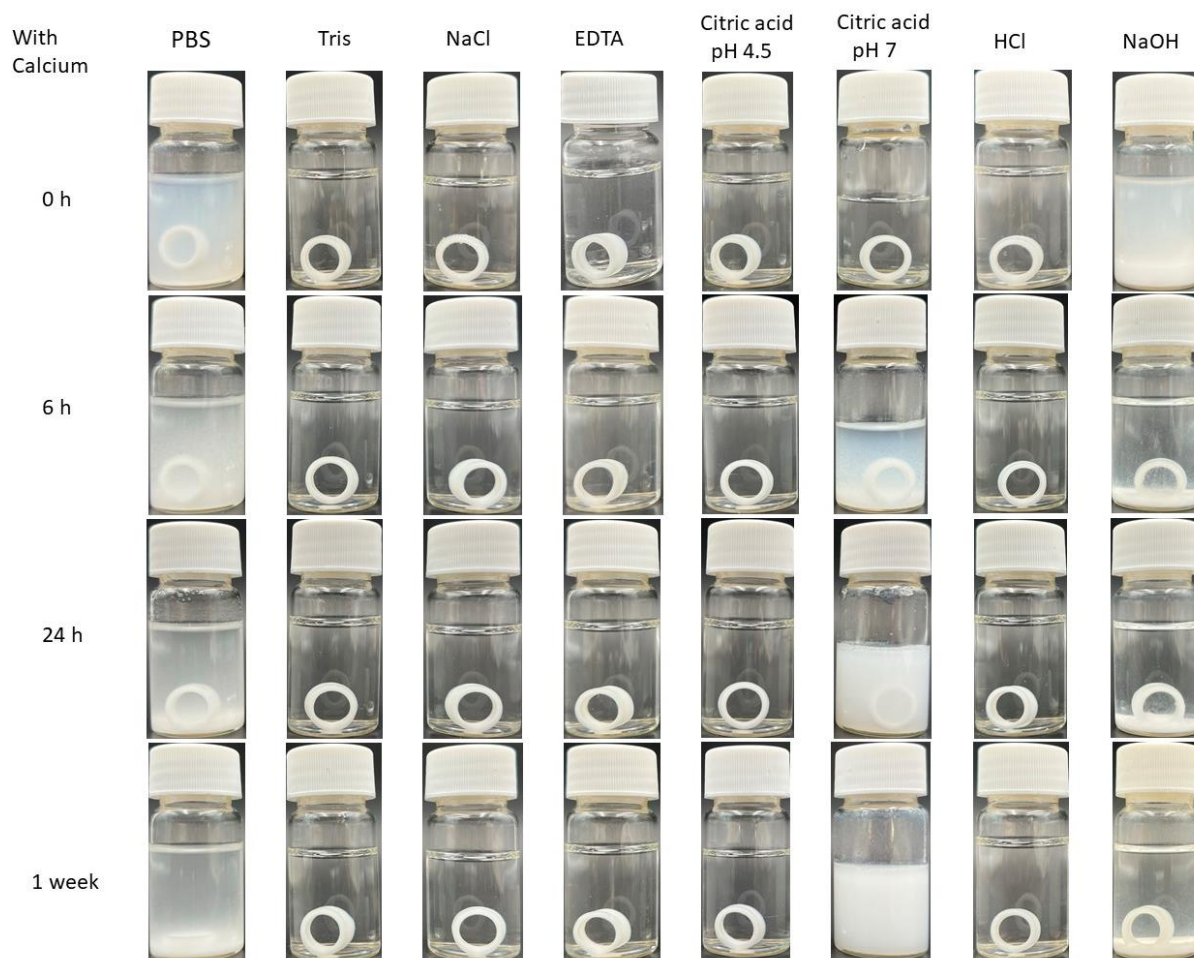
TRIS, EDTA and citrate from citric acid forms complexes with calcium from scaffolds and therefore degradation occurs. As for the phosphate buffer solution calcium was removed from the scaffold through precipitation of calcium phosphates which become visible by adding an excess of calcium ions. Pictures taken for described process are visible in **Figure 41**.





**Figure 41** Scaffolds in solutions described in **Table 8** immediately after putting them in the solutions and after 6 hours, 24 hours and 1 week

On the other hand, solutions with added excess calcium chloride show no signs of degradation. It is to be concluded that calcium forms soluble complexes with TRIS, EDTA and citrate. Therefore, no “free” groups were left for calcium from scaffold to form complexes and hence no degradation process occurred. PBS and NaOH from insoluble salts which precipitated on the bottom however did not affect scaffold stability. From the **Figure 42** it is visible that all scaffolds remained their original shape even after 1 week of being in the solutions.

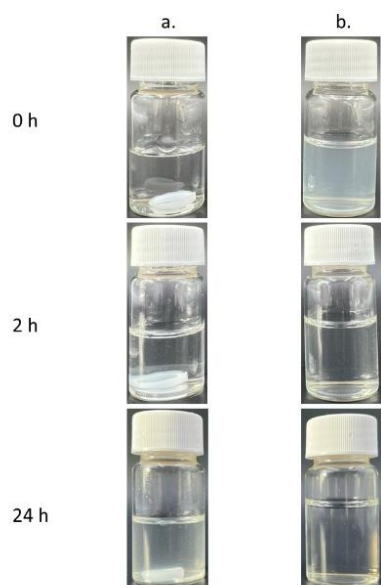


**Figure 42** Scaffolds in solutions described in **Table 8** with 100 mg of  $\text{CaCl}_2$  in each immediately after putting them in the solutions and after 6 hours, 24 hours and 1 week.

#### 4.8.2. Cellulase

After putting the scaffolds (either in solid state or dissolved in EDTA solution as described in paragraph 3.3.7.2) in distilled water, adjusting the pH to 5 and adding 1 mg of cellulase (3-10 units/mg), pictures were taken after 2 hours and after 24 hours. From **Figure 43** it is visible that the solution with solid scaffold became slightly cloudy, while the solution (which is already cloudy from the nanocellulose fibers) with dissolved scaffold became slightly clear after 2 hours and completely clear after 24 hours. This indicates that the solid scaffold started to degrade due to the influence of the cellulase enzyme and therefore a slight cloudiness occurred from the remaining nanocellulose fibers. As for the dissolved scaffold, the cloudy solution became clear due to the

cellulase activity that broke down the cellulose fibers and molecules into sugar mono and oligomer i.e. glucose, cellobiose etc. (described in next two paragraphs).



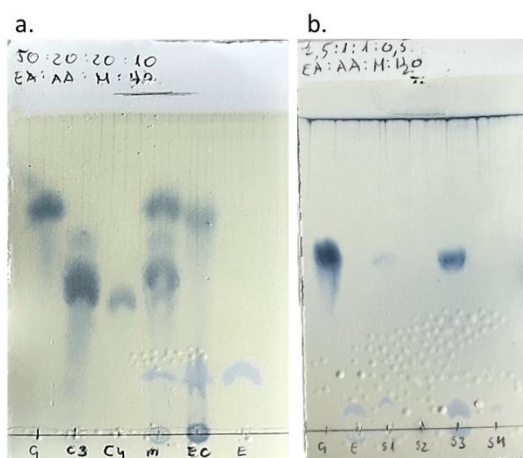
**Figure 43** Scaffold degradation process using cellulase enzyme for (a.) approximately 100 mg of scaffold in distilled water with 1 mg of cellulase added and (b.) approximately 1,5 mL of scaffold dissolved in EDTA and 1 mg of cellulase added.

#### 4.8.2.1. Thin layered chromatography

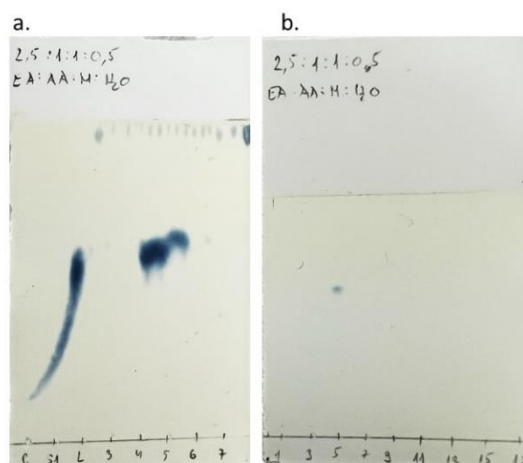
To assess the composition of the enzyme treated, solution thin layer chromatography was performed. From the **Figure 44 (a.)** it is visible that sample does not contain only glucose, but EDTA as well. A second purification was performed using ethanol as described in paragraph 3.3.7.2 to remove the alginate. From **Figure 44 (b.)** it can be concluded that glucose still was not isolated from the EDTA in the mixture, therefore column chromatography was performed. After all fractions were collected, they were run on a TLC plate and the results are shown in **Figure 45**. Samples that were suspected of containing glucose were combined and further analyzed by NMR spectroscopy.

**Table 13** Column chromatography process data

	<b>Amount</b>
<b>Silica gel</b>	10 mL
<b>Fractions</b>	3 mL
<b>Raw product</b>	0.0892 g
<b>End product</b>	0.0464 g



**Figure 44** Thin layer chromatography for (a.) G-glucose solution, C3-celotriose, C4-celotetraose, m-all samples mixed, EC-degraded scaffold in EDTA with added cellulase enzyme, E-EDTA and (b.) G-glucose, E-EDTA, S1-purified sample with methanol, S2-residue from S1, S3-purified S1 sample second time with ethanol, S4-residue from S3



**Figure 45** Chromatography fractions tested with TLC. No EDTA present in fractions. Fractions 5 and 6 collected for NMR.

### 4.8.2.2. NMR

Glucose, like many different sugars, exists in an equilibrium between different ring forms anomers. More than 99% of all glucose molecules occur as a  $\alpha$  and  $\beta$  D-glucopyranose, more of that being  $\beta$ -D-glucopyranose.<sup>105,106</sup> The rotation of anomeric protons ( $\alpha$ H1 and  $\beta$ H1) can be observed by monitoring the  $^1\text{H}$  NMR spectrum. Those rotations can be seen from NMR spectra of the tested sample (Figure 47) and results correspond to the ones in literature.<sup>107</sup>

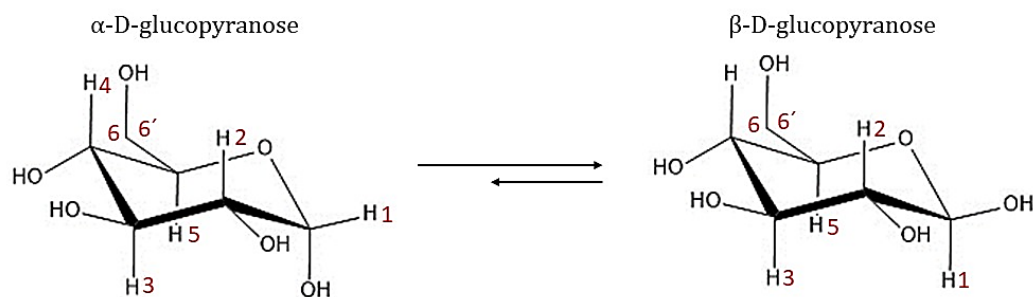


Figure 46 Structural formula of D-glucose and its anomeric configurations

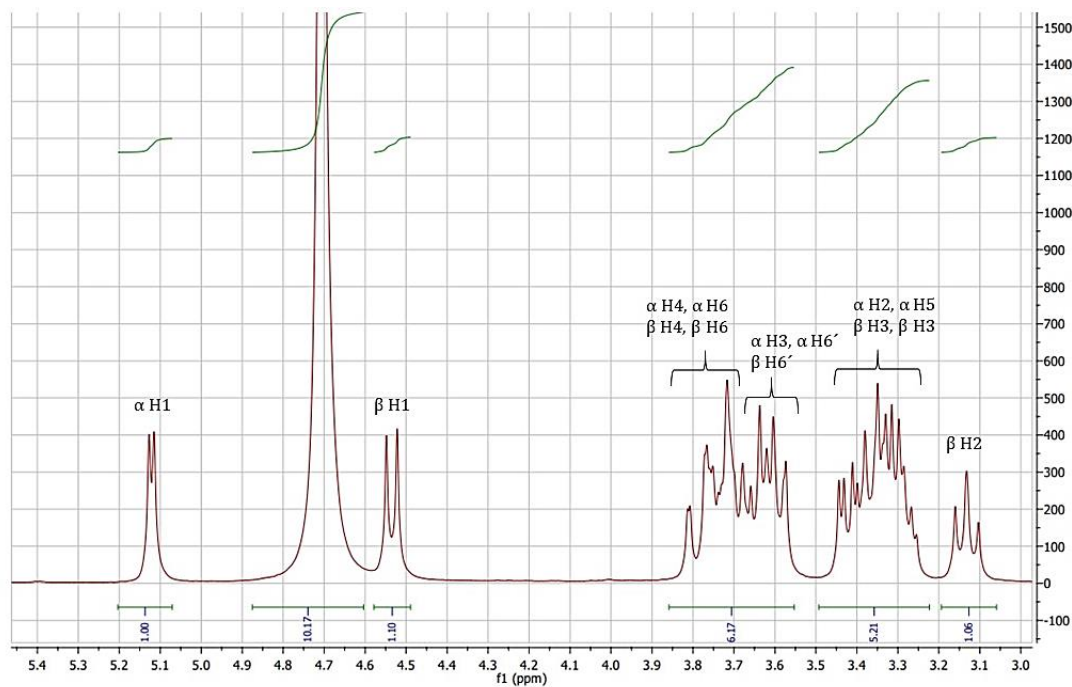
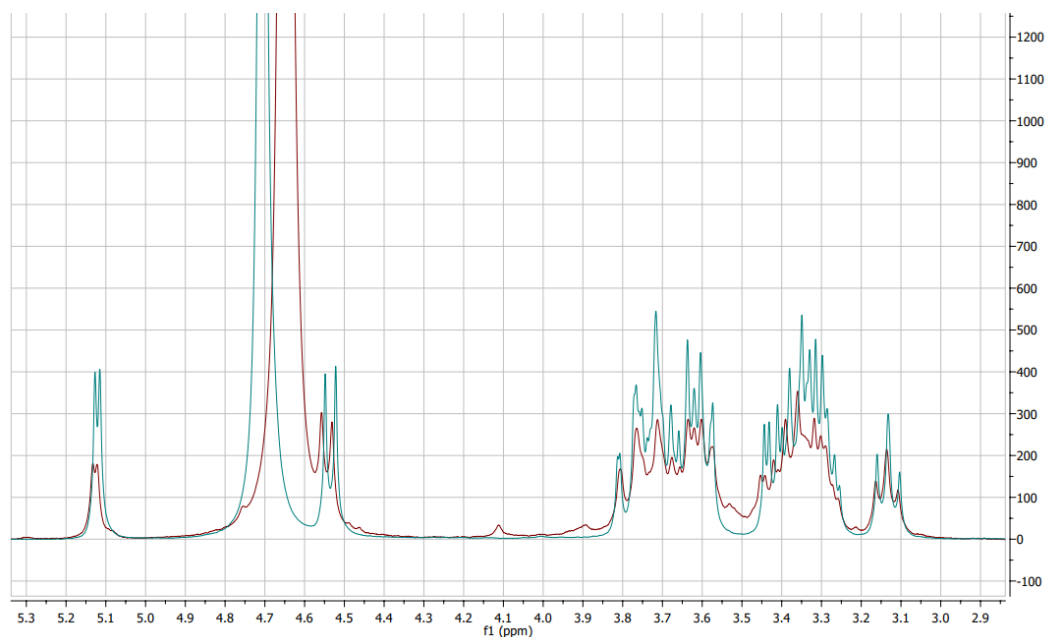


Figure 47 300 MHz  $^1\text{H}$  NMR spectra of the tested sample in  $\text{D}_2\text{O}$ .

**Figure 48** corresponding  $^1\text{H-NMR}$  spectrum, shows glucose and tested material's signals, which overlap. All signals approximately have the same intensity which implies that they belong to the same species. Lower peaks of the tested sample could be due to the lower concentration of the material used for testing.



**Figure 48** NMR comparison of unknown sample (red) and known sample of glucose (green)



## 5. CONCLUSIONS

The aim of this thesis was to investigate and optimize a bio-ink consisting of NFC, Alg and CaCO<sub>3</sub>, in order to obtain scaffolds with properties suitable for future tissue engineering or biomimetic fibrous materials that could be used as vascular grafts. The bio-inks could be extruded with a commercial 3D printer. As mentioned earlier, some of the most important properties for the application of scaffolds in biomedicine are biocompatibility, structural integrity, and the ability to control degradation. Calcium as a component of the ink brings many benefits to the fabricated scaffolds. Through leaching tests, it was concluded that the leaching of calcium can be optimized by using solutions with appropriate calcium concentration for different inks. Further, calcium ions in the scaffolds allow to control degradation processes, as they form complexes with various anions. In that regard, it could be experimentally demonstrated that the degradation can be stimulated by addition of PBS, EDTA, or citric acid solution, after adjusting the pH-value.

In addition, for the formation and maintenance of healthy tissue, nutrient supply to the tissue is important. Therefore, diffusion tests were performed to test the permeability of different solutes through the printed scaffolds. This showed that ions and smaller molecules such as riboflavin and glucose were permeable, while diffusion of larger molecules such as BSA and dextran was inhibited.

Mechanical properties were also tested with tensile and cycle tests and correlated to *in situ* calcium concentrations in the scaffolds. Specimens printed from inks with a high calcium concentration, and scaffolds stored in solutions with higher calcium concentration exhibited higher maximum stress than scaffolds with lower a calcium content. This reflects the network density of the cross-links. In addition, fiber orientation plays an important role in maximum stress and elongation achievable. It was confirmed that scaffolds with a fiber orientation in the same direction as the loading stress achieve higher maximum stress than the scaffolds with reversed fiber orientation. Additionally, a change in maximum stress was observed over time after subjecting the scaffolds to 10 cycles. After the first cycle, some scaffolds showed an increase in maximum stress. For this reason, cyclic testing suggests that fiber orientation may be changed when the material is subjected to tensile stress.

Lastly, one of the most important properties for materials in tissue engineering, non-cytotoxicity, was tested and obtained results confirm that scaffolds fabricated in this work are allowing cell

growth which is promising for further optimization and application in tissue engineering and biomedicine.



## 6. LIST OF PUBLICATIONS AND TALKS

- [1.] Gudelj, M.; Šurina, P.; Jurko, L.; Prkić, A.; Bošković, P. The Additive Influence of Propane-1,2-Diol on SDS Micellar Structure and Properties. *Molecules (Basel, Switzerland)* **2021**, *26* (12). DOI: 10.3390/molecules26123773. Published Online: Jun. 21, 2021
- [2.] Lackner, F.; Šurina P.; Fink J.; Kotzbeck P.; Stana J.; Grab M.; Tsilimparis N.; Mohan T.; Stana Kleinschek K. and Kargl R. 4-Axis 3D printing of tubular vascular tissue models and cell culture substrates with anisotropic nanofiber orientation – manuscript under review, August 2023  
Lackner, F.; Šurina P.; Fink J.; Kotzbeck P.; Stana J.; Grab M.; Tsilimparis N.; Mohan T.; Kargl R.; and Stana Kleinschek K. 3D Printing and Characterization of Vascular Models from Polysaccharides – EPNOE, 2023, talk
- [3.] Mohan T., Lackner, F.; Šurina P., Steindorfer T., Kargl R. and Stana Kleinschek K. Nanocellulose production and application in tissue engineering – EPNOE, 2023, poster
- [4.] Mohan T., Lackner, F.; Šurina P., Steindorfer T., Kargl R. and Stana Kleinschek K. Advanced surface and processing techniques for the design of multifunctional 2D and 3D polymeric materials – EPNOE, 2023, poster

## 7. ABBREVIATIONS

<b>3D</b>	three dimensional
<b>Alg</b>	alginate
<b>BC</b>	bacterial cellulose
<b>BCA</b>	bicinchoninic acid
<b>BSA</b>	bovine serum albumin
<b>CI</b>	cellulose I
<b>CII</b>	cellulose II
<b>CIII</b>	cellulose III
<b>CIV</b>	cellulose IV
<b>CNC</b>	cellulose nanocrystals
<b>CNF</b>	cellulose nanofibers
<b>D</b>	diffusion coefficient
<b>DIW</b>	direct ink writing
<b>DTAF</b>	dichlorotriazinyl aminofluorescein
<b>EDTA</b>	ethylenediaminetetraacetic acid
<b>GDL</b>	glucono- $\delta$ -lactone
<b>J</b>	flux
<b>MMD</b>	molecular mass distribution
<b>NFC</b>	nanofibrillated cellulose
<b>NMR</b>	nuclear magnetic resonance
<b>PBS</b>	phosphorus buffer solution
<b>PC</b>	plant cellulose
<b>PEG</b>	polyethyleneglycol
<b>RGD</b>	arginine-glycine-aspartate
<b>TLC</b>	thin layer chromatography
<b>TE</b>	tissue engineering
<b>WD</b>	wound dressing

## 8. LIST OF FIGURES

<b>Figure 1</b> Biomaterials throughout history until today <sup>10-12</sup> .....	3
<b>Figure 2 (a.)</b> Cellulose repeat unit showing $\beta$ 1 $\rightarrow$ 4 glycosidic bond <sup>22</sup> <b>(b.)</b> intermolecular (red) and intramolecular (blue) hydrogen bonding in cellulose <sup>30</sup> .....	5
<b>Figure 3</b> Schematic representation of the crystalline and amorphous region of cellulose, crystalline region is obtained by hydrogen bonds and Van der Waals forces, when they are disrupted amorphous region occurs .....	6
<b>Figure 4</b> Cellulose polymorphs conversions .....	7
<b>Figure 5</b> Plant cellulose hierarchical structure. Cellulose chains are bond together with hydrogen bonds and Van der Waals interactions forming microfibrils. Crystalline and amorphous regions aggregate and form fibrils which are held together with hemicellulose and lignin to form fibers. <sup>43</sup> .....	8
<b>Figure 6</b> Schematic representation of CNF and CNC production.....	8
<b>Figure 7</b> Alginate chemical structure <sup>65</sup> .....	11
<b>Figure 8</b> “Egg-box” structure as a result of interaction between alginate G blocks and Ca <sup>2+</sup> <sup>70</sup> ...	13
<b>Figure 9</b> Flow curves of Newtonian and non-Newtonian fluids .....	16
<b>Figure 10</b> GeSiM BioScaffolder 3.2. (GeSim, Germany) .....	21
<b>Figure 11</b> Used printhead with 4 different axis. Axis 7 which features Internal Heating (a.), Axis 5 with cartridge dispenser (50 mL) and plastic nozzle (410 $\mu$ m) (b.), Axis 3 that features Internal Cooler (c.) and Axis 1 (Piezo Pipette Nano, Z-sensor) (d.).....	21
<b>Figure 12</b> Target tray with the petri dish selected for printing (PointPrint_b) .....	22
<b>Figure 13</b> Different fiber alignment in scaffolds.....	23
<b>Figure 14</b> General settings for printing sheet scaffold.....	24
<b>Figure 15</b> Scaffold after crosslinking .....	25
<b>Figure 16</b> Hole punching tool .....	26
<b>Figure 17</b> Q-tec punching knife DIN 53504 S3A used to punch out scaffolds for tensile testing <sup>88</sup> .....	28
<b>Figure 18</b> Dimensions of the punched out scaffold ready for tensile testing according to DIN 53504 S3A <sup>88</sup> .....	29
<b>Figure 19</b> Motic: Panthera TEC MAT BD-T (6x4), microscope with Epi-LED fluorescence attachment <sup>89</sup> .....	30

**Figure 20** Diffusion cell..... 31

**Figure 21** Schematic illustration of column chromatography technique..... 37

**Figure 22** Remaining w% of calcium in the scaffolds leached in different leaching solutions at the end of the leaching process after five cycles. Line indicated the starting amount of calcium. .... 39

**Figure 23** Changes in w% of calcium in the different scaffolds (regarding different ink concentration) leached in different leaching solutions at the end of the leaching process after five cycles. .... 41

**Figure 24** Amount of calcium leached into the crosslinking solution and storage solutions in 24 hours for each solution for LOW, MEDIUM and HIGH inks leached in LOW Ca<sup>2+</sup>, MEDIUM Ca<sup>2+</sup> and HIGH Ca<sup>2+</sup> storage solutions. .... 41

**Figure 25** Tensile stress-strain curves for scaffolds stored in different storage solutions and with different fiber alignment. **Ca\_LOW**, **Ca\_MEDIUM** and **Ca\_HIGH** have longitudinal fiber alignment, whereas **Ca\_MEDIUM\_P** has perpendicular fiber alignment relative to the pulling direction. .... 44

**Figure 26** Comparison of the mechanical properties (maximum stress and tensile modulus) for scaffolds printed using **Medium ink** (**Table 4**) leached in different storage solutions (**Table 6**). Values on x-axis indicate remaining Ca concentration in w% after leaching. .... 45

**Figure 27** Cycle tests stress-strain graphs for scaffold with different fiber alignment (a. longitudinal, b. perpendicular and c. grid alignment) tested with speed 10 mm/min and 25 % strain ..... 46

**Figure 28** Cycle tests stress-strain graphs for scaffold with different fiber alignment (a. longitudinal, b. perpendicular and c. grid alignment) tested with speed 50 mm/min and 10 % strain ..... 47

**Figure 29** Cycle tests stress-strain graphs for scaffold with different fiber alignment (a. longitudinal, b. perpendicular and c. grid alignment) tested with speed 50 mm/min and 25 % strain ..... 47

**Figure 30** Maximum and minimum stress during cycle testing for (a.) speed 50 mm/min, strain 10%, (b.) speed 10 mm/min, strain 25% and (c.) speed 50 mm/min, strain 25% ..... 48

**Figure 31** Brightfield microscopic pictures of different ink components..... 49

**Figure 32** Darkfield microscopic pictures of ink with calcium carbonate (left) and without (right) ..... 49

**Figure 33** Concentration profiles over time for all tested substances..... 51

<b>Figure 34</b> Diffusion coefficient versus time and concentration versus time for sodium and calcium chloride .....	52
<b>Figure 35</b> Concentration versus time for riboflavin diffusion test through a. ZelluTrans membrane, b. 1 layered, c.2 layered and d. 3 layered scaffold membrane. ....	53
<b>Figure 36</b> Concentration versus time for dextran (10 kDa) diffusion test through a. ZelluTrans membrane, b. 1 layered, c. 2 layered and d. 3 layered scaffold membrane. ....	54
<b>Figure 37</b> Concentration versus time for BSA diffusion test through a. ZelluTrans membrane and b. 2 layered scaffold membrane .....	55
<b>Figure 38</b> Concentration versus time for glucose diffusion test through a. ZelluTrans membrane, b. 2 layered and c. 3 layered scaffold membrane. ....	56
<b>Figure 39</b> Cell viability test results tested for a. 24 hours and b. 48 hours on HEK 293 cells. ....	57
<b>Figure 40</b> Cell viability test results tested for a. 24 hours and b. 48 hours on HUVECs cells. ....	57
<b>Figure 41</b> Scaffolds in solutions described in <b>Table 8</b> immediately after putting them in the solutions and after 6 hours, 24 hours and 1 week .....	59
<b>Figure 42</b> Scaffolds in solutions described in <b>Table 8</b> with 100 mg of CaCl <sub>2</sub> in each immediately after putting them in the solutions and after 6 hours, 24 hours and 1 week. ....	60
<b>Figure 43</b> Scaffold degradation process using cellulase enzyme for (a.) approximately 100 mg of scaffold in distilled water with 1 mg of cellulase added and (b.) approximately 1,5 mL of scaffold dissolved in EDTA and 1 mg of cellulase added. ....	61
<b>Figure 44</b> Thin layer chromatography for (a.) G-glucose solution, C3-celotriose, C4-celotetraose, m-all samples mixed, EC-degraded scaffold in EDTA with added cellulase enzyme, E-EDTA and (b.) G-glucose, E-EDTA, S1-purified sample with methanol, S2-residue from S1, S3-purified S1 sample second time with ethanol, S4-residue from S3.....	62
<b>Figure 45</b> Chromatography fractions tested with TLC. No EDTA present in fractions. Fractions 5 and 6 collected for NMR. ....	62
<b>Figure 46</b> Structural formula of D-glucose and its anomeric configurations .....	63
<b>Figure 47</b> 300 MHz <sup>1</sup> H NMR spectra of the tested sample in D <sub>2</sub> O. ....	63
<b>Figure 48</b> NMR comparison of unknown sample (red) and known sample of glucose (green) ...	64

## 9. LIST OF TABLES

<b>Table 1</b> Comparison of different properties for plant and bacterial cellulose <sup>43</sup> .....	9
<b>Table 2</b> Plant and bacterial cellulose applications <sup>43</sup> .....	10
<b>Table 3</b> Alginate applications in various fields .....	14
<b>Table 4</b> Different inks used for 3D printing .....	20
<b>Table 5</b> Printing parameters for DIW (*different layered scaffolds were printed for different tests) .....	23
<b>Table 6</b> Storage solutions components .....	25
<b>Table 7</b> Calcium concentration in the ink and storage solution for Low, Medium, and High inks used for printing disks for cell viability testing .....	26
<b>Table 8</b> Solutions used for scaffold degradation process (pH values were set using 0,1 M NaOH) .....	35
<b>Table 9</b> Diffusion coefficients for NaCl, CaCl <sub>2</sub> , riboflavin, dextran (20 kDa), BSA and glucose measured through different membranes and compared to literature values. ....	50
<b>Table 10</b> Diffusion coefficients for NaCl and CaCl <sub>2</sub> for different membranes calculated at 8 hours. .....	52
<b>Table 11</b> Diffusion coefficients for riboflavin for different membranes calculated at 8 hours ....	53
<b>Table 12</b> Diffusion coefficients for glucose for different membranes calculated at 8 hours. ....	56
<b>Table 13</b> Column chromatography process data .....	62

## 10. References

- (1) Moon, R. J.; Martini, A.; Nairn, J.; Simonsen, J.; Youngblood, J. Cellulose nanomaterials review: structure, properties and nanocomposites. *Chemical Society reviews* **2011**, *40* (7), 3941–3994. DOI: 10.1039/c0cs00108b. Published Online: May. 12, 2011.
- (2) Lin, N.; Dufresne, A. Nanocellulose in biomedicine: Current status and future prospect. *European Polymer Journal* **2014**, *59*, 302–325. DOI: 10.1016/j.eurpolymj.2014.07.025.
- (3) Guang Yang; Muhammad Wajid Ullah and Zhijun Shi. *Nanocellulose: Synthesis, structure, properties and applications*; World Scientific, 2021.
- (4) Abitbol, T.; Rivkin, A.; Cao, Y.; Nevo, Y.; Abraham, E.; Ben-Shalom, T.; Lapidot, S.; Shoseyov, O. Nanocellulose, a tiny fiber with huge applications. *Current opinion in biotechnology* **2016**, *39*, 76–88. DOI: 10.1016/j.copbio.2016.01.002. Published Online: Feb. 28, 2016.
- (5) Chia, H. N.; Wu, B. M. Recent advances in 3D printing of biomaterials. *Journal of biological engineering* **2015**, *9*, 4. DOI: 10.1186/s13036-015-0001-4. Published Online: Mar. 1, 2015.
- (6) Lackner, F.; Knechtel, I.; Novak, M.; Nagaraj, C.; Dobaj Štiglic, A.; Kargl, R.; Olschewski, A.; Stana Kleinschek, K.; Mohan, T. 3D-Printed Anisotropic Nanofiber Composites with Gradual Mechanical Properties. *Adv Materials Technologies* **2023**, *4*, 2201708. DOI: 10.1002/admt.202201708.
- (7) Lee, K. Y.; Mooney, D. J. Alginate: properties and biomedical applications. *Progress in polymer science* **2012**, *37* (1), 106–126. DOI: 10.1016/j.progpolymsci.2011.06.003.
- (8) Novak, M. *3D printing, stabilization and characterization of nanofibrillated cellulose-alginate scaffolds*.
- (9) Ratner, B. D.; Bryant, S. J. Biomaterials: where we have been and where we are going. *Annual review of biomedical engineering* **2004**, *6*, 41–75. DOI: 10.1146/annurev.bioeng.6.040803.140027.
- (10) Vallet-Regí, M. Evolution of Biomaterials. *Front. Mater.* **2022**, *9*, 8605. DOI: 10.3389/fmats.2022.864016.
- (11) Todros, S.; Todesco, M.; Bagnò, A. Biomaterials and Their Biomedical Applications: From Replacement to Regeneration. *Processes* **2021**, *9* (11), 1949. DOI: 10.3390/pr9111949.
- (12) Navarro, M.; Michiardi, A.; Castaño, O.; Planell, J. A. Biomaterials in orthopaedics. *Journal of the Royal Society, Interface* **2008**, *5* (27), 1137–1158. DOI: 10.1098/rsif.2008.0151.
- (13) Hasanin, M. S. Cellulose-Based Biomaterials: Chemistry and Biomedical Applications. *Starch Stärke* **2022**, *74* (7-8), 2200060. DOI: 10.1002/star.202200060.

- (14) Millon, L. E.; Wan, W. K. The polyvinyl alcohol-bacterial cellulose system as a new nanocomposite for biomedical applications. *Journal of biomedical materials research. Part B, Applied biomaterials* **2006**, *79* (2), 245–253. DOI: 10.1002/jbm.b.30535.
- (15) Augst, A. D.; Kong, H. J.; Mooney, D. J. Alginate hydrogels as biomaterials. *Macromolecular bioscience* **2006**, *6* (8), 623–633. DOI: 10.1002/mabi.200600069.
- (16) Sun, J.; Tan, H. Alginate-Based Biomaterials for Regenerative Medicine Applications. *Materials (Basel, Switzerland)* **2013**, *6* (4), 1285–1309. DOI: 10.3390/ma6041285. Published Online: Mar. 26, 2013.
- (17) Ullah, S.; Chen, X. Fabrication, applications and challenges of natural biomaterials in tissue engineering. *Applied Materials Today* **2020**, *20*, 100656. DOI: 10.1016/j.apmt.2020.100656.
- (18) Nobles, D. R.; Romanovicz, D. K.; Brown, R. M. Cellulose in Cyanobacteria. Origin of Vascular Plant Cellulose Synthase? *Plant Physiology* **2001**, *127* (2), 529–542. DOI: 10.1104/pp.010557.
- (19) Payne, C. M.; Knott, B. C.; Mayes, H. B.; Hansson, H.; Himmel, M. E.; Sandgren, M.; Ståhlberg, J.; Beckham, G. T. Fungal cellulases. *Chemical reviews* **2015**, *115* (3), 1308–1448. DOI: 10.1021/cr500351c. Published Online: Jan. 28, 2015.
- (20) Zhao, Y.; Li, J. Excellent chemical and material cellulose from tunicates: diversity in cellulose production yield and chemical and morphological structures from different tunicate species. *Cellulose* **2014**, *21* (5), 3427–3441. DOI: 10.1007/s10570-014-0348-6.
- (21) Brown, R. M. Cellulose structure and biosynthesis: What is in store for the 21st century? *J. Polym. Sci. A Polym. Chem.* **2004**, *42* (3), 487–495. DOI: 10.1002/pola.10877.
- (22) Chami Khazraji, A.; Robert, S. Interaction Effects between Cellulose and Water in Nanocrystalline and Amorphous Regions: A Novel Approach Using Molecular Modeling. *Journal of Nanomaterials* **2013**, *2013* (3), 1–10. DOI: 10.1155/2013/409676.
- (23) Siqueira, G.; Bras, J.; Dufresne, A. Cellulosic Bionanocomposites: A Review of Preparation, Properties and Applications. *Polymers* **2010**, *2* (4), 728–765. DOI: 10.3390/polym2040728.
- (24) Mahmud, M. M.; Perveen, A.; Jahan, R. A.; Matin, M. A.; Wong, S. Y.; Li, X.; Arafat, M. T. Preparation of different polymorphs of cellulose from different acid hydrolysis medium. *International journal of biological macromolecules* **2019**, *130*, 969–976. DOI: 10.1016/j.ijbiomac.2019.03.027. Published Online: Mar. 4, 2019.
- (25) Assis, S. C. de; Morgado, D. L.; Scheidt, D. T.; Souza, S. S. de; Cavallari, M. R.; Ando Junior, O. H.; Carrilho, E. Review of Bacterial Nanocellulose-Based Electrochemical Biosensors:



Functionalization, Challenges, and Future Perspectives. *Biosensors* **2023**, *13* (1). DOI: 10.3390/bios13010142. Published Online: Jan. 14, 2023.

(26) Etale, A.; Onyianta, A. J.; Turner, S. R.; Eichhorn, S. J. Cellulose: A Review of Water Interactions, Applications in Composites, and Water Treatment. *Chemical reviews* **2023**, *123* (5), 2016–2048. DOI: 10.1021/acs.chemrev.2c00477. Published Online: Jan. 9, 2023.

(27) Medronho, B.; Lindman, B. Brief overview on cellulose dissolution/regeneration interactions and mechanisms. *Advances in colloid and interface science* **2015**, *222*, 502–508. DOI: 10.1016/j.cis.2014.05.004. Published Online: May. 28, 2014.

(28) Estela, R.; Luis, J. Hydrolysis of Biomass Mediated by Cellulases for the Production of Sugars. DOI: 10.5772/53719.

(29) Yu, Y.; Wu, H. Significant Differences in the Hydrolysis Behavior of Amorphous and Crystalline Portions within Microcrystalline Cellulose in Hot-Compressed Water. *Ind. Eng. Chem. Res.* **2010**, *49* (8), 3902–3909. DOI: 10.1021/ie901925g.

(30) Phanthong, P.; Reubroycharoen, P.; Hao, X.; Xu, G.; Abudula, A.; Guan, G. Nanocellulose: Extraction and application. *Carbon Resources Conversion* **2018**, *1* (1), 32–43. DOI: 10.1016/j.crcon.2018.05.004.

(31) O'sullivan A. C. Cellulose: the structure slowly unravels **1997**, 173–207.

(32) Wada, M.; Heux, L.; Sugiyama, J. Polymorphism of cellulose I family: reinvestigation of cellulose IVI. *Biomacromolecules* **2004**, *5* (4), 1385–1391. DOI: 10.1021/bm0345357.

(33) Jin, E.; Guo, J.; Yang, F.; Zhu, Y.; Song, J.; Jin, Y.; Rojas, O. J. On the polymorphic and morphological changes of cellulose nanocrystals (CNC-I) upon mercerization and conversion to CNC-II. *Carbohydrate polymers* **2016**, *143*, 327–335. DOI: 10.1016/j.carbpol.2016.01.048. Published Online: Jan. 25, 2016.

(34) V. V. Klechkovskaya, Yu. G. Baklagina, N. D. Stepina, A. K. Khripunov, P. A. Buffat, E. I. Suvorova, I. S. Zhanaveskina, A. A. Tkachenko, and S. V. Gladchenko. Structure of cellulose.

(35) Pinho, E.; Soares, G. Functionalization of cotton cellulose for improved wound healing. *Journal of materials chemistry. B* **2018**, *6* (13), 1887–1898. DOI: 10.1039/c8tb00052b. Published Online: Mar. 16, 2018.

(36) Chang, C.; Lue, A.; Zhang, L. Effects of Crosslinking Methods on Structure and Properties of Cellulose/PVA Hydrogels. *Macromol. Chem. Phys.* **2008**, *209* (12), 1266–1273. DOI: 10.1002/macp.200800161.

- (37) Abe, K.; Yano, H. Formation of hydrogels from cellulose nanofibers. *Carbohydrate polymers* **2011**, *85* (4), 733–737. DOI: 10.1016/j.carbpol.2011.03.028.
- (38) Carvalho, J. P. F.; Silva, A. C. Q.; Silvestre, A. J. D.; Freire, C. S. R.; Vilela, C. Spherical Cellulose Micro and Nanoparticles: A Review of Recent Developments and Applications. *Nanomaterials (Basel, Switzerland)* **2021**, *11* (10). DOI: 10.3390/nano11102744. Published Online: Oct. 17, 2021.
- (39) Naomi, R.; Bt Hj Idrus, R.; Fauzi, M. B. Plant- vs. Bacterial-Derived Cellulose for Wound Healing: A Review. *International journal of environmental research and public health* **2020**, *17* (18). DOI: 10.3390/ijerph17186803. Published Online: Sep. 18, 2020.
- (40) Salimi, S.; Sotudeh-Gharebagh, R.; Zarghami, R.; Chan, S. Y.; Yuen, K. H. Production of Nanocellulose and Its Applications in Drug Delivery: A Critical Review. *ACS Sustainable Chem. Eng.* **2019**, *7* (19), 15800–15827. DOI: 10.1021/acssuschemeng.9b02744.
- (41) Lahiri, D.; Nag, M.; Dutta, B.; Dey, A.; Sarkar, T.; Pati, S.; Edinur, H. A.; Abdul Kari, Z.; Mohd Noor, N. H.; Ray, R. R. Bacterial Cellulose: Production, Characterization, and Application as Antimicrobial Agent. *International journal of molecular sciences* **2021**, *22* (23). DOI: 10.3390/ijms222312984. Published Online: Nov. 30, 2021.
- (42) Hu, D.; Liu, X. B.; She, H. Z.; Gao, Z.; Ruan, R. W.; Wu, D. Q.; Yi, Z. L. The lignin synthesis related genes and lodging resistance of *Fagopyrum esculentum*. *Biologia plant.* **2017**, *61* (1), 138–146. DOI: 10.1007/s10535-016-0685-4.
- (43) Amorim, J. D. P. de; Souza, K. C. de; Duarte, C. R.; da Silva Duarte, I.; Assis Sales Ribeiro, F. de; Silva, G. S.; Farias, P. M. A. de; Stingl, A.; Costa, A. F. S.; Vinhas, G. M.; Sarubbo, L. A. Plant and bacterial nanocellulose: production, properties and applications in medicine, food, cosmetics, electronics and engineering. A review. *Environ Chem Lett* **2020**, *18* (3), 851–869. DOI: 10.1007/s10311-020-00989-9.
- (44) Yardrung Suwannarat , Waritchon Ninlanon, Rungtiwa Suwannarat and Komsan Muisee. Production of Bacterial Cellulose from *Acetobacter xylinum* by using Rambutan Juice as a Carbon Source.
- (45) Mishra, R. K.; Sabu, A.; Tiwari, S. K. Materials chemistry and the futurist eco-friendly applications of nanocellulose: Status and prospect. *Journal of Saudi Chemical Society* **2018**, *22* (8), 949–978. DOI: 10.1016/j.jscs.2018.02.005.

- (46) Esa, F.; Tasirin, S. M.; Rahman, N. A. Overview of Bacterial Cellulose Production and Application. *Agriculture and Agricultural Science Procedia* **2014**, *2* (2), 113–119. DOI: 10.1016/j.aaspro.2014.11.017.
- (47) Klemm, D.; Heublein, B.; Fink, H.-P.; Bohn, A. Cellulose: fascinating biopolymer and sustainable raw material. *Angewandte Chemie (International ed. in English)* **2005**, *44* (22), 3358–3393. DOI: 10.1002/anie.200460587.
- (48) Gibson, L. J. The hierarchical structure and mechanics of plant materials. *Journal of the Royal Society, Interface* **2012**, *9* (76), 2749–2766. DOI: 10.1098/rsif.2012.0341. Published Online: Aug. 8, 2012.
- (49) Feng, X.; Ullah, N.; Wang, X.; Sun, X.; Li, C.; Bai, Y.; Chen, L.; Li, Z. Characterization of Bacterial Cellulose by *Gluconacetobacter hansenii* CGMCC 3917. *Journal of food science* **2015**, *80* (10), E2217-27. DOI: 10.1111/1750-3841.13010. Published Online: Sep. 9, 2015.
- (50) Wang, J.; Tavakoli, J.; Tang, Y. Bacterial cellulose production, properties and applications with different culture methods - A review. *Carbohydrate polymers* **2019**, *219*, 63–76. DOI: 10.1016/j.carbpol.2019.05.008. Published Online: May. 7, 2019.
- (51) Endes, C.; Camarero-Espinosa, S.; Mueller, S.; Foster, E. J.; Petri-Fink, A.; Rothen-Rutishauser, B.; Weder, C.; Clift, M. J. D. A critical review of the current knowledge regarding the biological impact of nanocellulose. *Journal of nanobiotechnology* **2016**, *14* (1), 78. DOI: 10.1186/s12951-016-0230-9. Published Online: Dec. 1, 2016.
- (52) Ciolacu, D. E.; Nicu, R.; Ciolacu, F. Cellulose-Based Hydrogels as Sustained Drug-Delivery Systems. *Materials (Basel, Switzerland)* **2020**, *13* (22). DOI: 10.3390/ma13225270. Published Online: Nov. 21, 2020.
- (53) Mishra, R. K.; Sabu, A.; Tiwari, S. K. Materials chemistry and the futurist eco-friendly applications of nanocellulose: Status and prospect. *Journal of Saudi Chemical Society* **2018**, *22* (8), 949–978. DOI: 10.1016/j.jscs.2018.02.005.
- (54) Zmejkoski, D.; Spasojević, D.; Orlovska, I.; Kozyrovska, N.; Soković, M.; Glamočlija, J.; Dmitrović, S.; Matović, B.; Tasić, N.; Maksimović, V.; Sosnin, M.; Radotić, K. Bacterial cellulose-lignin composite hydrogel as a promising agent in chronic wound healing. *International journal of biological macromolecules* **2018**, *118* (Pt A), 494–503. DOI: 10.1016/j.ijbiomac.2018.06.067. Published Online: Jun. 15, 2018.

- (55) Bideau, B.; Loranger, E.; Daneault, C. Nanocellulose-polypyrrole-coated paperboard for food packaging application. *Progress in Organic Coatings* **2018**, *123* (1), 128–133. DOI: 10.1016/j.porgcoat.2018.07.003.
- (56) Sarwar, M. S.; Niazi, M. B. K.; Jahan, Z.; Ahmad, T.; Hussain, A. Preparation and characterization of PVA/nanocellulose/Ag nanocomposite films for antimicrobial food packaging. *Carbohydrate polymers* **2018**, *184*, 453–464. DOI: 10.1016/j.carbpol.2017.12.068. Published Online: Jan. 3, 2018.
- (57) Cazón, P.; Vázquez, M. Bacterial cellulose as a biodegradable food packaging material: A review. *Food Hydrocolloids* **2021**, *113* (11), 106530. DOI: 10.1016/j.foodhyd.2020.106530.
- (58) Henriette M. C. Azeredo. Bacterial cellulose for food applications: International Journal of Advances in Medical Biotechnology.
- (59) Albuquerque, P. B. S.; Oliveira, W. F. de; Dos Santos Silva, P. M.; Dos Santos Correia, M. T.; Kennedy, J. F.; Coelho, L. C. B. B. Skincare application of medicinal plant polysaccharides - A review. *Carbohydrate polymers* **2022**, *277*, 118824. DOI: 10.1016/j.carbpol.2021.118824. Published Online: Oct. 28, 2021.
- (60) Stasiak-Róžańska, L.; Płoska, J. Study on the Use of Microbial Cellulose as a Biocarrier for 1,3-Dihydroxy-2-Propanone and Its Potential Application in Industry. *Polymers* **2018**, *10* (4). DOI: 10.3390/polym10040438. Published Online: Apr. 14, 2018.
- (61) Chantereau, G.; Sharma, M.; Abednejad, A.; Vilela, C.; Costa, E. M.; Veiga, M.; Antunes, F.; Pintado, M. M.; Sèbe, G.; Coma, V.; Freire, M. G.; Freire, C.S.R.; Silvestre, A.J.D. Bacterial nanocellulose membranes loaded with vitamin B-based ionic liquids for dermal care applications. *Journal of Molecular Liquids* **2020**, *302* (4), 112547. DOI: 10.1016/j.molliq.2020.112547.
- (62) Hisseine, O. A.; Wilson, W.; Sorelli, L.; Tolnai, B.; Tagnit-Hamou, A. Nanocellulose for improved concrete performance: A macro-to-micro investigation for disclosing the effects of cellulose filaments on strength of cement systems. *Construction and Building Materials* **2019**, *206* (11), 84–96. DOI: 10.1016/j.conbuildmat.2019.02.042.
- (63) Grishkewich, N.; Mohammed, N.; Tang, J.; Tam, K. C. Recent advances in the application of cellulose nanocrystals. *Current Opinion in Colloid & Interface Science* **2017**, *29*, 32–45. DOI: 10.1016/j.cocis.2017.01.005.
- (64) Xie, Y.; Zheng, Y.; Fan, J.; Wang, Y.; Yue, L.; Zhang, N. Novel Electronic-Ionic Hybrid Conductive Composites for Multifunctional Flexible Bioelectrode Based on in Situ Synthesis of

Poly(dopamine) on Bacterial Cellulose. *ACS applied materials & interfaces* **2018**, *10* (26), 22692–22702. DOI: 10.1021/acsami.8b05345. Published Online: Jun. 21, 2018.

(65) Eskens, O.; Villani, G.; Amin, S. Rheological Investigation of Thermoresponsive Alginate-Methylcellulose Gels for Epidermal Growth Factor Formulation. *Cosmetics* **2021**, *8* (1), 3. DOI: 10.3390/cosmetics8010003.

(66) Guo, Y.; Bae, J.; Fang, Z.; Li, P.; Zhao, F.; Yu, G. Hydrogels and Hydrogel-Derived Materials for Energy and Water Sustainability. *Chemical reviews* **2020**, *120* (15), 7642–7707. DOI: 10.1021/acs.chemrev.0c00345. Published Online: Jul. 8, 2020.

(67) Abasalizadeh, F.; Moghaddam, S. V.; Alizadeh, E.; Akbari, E.; Kashani, E.; Fazljou, S. M. B.; Torbati, M.; Akbarzadeh, A. Alginate-based hydrogels as drug delivery vehicles in cancer treatment and their applications in wound dressing and 3D bioprinting. *Journal of biological engineering* **2020**, *14*, 8. DOI: 10.1186/s13036-020-0227-7. Published Online: Mar. 13, 2020.

(68) Zhang, X.; Wang, K.; Hu, J.; Zhang, Y.; Dai, Y.; Xia, F. Role of a high calcium ion content in extending the properties of alginate dual-crosslinked hydrogels. *J. Mater. Chem. A* **2020**, *8* (47), 25390–25401. DOI: 10.1039/D0TA09315G.

(69) Navarro-Requena, C.; Pérez-Amodio, S.; Castaño, O.; Engel, E. Wound healing-promoting effects stimulated by extracellular calcium and calcium-releasing nanoparticles on dermal fibroblasts. *Nanotechnology* **2018**, *29* (39), 395102. DOI: 10.1088/1361-6528/aad01f.

(70) Auriemma, G.; Russo, P.; Del Gaudio, P.; García-González, C. A.; Landín, M.; Aquino, R. P. Technologies and Formulation Design of Polysaccharide-Based Hydrogels for Drug Delivery. *Molecules (Basel, Switzerland)* **2020**, *25* (14). DOI: 10.3390/molecules25143156. Published Online: Jul. 10, 2020.

(71) Stress relaxation behavior in gels with ionic and covalent crosslinks.

(72) Wang, F.; Li, Y.; Shen, Y.; Wang, A.; Wang, S.; Xie, T. The functions and applications of RGD in tumor therapy and tissue engineering. *International journal of molecular sciences* **2013**, *14* (7), 13447–13462. DOI: 10.3390/ijms140713447. Published Online: Jun. 27, 2013.

(73) Abka-Khajouei, R.; Tounsi, L.; Shahabi, N.; Patel, A. K.; Abdelkafi, S.; Michaud, P. Structures, Properties and Applications of Alginates. *Marine drugs* **2022**, *20* (6). DOI: 10.3390/md20060364. Published Online: May. 29, 2022.

(74) Teraoka I. *Polymer Solutions An Introduction to Physical Properties*; John Wiley & Sons, Inc., 2002.

- (75) Hernández-Sosa, A.; Ramírez-Jiménez, R. A.; Rojo, L.; Boulmedais, F.; Aguilar, M. R.; Criado-Gonzalez, M.; Hernández, R. Optimization of the Rheological Properties of Self-Assembled Tripeptide/Alginate/Cellulose Hydrogels for 3D Printing. *Polymers* **2022**, *14* (11). DOI: 10.3390/polym14112229. Published Online: May. 30, 2022.
- (76) Leu Alexa, R.; Ianchis, R.; Savu, D.; Temelie, M.; Trica, B.; Serafim, A.; Vlasceanu, G. M.; Alexandrescu, E.; Preda, S.; Iovu, H. 3D Printing of Alginate-Natural Clay Hydrogel-Based Nanocomposites. *Gels (Basel, Switzerland)* **2021**, *7* (4). DOI: 10.3390/gels7040211. Published Online: Nov. 14, 2021.
- (77) Stepto, R. F. T. Dispersity in polymer science (IUPAC Recommendations 2009). *Pure and Applied Chemistry* **2009**, *81* (2), 351–353. DOI: 10.1351/PAC-REC-08-05-02.
- (78) Xie, Y.; Park, J.-s.; Kang, S.-k. Studies on the Effect of Molecular Weight on Biodegradable Polymer Membrane. *IJBSBT* **2016**, *8* (3), 315–322. DOI: 10.14257/ijbsbt.2016.8.3.32.
- (79) DOBRYNIN, A.; RUBINSTEIN, M. Theory of polyelectrolytes in solutions and at surfaces. *Progress in polymer science* **2005**, *30* (11), 1049–1118. DOI: 10.1016/j.progpolymsci.2005.07.006.
- (80) Vos, P. de; Bucko, M.; Gemeiner, P.; Navrátil, M.; Svitel, J.; Faas, M.; Strand, B. L.; Skjak-Braek, G.; Morch, Y. A.; Vikartovská, A.; Lacík, I.; Kolláriková, G.; Orive, G.; Poncelet, D.; Pedraz, J. L.; Ansorge-Schumacher, M. B. Multiscale requirements for bioencapsulation in medicine and biotechnology. *Biomaterials* **2009**, *30* (13), 2559–2570. DOI: 10.1016/j.biomaterials.2009.01.014. Published Online: Feb. 7, 2009.
- (81) Laurén, P.; Somersalo, P.; Pitkänen, I.; Lou, Y.-R.; Urtti, A.; Partanen, J.; Seppälä, J.; Madetoja, M.; Laaksonen, T.; Mäkitie, A.; Yliperttula, M. Nanofibrillar cellulose-alginate hydrogel coated surgical sutures as cell-carrier systems. *PLoS one* **2017**, *12* (8), e0183487. DOI: 10.1371/journal.pone.0183487. Published Online: Aug. 22, 2017.
- (82) Xu, W.; Zhu, Y.; Ravichandran, D.; Jambhulkar, S.; Kakarla, M.; Bawareth, M.; Lanke, S.; Song, K. Review of Fiber-Based Three-Dimensional Printing for Applications Ranging from Nanoscale Nanoparticle Alignment to Macroscale Patterning. *ACS Appl. Nano Mater.* **2021**, *4* (8), 7538–7562. DOI: 10.1021/acsanm.1c01408.
- (83) Masoumi, N.; Copper, D.; Chen, P.; Cubberley, A.; Guo, K.; Lin, R.-Z.; Ahmed, B.; Martin, D.; Aikawa, E.; Melero-Martin, J.; Mayer, J. Elastomeric Fibrous Hybrid Scaffold Supports In Vitro and In Vivo Tissue Formation. *Advanced functional materials* **2017**, *27* (27). DOI: 10.1002/adfm.201606614. Published Online: Jun. 5, 2017.

- (84) Khatri, N. R.; Islam, M. N.; Cao, P.-F.; Advincula, R. C.; Choi, W.; Jiang, Y. Integrating helicoid channels for passive control of fiber alignment in direct-write 3D printing. *Additive Manufacturing* **2021**, *48*, 102419. DOI: 10.1016/j.addma.2021.102419.
- (85) Yan, J.; Demirci, E.; Gleadow, A. 3D short fibre orientation for universal structures and geometries in material extrusion additive manufacturing. *Additive Manufacturing* **2023**, *69*, 103535. DOI: 10.1016/j.addma.2023.103535.
- (86) Ee, L. Y.; Yau Li, S. F. Recent advances in 3D printing of nanocellulose: structure, preparation, and application prospects. *Nanoscale advances* **2021**, *3* (5), 1167–1208. DOI: 10.1039/d0na00408a. Published Online: Dec. 28, 2020.
- (87) Saadi, M. A. S. R.; Maguire, A.; Pottackal, N. T.; Thakur, M. S. H.; Ikram, M. M.; Hart, A. J.; Ajayan, P. M.; Rahman, M. M. Direct Ink Writing: A 3D Printing Technology for Diverse Materials. *Advanced materials (Deerfield Beach, Fla.)* **2022**, *34* (28), e2108855. DOI: 10.1002/adma.202108855. Published Online: Apr. 28, 2022.
- (88) Q-tec GmbH, "Cutting die, DIN 53504 S3A", <https://q-tec-gmbh.de/en/products/cutting-die/din-53504/din-53504-s3a/>.
- (89) Moticeurope, "Panthera TEC MAT BD-T" <https://moticeurope.com/en/panthera-tec-mat-bd-t-6x4.html>,
- (90) Rouwkema, J.; Koopman, B.; Blitterswijk, C.; Dhert, W.; Malda, J. Supply of nutrients to cells in engineered tissues. *Biotechnology & genetic engineering reviews* **2010**, *26*, 163–178. DOI: 10.5661/bger-26-163.
- (91) Bensefelt, T.; Wågberg, L. Unidirectional Swelling of Dynamic Cellulose Nanofibril Networks: A Platform for Tunable Hydrogels and Aerogels with 3D Shapeability. *Biomacromolecules* **2019**, *20* (6), 2406–2412. DOI: 10.1021/acs.biomac.9b00401. Published Online: May. 17, 2019.
- (92) Somasekharan, L. T.; Raju, R.; Kumar, S.; Geevarghese, R.; Nair, R. P.; Kasoju, N.; Bhatt, A. Biofabrication of skin tissue constructs using alginate, gelatin and diethylaminoethyl cellulose bioink. *International journal of biological macromolecules* **2021**, *189*, 398–409. DOI: 10.1016/j.ijbiomac.2021.08.114. Published Online: Aug. 20, 2021.
- (93) Junker, J. P. E.; Kamel, R. A.; Caterson, E. J.; Eriksson, E. Clinical Impact Upon Wound Healing and Inflammation in Moist, Wet, and Dry Environments. *Advances in wound care* **2013**, *2* (7), 348–356. DOI: 10.1089/wound.2012.0412.

- (94) Aparajita Singh; Sajal Halder; Geetha R. Menon; Sunil Chumber; Mahesh Chandra Misra; Lalit Kumar Sharma; Anurag Srivastava. Meta-analysis of Randomized Controlled Trials on Hydrocolloid Occlusive Dressing Versus Conventional Gauze Dressing in the Healing of Chronic Wounds **2004**, 27, 326–332.
- (95) Susilo, M. E.; Paten, J. A.; Sander, E. A.; Nguyen, T. D.; Ruberti, J. W. Collagen network strengthening following cyclic tensile loading. *Interface focus* **2016**, 6 (1), 20150088. DOI: 10.1098/rsfs.2015.0088.
- (96) Graiver, N.; Pinotti, A.; Califano, A.; Zaritzky, N. Diffusion of sodium chloride in pork tissue. *Journal of Food Engineering* **2006**, 77 (4), 910–918. DOI: 10.1016/j.jfoodeng.2005.08.018.
- (97) Pineda Hernandez, A. Diffusion of a Salt in an Aqueous Media:Chemical Engineering Undergraduate Honors Theses **2022**.
- (98) Ribeiro, A. C.F.; Barros, M. C.F.; Teles, A. S.N.; Valente, A. J.M.; Lobo, V. M.M.; Sobral, A. J.F.N.; Estes, M. A. Diffusion coefficients and electrical conductivities for calcium chloride aqueous solutions at 298.15K and 310.15K. *Electrochimica Acta* **2008**, 54 (2), 192–196. DOI: 10.1016/j.electacta.2008.08.011.
- (99) Stoppel, W. L.; White, J. C.; Horava, S. D.; Bhatia, S. R.; Roberts, S. C. Transport of biological molecules in surfactant-alginate composite hydrogels. *Acta biomaterialia* **2011**, 7 (11), 3988–3998. DOI: 10.1016/j.actbio.2011.07.009. Published Online: Jul. 14, 2011.
- (100) Ping Xia; Peter M. Bungay; Carter C. Gibson; Olga N. Kovbasnjuk; Kenneth R. Spring. Diffusion Coefficients in the Lateral Intercellular Spaces of Madin-Darby Canine Kidney Cell Epithelium Determined with Caged Compounds **1998**, 74, 3302–3312.
- (101) M. Arrio-Dupont; S. Cribier; G. Foucault; P.F. Devaux; A. d'Albis. Diffusion of fluorescently labeled macromolecules in cultured muscle cells **1996**, 70, 2327–2332.
- (102) Dhanya, N. P.; Sasikumar, P. R. Mutual Diffusion Studies of Bovine Serum Albumin in Water at Different Concentrations and pH with Laser Beam Deflection **2018**, 8 (3), 41–46.
- (103) Axelsson, A.; Persson, B. Determination of effective diffusion coefficients in calcium alginate gel plates with varying yeast cell content. *Appl Biochem Biotechnol* **1988**, 18 (1), 231–250. DOI: 10.1007/BF02930828.
- (104) Howard, D.; Buttery, L. D.; Shakesheff, K. M.; Roberts, S. J. Tissue engineering: strategies, stem cells and scaffolds. *Journal of anatomy* **2008**, 213 (1), 66–72. DOI: 10.1111/j.1469-7580.2008.00878.x. Published Online: Apr. 15, 2008.



(105) Zhu, Y.; Zajicek, J.; Serianni, A. S. Acyclic forms of 1-(13)Caldohexoses in aqueous solution: quantitation by (13)C NMR and deuterium isotope effects on tautomeric equilibria. *The Journal of organic chemistry* **2001**, *66* (19), 6244–6251. DOI: 10.1021/jo010541m.

(106) Alexandersson, E.; Nestor, G. Complete 1H and 13C NMR spectral assignment of d-glucofuranose. *Carbohydrate research* **2022**, *511*, 108477. DOI: 10.1016/j.carres.2021.108477. Published Online: Nov. 9, 2021.

(107) H., V. Unravelling Glycobiology by NMR Spectroscopy. DOI: 10.5772/48136.

## 11. METHODOICAL PART

### Detailed lesson plan

**First and last name:** Paola Šurina

**Date:** September 2023

#### Lecture topic

3D printing of biomaterials

#### Aim of the lesson

Introduce students to direct ink writing and properties that materials must have for such purpose.

#### Misconceptions found in literature

1. ***“3D printing is great but it only makes plastic objects.”/“Direct ink writing (DIW) is only for ink-type substances.”***

The cartridges that feed a 3D printing machine can be loaded with many materials other than plastic, for example: clay, cement, silicone, biomaterials and even chocolate and sugar.

While it is called “ink writing”, DIW can use a wide range of materials, including metals, ceramics, and polymers, depending on the printer and application. Selection of materials continues to expand as researchers develop new ink formulations.

2. ***“I understand that soon human hearts can be 3D printed.”***

A replica of the human heart can be printed, but this does not mean that it will function in the human body.

3. ***“Plastic is another name for polymer.”***

While all plastics are polymers, not all polymers are plastic. Polymers are long chains of molecules. The chains may be composed of monomers that form plastics, but many biomolecules also polymerize to form starches (polymers of sugars), proteins (polymers of amino acids), and DNA (polymers of nucleotides). Additionally, films, paints, elastomers, fibres, gels, and adhesives are all polymers.

4. ***“All biomaterials are natural”***

While some biomaterials are derived from natural sources like cellulose, collagen and silk, many are synthetic (e.g. polyethylene, silicone) or a combination of synthetic and natural materials.

5. ***“All biomaterials for biomedical application have to have the same properties.”***

Not all biomaterials for biomedical applications have to have the same properties. The properties are tailored to meet specific requirements based on the intended use. Different biomedical applications demand distinct properties, and biomaterials are customized accordingly.

6. ***“Because paper can be easily recycled, there is no need to cut down new trees.”***

It is true that paper can be recycled; however, the fibers in paper products cannot be recycled infinitely. Most paper fibers can only be used and recycled about 4 to 6 times before they become so short that they are no longer useful. Paper manufacturers must use some new fibers in their products; the percent of new fibers required is dependent upon the specific paper product.

Certainly, by recycling most of the paper used, the number of new fibers from trees is greatly reduced, but there will always be a need for new, replacement fibers even if demand for paper products remains at a constant level.

**7. “3D bioprinting is a fully mature technology.”**

While promising, 3D bioprinting is still evolving and faces technical challenges that need to be addressed before widespread clinical use.

**8. “3D bioprinting gives us instant product.”**

People sometimes expect immediate results from 3D bioprinting. However, there is a lot going on before and after actual printing process such as ink preparation before and crosslinking after printing.

**Keywords students should know**

Polymers, biomaterials

**Keywords students should adopt throughout this lecture**

Direct ink writing, 3D printing, Bingham plastic, shear thickening and thinning, yield stress, crosslinking, anisotropy, maximum tensile strength

**Limitations – difficulties that can occur throughout this lecture**

Due to the multidisciplinary nature of the lesson difficulties in understanding might occur therefore it is important to carefully go over each chapter of the POGIL worksheet and fulfil student’s knowledge.

Not being able to show the whole printing process and samples in real life might create difficulties for students to understand and visualize the process of 3D bioprinting. However, animations and videos will help with that.

A lot of keywords and concepts are introduced to students in this lecture which could cause information overload on students. For that reason, this lecture can be divided into several parts depending on the teacher’s assessment and students’ concentration.

**Basic concepts (basic ideas)**

- 3D bioprinting is an innovative technology that combines 3D printing with biology and chemistry to create structures, tissues and even organs for biomedical applications.
- Direct ink writing (DIW) is a part of 3D printing technology that represents an extrusion-based additive manufacturing (AM) process that allows a wide range of materials to be fabricated into desired 3D structures. Different materials in the form of inks can be extruded through small nozzle layer by layer until the software designed structure is obtained.
- Rheology is an important factor that affects 3D printing process and outcome. These includes viscosity, shear thinning behaviour, and yield stress.
- Crosslinking is a process in which polymer chains are chemically or physically linked creating a stronger and more stable material.
- Cellulose, known for its biocompatibility, biodegradability and mechanical strength has emerged as a promising material for 3D manufacturing in field of biomedicine and tissue engineering.
- Anisotropic materials have different properties in different directions. It is the opposite of isotropic. Wood and composite materials are good examples of anisotropic materials. For

example, it is easier to break a piece of wood along the grain (parallel to the wood fibers) than across the grain. This is because wood fibers provide structural strength along the grain. Properties of these materials are dependent on directions; it means they show different properties in different directions. This type of behavior of these materials is called anisotropy.

- Tensile Testing is a form of tension testing and is a destructive engineering and materials science test whereby controlled tension is applied to a sample until it fully fails. This is one of the most common mechanical testing techniques.

### **Lecture outcomes**

- I-1.** To understand 3D printing process step by step.
- I-2.** To develop an understanding regarding the characteristics of the materials to be used as biomaterial.
- I-3.** To understand the shear stress vs. shear rate graph for Bingham plastic, Newtonian fluids, dilatant and pseudoplastic fluids.
- I-4.** To describe events that occur while crosslinking at submicroscopic level and link them with macroscopic results.
- I-5.** To give examples of materials/objects with anisotropic behavior.

### **Activity/question for outcome check**

- I-1.** Arrange the following steps in the correct order for 3D printing:
  - \_\_\_ post processing - cooling and/or solidifying the material
  - \_\_\_ preparing/designing the 3D model
  - \_\_\_ 3D printing
  - \_\_\_ selecting/designing the material for printing
  - \_\_\_ testing
  - \_\_\_ setting up the 3D printer
- I-2.** Name some of the properties hydrogels have to possess to be applicable in biomedicine.
- I-3.** Use empty graphs to draw shear stress vs shear rate curves for samples you were given (toothpaste, icing, honey/corn syrup and corn starch).
- I-4.** Show the calcium crosslinking between two alginate polymer chains.
- I-5.** Name at least two examples of an anisotropic objects/materials.

### **Submicroscopic and macroscopic linkage**

By examining and comparing **SAMPLE 1** (ink) and **SAMPLE 2** (crosslinked specimen) students are noticing differences in physical properties such as stiffness, shape and elasticity. After looking at the crosslinking scheme in the POGIL sheet, they are getting insight into submicroscopic explanation of crosslinking that is explaining the differences between **SAMPLE 1** and **SAMPLE 2**.

### Articulation (lecture preview)

<b>STRUCTURAL ELEMENT OF THE LECTURE</b>	<b>STUDENT ACTIVITIES</b>	<b>SOCIOLOGICAL FORM OF TEACHING</b>	<b>DURATION</b>
Introduction	Listening, thinking, concluding	Frontal work, conversation method	7
Body	Predicting, observing, analysing, thinking, concluding, listening, problem solving	Group activities, individual activities, conversation method, frontal work	73
Repetition	Connecting, analysing, thinking and solving tasks and problems	<i>Individual activities, conversation method, frontal work</i>	10

### Elaboration of the lecture by sources of knowledge and key terms

#### Source of knowledges

<b>Source of knowledge</b>		<b>A concrete description of what is to be achieved with each of the mentioned source of knowledge (list the advantages and possible disadvantages)</b>
type	Meaning	
PPT slide 1 (pictures), Cellulose (in a form of sponge or pulp), PLA (surgical sutures), contact lenses (PMMA, silicone hydrogel polymers), alginate, titanium alloy	Examples of biomaterials	By presenting these materials to the students (either at PPT or in person, if possible), I will ask them what they are, what they are used for, and what they are made of. If necessary, I will let students use Internet search engines on their phones to help them. Further, I am asking them what are the methods for making contact lenses or hip replacements. I expect answers as cutting, machining, refining or by using mould (for contact lenses). I am leading students to conclude that they can also be 3D printed for better customization and reduction of waste. These materials and products will help students become familiar with the lecture topic and help them get started with the POGIL worksheet.

or cobalt chrome (hip replacement picture) ...		
PPT slide 2	Lecture topic	Students are introduced with lecture topic.
Task 1	“3D printing” section of the POGIL	Students get insight on how 3D printing technology works and understanding of direct ink writing as a category of 3D printing. Also, they are introduced to 3D bioprinting by thinking and analysing and discussing about the word “bioprinting”.
PPT slide 3, video 1, 2	Direct ink writing	Animations will help students visualize DIW process. This animation is also used in “ <i>Rheology of the ink for DIW</i> ” section of the POGIL for students to conclude what rheological properties and viscosity ink must possess.
Task 2	“ <i>Biomaterials in bioprinting</i> ” section of the POGIL	By series of questions students are concluding the importance of 3D printing for medical purposes and properties that biomaterials must have. Also, appropriate rheological properties are discussed in this section.
Task 3	“ <i>Rheology of the ink for DIW</i> ” section of the POGIL	Students are getting introduced in rheological properties of the ink used for DIW. They are learning about shear stress and shear rate, as well as shear thinning and shear thickening behaviour. They will also learn how to draw a shear stress vs. shear rate graph for Bingham plastic, dilatant, Newtonian fluid and pseudoplastic fluid.
Task 4	“ <i>Polymer crosslinking</i> ” section of the POGIL, “ <i>ALGINATE WORMS</i> ” experiment	By doing experiment “ <i>ALGINATE WORMS</i> ” students will get an insight on polymer crosslinking. Also, critical thinking which is a result of the questions asked through this sections student will conclude the importance of the polymer crosslinking for its further applications. By drawing the calcium crosslinked polymer chains, students will get better understanding at microscopic events during crosslinking process (sodium and alginate exchange).
SAMPLE 1	Ink used for 3D bioprinting	Students will notice viscosity of the ink and its possibility to flow making it suitable for printing.
SAMPLE 2	Crosslinked scaffold prepared from the ink representing SAMPLE 1	Looking and feeling the SAMPLE 2 students can notice that crosslinked scaffold is solid and stiff structure when comparing to the SAMPLE 1. That observation helps them to understand crosslinking process and result of the crosslinking.
PPT slide 4 and 5, video 3, 4 and video 5	Videos of the SAMPLE 1 and SAMPLE 2	Only used if it is not possible to show SAMPLE 1 and SAMPLE 2 in person. It shows differences between physical properties between ink and crosslinked scaffolds.

Task 5	“ <i>Isotropic and anisotropic materials</i> ” section of the POGIL	Students will learn about isotropic and anisotropic behaviour of materials. They will be able to give examples of anisotropic materials and their behaviour. They will also be introduced to tensile testing by completing the tasks with tensile testing results.
PPT slide 6, video 6 and 7	Tensile testing video	Students can now visualize the tensile testing experiment.
Task 6	“ <i>Tensile testing</i> ” section of the POGIL	This section is closely related to the previous one. It helps student to understand the importance of anisotropic behaviour of material. Students will be introduced to stress/strain graph, yield point and maximum tensile strength. They will also be able to read stress strain graphs after completing tasks in this section.
Worksheet	Questions for repetition	Gives feedback

## Keywords

KEYWORD	A detailed description of how the students will be led to understand the key concept (specify teaching methods, cognitive procedures, pictures, diagrams, graphs, animations...)
Direct ink writing	By reading the introduction part of “ <i>3D printing</i> ” and watching animation on PPT
3D bioprinting	Witt critical thinking induced by question: “ <i>What do you think prefix bio- in bioprinting stands for and what does it refers to?</i> ”, and discussing with their team students will conclude that bio stands for biology or biological and it refers to the use of biological materials and that bioprinting refers to creating structures and tissues that mimic natural ones.
Bingham plastic, shear thinning and thickening	With the help of the graph in task 9. students will conclude the differences in those three terms. Also, during the experiment described in task 11. they will observe the behaviour of each term described and link it to the material observed.
Shear stress, shear rate and yield stress	Those terms are described in the introduction part of the “ <i>Rheology of the ink for DIW</i> ” with provided examples in order to complement the understandings. From the task 9. they will get introduced with symbols and measuring units of the shear rate and shear stress.
Crosslinking	“ <i>ALGINATE WORMS</i> ” experiment nicely shows crosslinking process of alginate polymer. When pouring sodium alginate suspension into the calcium chloride solution students will observe how alginate thickens and takes on a gel like texture. When transferring alginate into the sodium chlorine solution they will observe dissolving of alginate which indicates exchange of the calcium and sodium ions important for crosslinking process.
Anisotropy	Anisotropy is described in the “ <i>Isotopic and anisotropic materials</i> ” section. Students will think about everyday object that have anisotropic behaviour and, in that way, get a better understanding. Also, when checking the

	answers, they will explain why are those objects/materials anisotropic with the teachers help which will also deepen their understandings.
Maximum tensile strength	This term will be explained in the introduction part of the “ <i>Tensile testing</i> ” section.

### **Lecture flow:**

#### **INTRODUCTION:**

To start the class, I am presenting some of the examples of biomaterials and their use. Following I will ask the students several questions: “What do you see?”, “What are this product made of?”, “What are the methods of making some of these products?” ... By series of questions I am leading students into the 3D printing as a topic of this lesson focusing on biomaterials used for such purpose.

#### **BODY:**

Lecture is based on the POGIL workshop, which prompts students to think and come to their own conclusions. As a teacher I am leading students on a right track and if necessary asking additional questions and using a conversation method to fulfil their understandings.

#### **END:**

Students are answering questions and tasks to get an insight of their understanding.

### **Student record plan**

Students are writing everything in their POGIL worksheets.

### **Emotional assessment**

I expect that the students will be very interested in the topic and will ask many questions.

### **Homework**

Repetition sheet if not completed in the lecture. Evaluation should be done at the beginning of the next lecture.

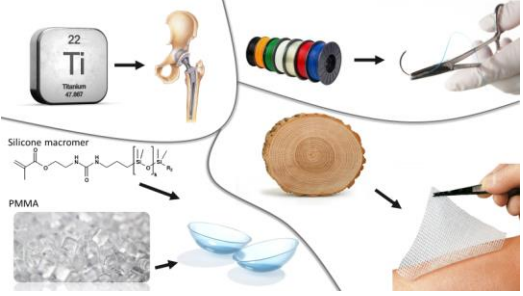

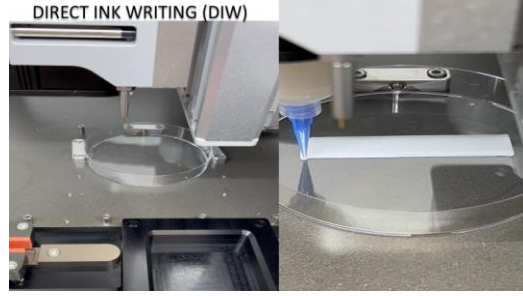
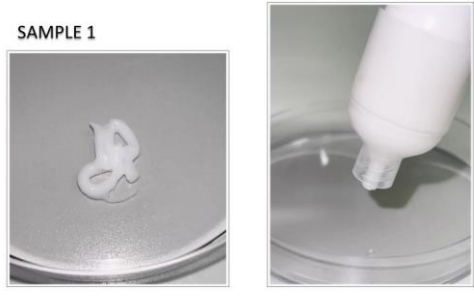
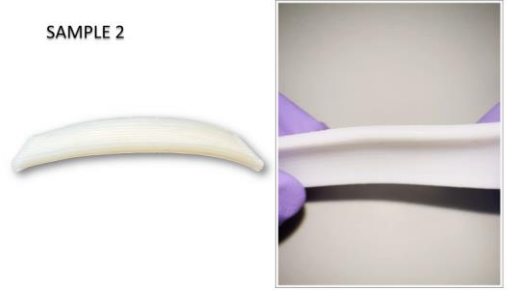
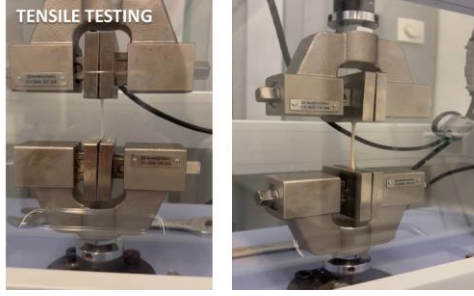
### **Literature**

- [1.] Šurina, P. *Optimization and in-depth analysis of alginate nanocellulose hydrogels for 3D printing of vascular and integumentary systems*, Master thesis, September 2023
- [2.] Lackner, F.; Šurina P.; Fink J.; Kotzbeck P.; Stana J.; Grab M.; Tsilimparis N.; Mohan T.; Stana Kleinschek K. and Kargl R. *4-Axis 3D printing of tubular vascular tissue models and cell culture substrates with anisotropic nanofiber orientation* – manuscript under review, August 2023



**Additions**

**PPT**

<p><b>1.</b></p>  <p>22 <b>Ti</b> Titanium 47.88</p> <p>Silicone macromer</p> <p>PMMA</p>	<p><b>2.</b></p>  <p>3D printing of biomaterials</p>
<p><b>3.</b></p> <p>DIRECT INK WRITING (DIW)</p> 	<p><b>4.</b></p> <p>SAMPLE 1</p> 
<p><b>5.</b></p> <p>SAMPLE 2</p> 	<p><b>6.</b></p> <p>TENSILE TESTING</p> 

## POGIL worksheet

Name and surname: \_\_\_\_\_

Date: \_\_\_\_\_

# 3D BIOPRINTING OF BIOMATERIALS

## 3D printing

*3D printing is an innovative manufacturing process that builds objects layer by layer, typically from digital designs. Direct ink writing (DIW) is a specific 3D printing technique that precisely deposits materials in form of ink or paste through nozzle to build a three-dimensional structure. This method is known for versatility and its applications in fields like biomedicine, architecture and advanced materials development.*

1. **What is the difference between a 3D printer and traditional inkjet printer?**

---

---

2. **Why is 3D printing also referred as additive layer manufacturing?**

---

3. **Arrange the following steps in the correct order for 3D printing process:**

- \_\_\_ post processing – crosslinking, cooling and/or solidifying the material
- \_\_\_ preparing/designing the 3D model
- \_\_\_ 3D printing
- \_\_\_ selecting/designing the material for printing
- \_\_\_ testing
- \_\_\_ setting up the 3D printer

4. **Name at least 5 everyday object that can be 3D printed.**

---

---

5. **What do you think prefix bio- in bioprinting stands for and what does it refers to?**

---

---

---

## Biomaterials in bioprinting

*Biomaterials in bioprinting are specialized materials designed to interact with and support living cells and tissues during and after 3D printing process. They serve as a building blocks for creating functional and biocompatible structures, making bioprinting promising technology for applications in regenerative medicine and tissue engineering.*

6. **What do you think what properties do biomaterials have to possess to:**
- a) be printable (*to be able to extrude them by pressure from the nozzle onto the printing surface*)?  
\_\_\_\_\_
- b) be compatible with living cells and tissues? \_\_\_\_\_
7. **Are there any environmental benefits of 3D printing with biodegradable materials compared to traditional manufacturing methods? If yes, what are those?**  
\_\_\_\_\_  
\_\_\_\_\_
8. **Explain how 3D printing with biomaterials revolutionizes the field of medicine.**  
\_\_\_\_\_  
\_\_\_\_\_  
\_\_\_\_\_

## Rheology of the ink for DIW

*The rheology of ink in DIW is a crucial factor that influences the process and outcome of 3D printing. Rheology refers to the study of how materials flow and deform under various forces. In the context of DIW, understanding the rheological properties of the ink is essential for achieving precise and controlled deposition of material layers. These properties include viscosity, shear thinning behavior, and yield stress.*

*Shear stress – a stress that is applied parallel or tangential to the face of a material*

*Examples:*

- 1. Think of shear stress like the force that makes one layer of a fluid slide past another.*
- 2. Imagine you have a deck of cards and you want to slide the top card off the deck with your finger. The force you apply with your finger to make that card move is similar to shear stress.*

*Shear rate – the rate of change in velocity at which one layer of fluid passes over an adjacent layer*

*Examples:*

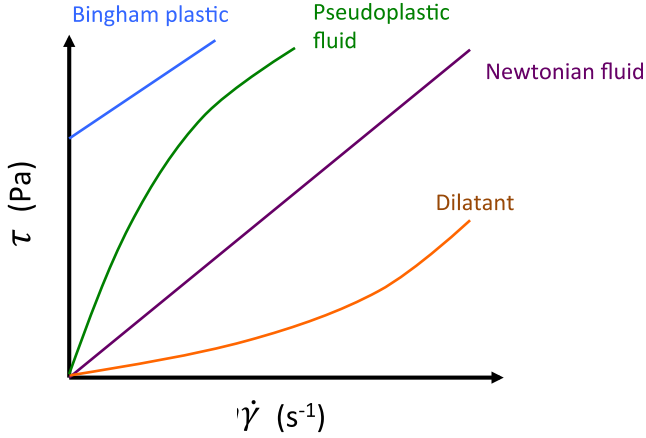
- 1. Shear rate is how fast those layers of fluid past each other.*
- 2. Imagine you are pushing that card at a certain speed. The rate at which you are making it move is similar to shear rate.*

*Yield stress – a minimum stress at which a solid will undergo permanent deformation or plastic flow without significant increase in the load or external force*

*Example:*

When you try to pour ketchup in a bottle, you need to apply a certain amount of force (squeeze the bottle) to overcome an initial resistance. Once you surpass this yield stress the ketchup starts to flow easily.

9. Examine the following shear stress vs. shear rate graph and answer the questions.



a) Fill in the following sentences:  
 Shear stress is represented by τ symbol and measuring unit is Pa.  
 Shear rate is represented by γ̇ symbol and measuring unit is s⁻¹.

b) Match the terms on the left with the correct description on the right.

Bingham plastic	shear thickening behaviour
Pseudoplastic fluid	has yield stress
Newtonian fluid	shear thickening behaviour
Dilatant	viscosity is not affected by shear rate

c) Fill in the blanks for flow behaviour index (*n*) with following symbols: =, < and >

- n* < 1 for a pseudoplastic fluid
- n* = 1 for a Newtonian fluid
- n* > 1 for a dilatant fluid

10. How can too low and too high viscosity of the ink affect the printing process?

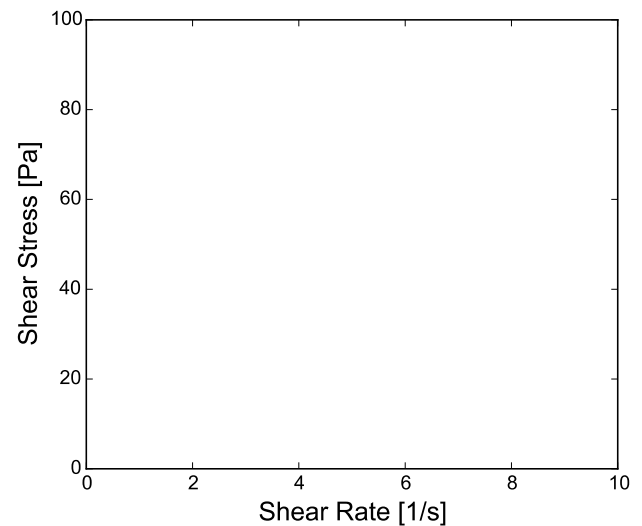
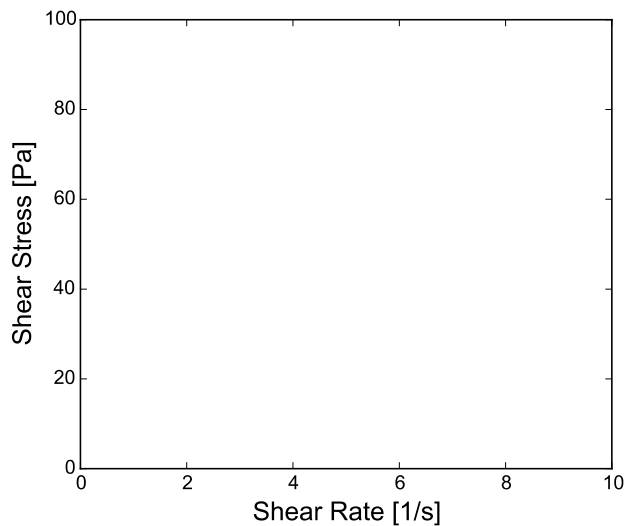
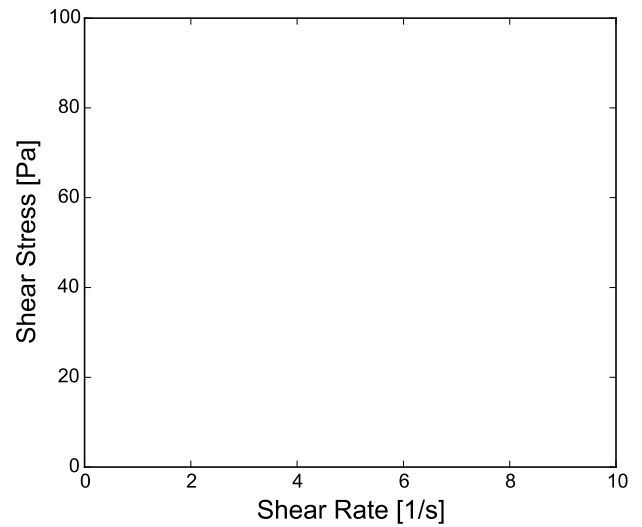
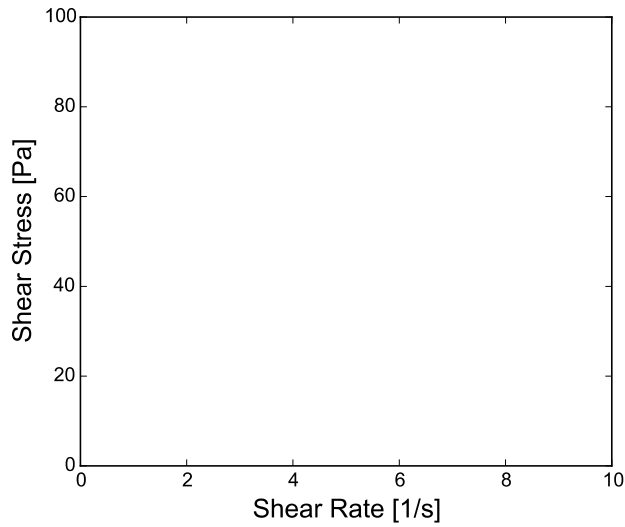
---



---

11. Your team should prepare a figure containing estimated shear stress vs. shear rate curves for each of the materials you were given. Work as a team to feel, pour, squish, squeeze, ..., and deform the four materials (A-D) provided to your group. One of the materials in your possession is similar to a Bingham plastic in that it has a yield stress (behaves as a fluid above the yield stress and like a solid below this stress level). Clearly indicate this fluid's yield stress in your plot.

**HINT: Your plot will not look like the example in task 9! Really think critically about how each of your fluid samples flows. How viscous is it? When does it flow? How easily does it flow? Use the empty graphs below to draft and finalize your figure.**



**12. Name rheological properties ink must have to be extrudable through the printer nozzle and briefly explain.**

---

---

---

---

## Polymer crosslinking

*In DIW 3D printing, crosslinking plays a crucial role and is essential in various fields. By finishing tasks in this section, you will find out reason behind this and get introduced with crosslinking process.*

**13. Follow the next procedure to finish the experiment. Write down your observations and conclusion.**

### **“ALGINATE WORMS”**

#### **Equipment:**

- Eye protection
- Dropping pipette/syringe
- Beakers, 150 cm<sup>3</sup> x 2

#### **Chemicals:**

- Sodium alginate suspension (2% solution)
- Sodium chloride solution (5% solution)
- Calcium chloride solution (5% solution)
- Food coloring

Always wear eye protection!

#### **Procedure:**

1. Prepare the solutions written in “**Chemicals**”. Label the beakers clearly.
2. Add few drops of food coloring to the sodium alginate suspension.
3. Using the pipette or syringe, squirt the sodium alginate into the calcium chloride solution. Observe the changes.
4. Transfer the mass from calcium chloride solution to the sodium chloride solution.
5. Swirl both beakers gently and observe what happens to the worms in each one.
6. You can remove and squeeze the worms as well as observing their appearance.
7. You will need to wait a few minutes for all the reactions to be complete.

Observations:

---

---

---

Conclusion:

---

---

---

Circle the correct answer:

When crosslinked with divalent cations, physical/chemical double networks occur between alginate polymer chains, often called “egg-box” structures.

**14. Examine SAMPLE 1 and SAMPLE 2 and answer the questions.**

*Both samples are composed of nanofibrilated cellulose (NFC), alginate and CaCO<sub>3</sub>.*

Observations:

What is the difference between the samples?

---

---

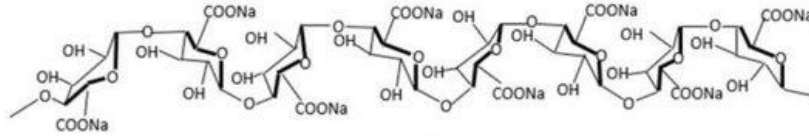
---

Why is SAMPLE 1 different than SAMPLE 2 even though they both contain  $\text{CaCO}_3$ ? What do you need to add to SAMPLE 1 in order to turn it to SAMPLE 2?

---

---

15. Sodium alginate is a polymer which can be extracted from brown seaweed and kelps. It is one of the structural polymers that help to build the cell walls of these plants. It has some unusual properties and a wide variety of uses. Next picture shows sodium alginate structure:



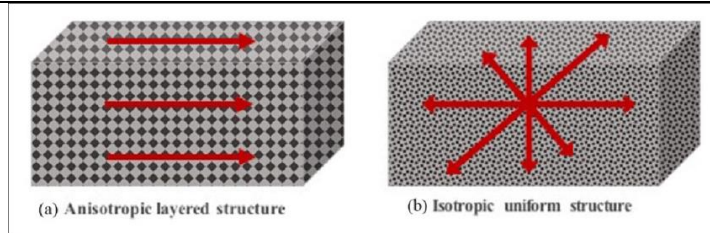
In this empty space show the crosslinking networks between two alginate polymer chains:  
(*HINT: Last sentence in task 13 might help you!*)

16. What is crosslinking in the context of a material science and why is it important in various industries?
- 
- 

### Isotropic and anisotropic materials

*The word isotropic is derived from Greek words isos meaning equal and tropos meaning way. Some materials such as metals, diamonds, glasses, etc. exhibit the same material properties (such as strength, stiffness) in all directions, these materials are known as isotropic materials and this type of behavior of these materials is known as isotropy.*

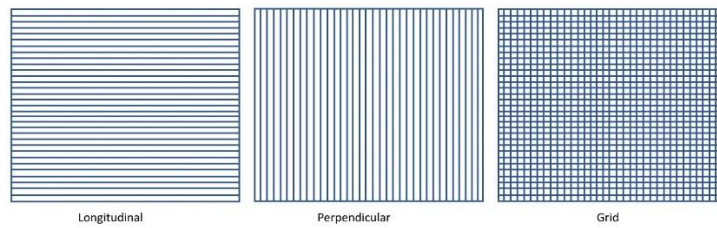
*The word anisotropic is also derived from the Greek words and means without, isos means equal and tropos means way. Thus, anisotropic meaning has different properties in different directions. It is the opposite of isotropic. Wood and composite materials are good examples of anisotropic materials. For example, it is easier to break a piece of wood along the grain (parallel to the wood fibers) than across the grain. This is because wood fibers provide structural strength along the grain. Properties of these materials are dependent on directions; it means they show different properties in different directions. This type of behavior of these materials is called anisotropy.*



*Anisotropic surfaces have clear directionality, differ considerably in roughness and the materials properties are not the same at all points or directions.*

*Isotropic surfaces have the same topography independent of measuring direction and the physical property is the same at any point/direction through the material.*

*When 3D printing with semi-solid inks that contain fibrous materials shear forces in the nozzle of the printer are aligning fibers in the direction of printing. In that way anisotropic materials can be aligned in a desired way. For example, in longitudinal, perpendicular and grid way as shown below.*



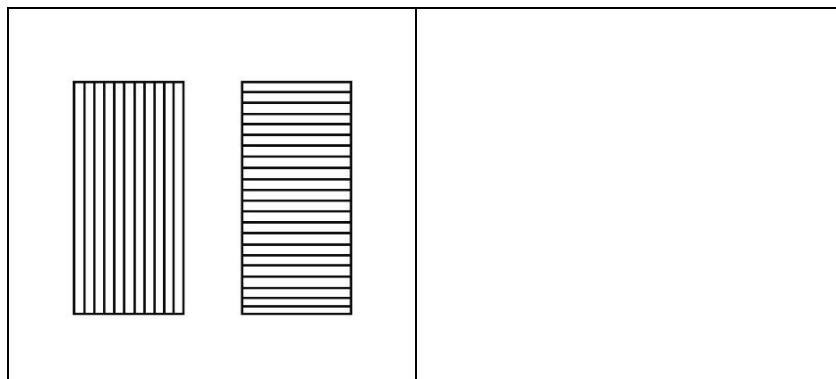
17. Name at least two examples of an anisotropic objects/materials.

---

18. Why is anisotropy significant in tissue engineering?

---

19. Next schematic representation shows scaffolds with different fiber alignment after printing. When put in water they show noticeable swelling. In the empty space draw the scaffolds after swelling paying attention on the fibers.



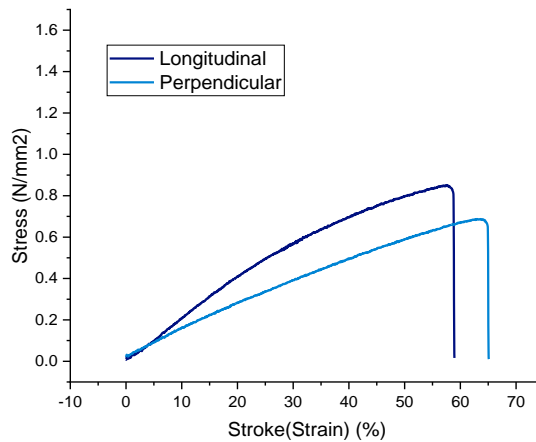


## Tensile testing

*Tensile test is a simple but crucial experiment in material science and engineering used to understand how a material responds to stretching or pulling force. The tensile machine pulls or stretches a material sample slowly and steadily in one direction, trying to make sample longer. As the machine stretches it measures two things: how much it's stretching the sample (THE STRAIN) and how much force it's applying (THE STRESS). The data collected is used to create a graph (shown in task 20.). Eventually the material might reach a point where it starts deforming permanently. This is called YIELD POINT. If you keep stretching the material above that point, it will continue to deform until it eventually breaks. The point where it breaks is the ultimate tensile strength or MAXIMUM STRESS of the material.*

*Watch video on the presentation to help you visualize the process.*

20. Next graph shows stress strain curves of perpendicularly and longitudinally printed scaffolds. Examine the graph and answer the questions.



- a) What is the measuring unit for tensile stress? \_\_\_\_\_
- b) What is the measuring unit for tensile strain? \_\_\_\_\_
- c) What is maximum tensile strength and how is it determined from a stress-strain curve?

\_\_\_\_\_

\_\_\_\_\_

- d) Which of the scaffold shows higher maximum tensile strength? \_\_\_\_\_

- e) Explain why do you think that is. \_\_\_\_\_

\_\_\_\_\_

- f) What is happening with perpendicular scaffold during tensile loading?

\_\_\_\_\_

\_\_\_\_\_

## POGIL answers

### 3D BIOPRINTING OF BIOMATERIALS

(answers)

**1. What is the difference between a 3D printer and traditional inkjet printer?**

*A traditional inkjet printer produces flat two-dimensional images, while a 3D printer creates three-dimensional objects by adding material layer by layer.*

**2. Why is 3D printing also referred as additive layer manufacturing?**

*Because it adds material layer by layer to build an object.*

**3. Arrange the following steps in the correct order for 3D printing process:**

- \_5\_ post processing - cooling and/or solidifying the material*
- \_2\_ preparing/designing the 3D model*
- \_4\_ 3D printing*
- \_1\_ selecting/designing the material for printing*
- \_6\_ testing*
- \_3\_ setting up the 3D printer*

*(Students may be confused by the order of first and second step therefore it is important to explain that both answers are correct. In some cases, you might start by choosing the material based on its properties and suitability for a particular application. In other cases, you can design an object first and then choose the material based on that. For example, after designing some objects that have a lot of overhanging parts you could choose better, stiffer material).*

**4. Name at least 5 everyday object that can be 3D printed.**

*Phone cases, key chains, custom jewelry, toy figurines, household tools, educational models...*

**5. What do you think prefix bio- in bioprinting stands for and what does it refers to?**

*It stands for biology or biological and it refers to the use of biological materials. Bioprinting refers to creating structures and tissues that mimic natural ones for application in medicine, tissue engineering and more. Also, bioprinting may imply to bio inks that contains natural living cells.*

**6. What do you think what properties do biomaterials have to possess to:**

- c) be printable (to be able to extrude them by pressure from the nozzle onto the printing surface)?  
They have to possess appropriate rheological properties such as low viscosity.*
- d) be compatible with living cells and tissues?? Non-toxic and support growth and proliferation of living cells and tissues. They should not cause an immune response or harm the cells.*

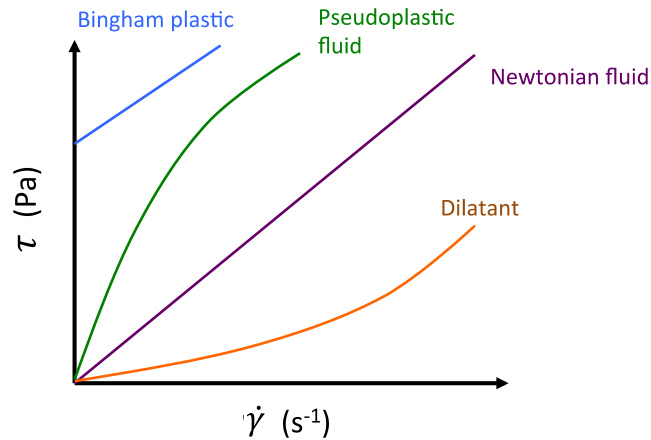
**7. Are there any environmental benefits of 3D printing with biodegradable materials compared to traditional manufacturing methods? If yes, what are those?**

*3D printing with biodegradable materials can reduce waste and environmental impact compared to the traditional manufacturing methods that generate more waste.*

**8. Explain how 3D printing with biomaterials revolutionizes the field of medicine.**

*It enables personalized medicines and medical devices to suit better need of a patient.*

9. Examine the following shear stress vs. shear rate graph and answer the questions.



a) Fill in the following sentences:

Shear stress is represented by  $\tau$  symbol and measuring unit is Pa.

Shear rate is represented by  $\dot{\gamma}$  symbol and measuring unit is 1/s.

b) Match the terms on the left with the correct description on the right.

Bingham plastic	—	shear thickening behaviour
Pseudoplastic fluid	—	has yield stress
Newtonian fluid	—	shear thickening behaviour
Dilatant	—	viscosity is not affected by shear rate

c) Fill in the blanks for flow behaviour index ( $n$ ) with following symbols: =, < and >

$n < 1$  for a pseudoplastic fluid

$n = 1$  for a Newtonian fluid

$n > 1$  for a dilatant fluid

10. How can too low viscosity and too high viscosity of the ink affect the printing process?

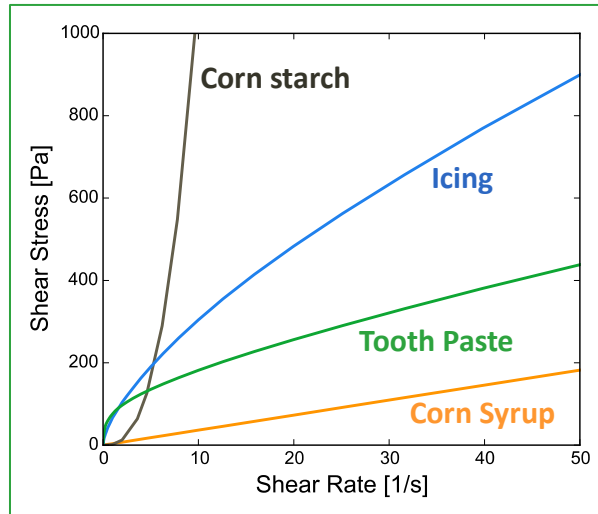
*Low viscosity may lead to poor shape retention, while high viscosity might be hard to extrude through the nozzle.*

11. Your team should prepare a figure containing estimated shear stress vs. shear rate curves for each of the materials you were given. Work as a team to feel, pour, squish, squeeze ..., and deform the four materials (A-D) provided to your group.

One of the materials in your possession is similar to a Bingham plastic in that it has a yield stress. Clearly indicate this fluid's yield stress in your plot.

**HINT:** Your plot will not look like the example one in the slides! Really think critically about how each of your fluid samples flows. How viscous is it? When does it flow? How easily does it flow?

Use the empty graphs below to draft and finalize your figure.



- *Corn syrup is a viscous Newtonian fluid. Its flow curve should be a straight line.*
- *Corn starch is shear-thickening. At increasing shear rates, this suspension behaves more like a solid, only deforming under ever-increasing shear stresses.*
- *At most shear rates, icing has a higher apparent viscosity than the tooth paste.*
- *The tooth paste has a yield stress of ~15-30 Pa; when applied shear stress is below this yield stress, it does not flow.*

**12. Name rheological properties ink must have to be extrudable through the printer nozzle and briefly explain.**

*Their viscosity should decrease while applying pressure meaning they should have shear thinning behaviour (allows ink to flow more readily when pressure is applied making it easier to deposit precise layers and returns to its original viscosity after the pressure is removed) and yield stress property (crucial for preventing unintended flow of ink when not under extrusion pressure).*

**13. Follow the next procedure to finish the experiment. Write down your observations and conclusion.**

Observations:

- *sodium alginate suspension has thicker consistency and higher viscosity than other solutions*
- *when adding sodium alginate to calcium chloride solution it thickens and takes on a gel like texture*
- *worms are dissolving in sodium chloride solution*

Conclusion:

- *when adding sodium alginate to the calcium chloride solution, crosslinking of alginate polymer occurs*
- *calcium ions are taking sodium ions place and due to the divalent of the calcium, alginate polymer chains are attracted to each other by electrostatic forces*

**Circle the correct answer:**

When crosslinked with divalent cations, physical chemical double networks occur between alginate polymer chains, often called “egg-box” structures.

**14. Examine SAMPLE 1 and SAMPLE 2 and answer the question.**

Both samples are composed of nanofibrilated cellulose (NFC, 3 w%), alginate and  $\text{CaCO}_3$ .

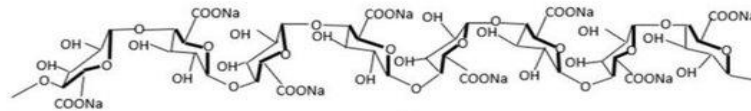
What is the difference between the samples?

*SAMPLE 1 has no stable structure, it flows when pressure is applied compared to SAMPLe 2. It also has shear thinning behaviour because its viscosity decreases as pressure is applied. SAMPLe 2 shows stiffer structure.*

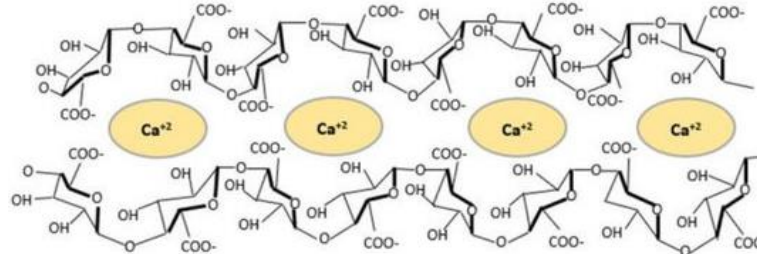
Why is SAMPLe 1 different that SAMPLe 2 even though they both contain  $\text{CaCO}_3$ ? What do you need to add to SAMPLe 1 in order to turn it to SAMPLe 2?

*$\text{CaCO}_3$  has low solubility in water. In order to make  $\text{CaCO}_3$  more soluble and crosslink the alginate polymer chains, acid needs to be added.*

15. **Sodium alginate is a polymer which can be extracted from brown seaweed and kelps. It is one of the structural polymers that help to build the cell walls of these plants. It has some unusual properties and a wide variety of uses. Next picture shows sodium alginate structure:**



In this empty space show the calcium crosslinking between two alginate polymer chains:



16. **What is crosslinking in the context of a material science and why is it important in various industries?**

*Crosslinking is the process of chemically or physically connecting polymer chains to create network-like structure. It is crucial in industries because it enhances material strength, stability and durability.*

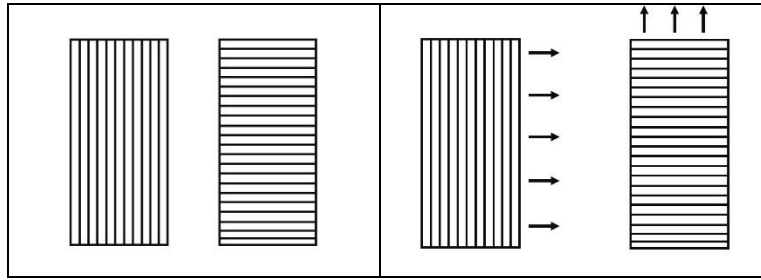
17. **Name at least two examples of an anisotropic objects/materials.**

*Muscles in the body, wooden pencil, graphite, paper, crystals, plant stem, fishing rod...*

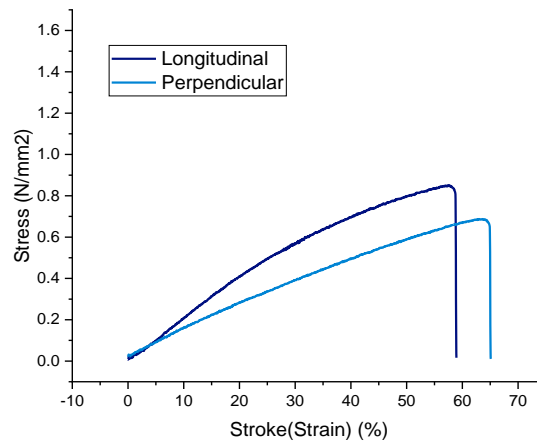
18. **Why is anisotropy significant in tissue engineering?**

*Anisotropy is important in tissue engineering because it helps replicate natural alignment and properties of tissues. This is crucial for achieving functional and biomechanical replicas of tissues.*

19. **Next schematic representation shows scaffolds with different fiber alignment after printing. When put in water they show noticeable swelling. In the empty space draw the scaffolds after swelling paying attention on the fibers.**



20. Next graph shows stress strain curves of perpendicularly and longitudinally printed scaffolds. Examine the graph and answer the questions.



- What is the measuring unit for tensile stress?  $N/mm^2$
- What is the measuring unit for tensile strain? %
- What is maximum tensile strength and how is it determined from a stress-strain curve?  
*It is the maximum stress a material can withstand before it breaks. It is determined by finding the highest point on the stress-strain curve.*
- Which of the scaffold shows higher maximum tensile strength? *Longitudinal one*
- Explain why do you think that is.  
*The answer lies in anisotropic behaviour of the material. The force is applied in longitudinal direction and it is aligned with the natural orientation of the longitudinal scaffold and that allows for more efficient load along the fibers.*

## Repetition worksheet

1. What is 3D printing and how it differs from traditional manufacturing methods?

---

---

---

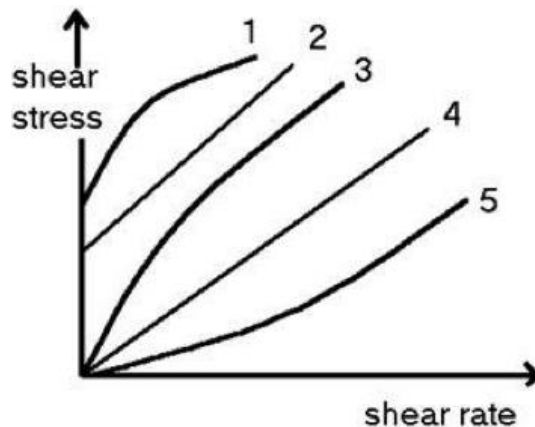
2. Briefly explain whole 3D printing process.

---

---

---

3. Refer to the following graph for questions. For the materials depicted in the graph please answer these questions. Only one per question.



- A.** Which material may be extremely difficult to pump using a piston pump because it thickens with increased shear stress?  
a)1 b)2 c)3 d)4 e)5
- B.** Which fluid flows directly proportional to the force applied to it, has no yield value and is termed Newtonian?  
a)1 b)2 c)3 d)4 e)5
- C.** Which material shows the highest yield stress value?  
a)1 b)2 c)3 d)4 e)5

**D.** Which material is pseudoplastic and demonstrates shear thinning but no yield value?  
a)1 b) 2 c)3 d)4 e)5

**E.** Which rheological profile might be preferred for a cosmetic emulsion because it has both a high yield value and is shear thinning?  
a)1 b) 2 c)3 d)4 e)5

4. How does anisotropy affect the behavior of materials like wood and paper?

---

---

5. What is happening with perpendicular scaffold during longitudinal tensile loading?

---

---

6. Think and name one or more real-world problems that 3D printing might solve.

---

---



## Repetition worksheet answers

1. What is 3D printing and how it differs from traditional manufacturing methods?  
*3D printing also known as additive manufacturing is a process of creating a three-dimensional objects layer by layer from a digital model. It differs from traditional manufacturing in a way that it doesn't involve subtracting material (e.g. cutting, drilling...) from a solid block to shape a model.*
2. Briefly explain whole 3D printing process.  
*Selecting/designing the material for printing, preparing/designing the 3D model, setting up the 3D printer, 3D printing, post processing – crosslinking, cooling and/or solidifying the material, testing.*
3. A. e) 5  
B. d) 4  
C. a) 1  
D. c) 3  
E. a) 1
4. How does anisotropy affect the behaviour of materials like wood and paper?  
*It influences properties like strength, flexibility and ease of tearing in these materials. For instance, wood is stronger along the grain while paper is easier to tear across the grain.*
5. What is happening with perpendicular scaffold during longitudinal tensile loading?  
*When applying force in longitudinal direction to the perpendicularly printed scaffolds, the force is trying to separate the fibers or attractions/bonds between them.*
6. Think and name one or more real-world problems that 3D printing might solve.  
*3D printing can help address problems like creating affordable prosthetics for people in need, reducing waste through custom manufacturing and producing replacement parts in machinery, producing personalized medicine...*